EXERGY ANALYSIS
OF
COMBINED CYCLE COGENERATION SYSTEMS

A THESIS SUBMITTED TO
THE GRADUATE SCHOOL OF NATURAL AND APPLIED SCIENCES
OF
MIDDLE EAST TECHNICAL UNIVERSITY

BY

CAN ÖZGÜR ÇOLPAN

IN PARTIAL FULFILLMENT OF THE REQUIREMENTS
FOR
THE DEGREE OF MASTER OF SCIENCE
IN
MECHANICAL ENGINEERING

MAY 2005

Approval of the Graduate School of Natural and Applied Sciences.

_____

Prof. Dr. Canan Özgen
Director

I certify that this thesis satisfies all the requirements as a thesis for the degree of Master of Science.

_____

Prof. Dr. Kemal İder
Head of Department

This is to certify that we have read this thesis and that in our opinion it is fully adequate, in scope and quality, as a thesis for the degree of Master of Science.

_____

Prof. Dr. Tülay Yeşin
Supervisor

Examining Committee Members

Prof. Dr. Hafit Yüncü	(METU, ME)	_____
Prof. Dr. Tülay Yeşin	(METU, ME)	_____
Prof. Dr. Yalçın A. Göğüş	(METU, AEE)	_____
Assoc. Prof. Dr. Cemil Yamalı	(METU, ME)	_____
Asst. Prof. Dr. Derek Baker	(METU, ME)	_____

I hereby declare that all information in this document has been obtained and presented in accordance with academic rules and ethical conduct. I also declare that, as required by these rules and conduct, I have fully cited and referenced all material and results that are not original to this work.

Name, Last name: Can Özgür ÇOLPAN

Signature :

ABSTRACT

EXERGY ANALYSIS
OF
COMBINED CYCLE COGENERATION SYSTEMS

Çolpan, Can Özgür
M.Sc., Department of Mechanical Engineering
Supervisor: Prof. Dr. Tülay Yeşin

May 2005, 120 pages

In this thesis, several configurations of combined cycle cogeneration systems proposed by the author and an existing system, the Bilkent Combined Cycle Cogeneration Plant, are investigated by energy, exergy and thermoeconomic analyses. In each of these configurations, varying steam demand is considered rather than fixed steam demand. Basic thermodynamic properties of the systems are determined by energy analysis utilizing main operation conditions. Exergy destructions within the system and exergy losses to environment are investigated to determine thermodynamic inefficiencies in the system and to assist in guiding future improvements in the plant. Among the different approaches for thermoeconomic analysis in literature, SPECO method is applied. Since the systems have more than one product (process steam and electrical power), systems are divided into several subsystems and cost balances are applied together with the auxiliary equations. Hence, cost of each product is calculated. Comparison of the configurations in terms of performance assessment parameters and costs per unit of exergy are also given in this thesis.

Keywords: Combined Cycle, Cogeneration, Energy, Exergy, Thermoeconomics

ÖZ

KOMBİNE ÇEVRİM KOJENERASYON SİSTEMLERİN
EKSERJİ ANALİZİ

Çolpan, Can Özgür
Yüksek Lisans, Makina Mühendisliği Bölümü
Tez Yöneticisi: Prof. Dr. Tülay Yeşin

Mayıs 2005, 120 sayfa

Bu tezde, yazar tarafından oluşturulan çeşitli konfigürasyonlarda kombine çevrim kojenerasyon sistemleri ve mevcut bir sistem olan Bilkent kombine kojenerasyon santrali, enerji, ekserji ve termoekonomik analizlerle incelenmiştir. Her bir konfigürasyonda, sabit buhar talebi yerine değişken buhar talebi ele alınmıştır. Sistemlerin temel termodinamik özellikleri, başlıca operasyon durumları kullanılarak, enerji analiziyle kararlaştırıldı. Sistemlerdeki ekserji yıkımları ve çevreye giden ekserji kayıpları, sistemdeki termodinamik verimsizlikleri incelemek ve gelecekteki yenilemelere yol göstermek için irdelendi. Literatürdeki, farklı termoekonomik analiz yaklaşımları arasından, SPECO metodu uygulanmıştır. Sistemlerin birden çok ürünü olmasından dolayı (proses buharı ve elektrik gücü), sistemler çeşitli altsistemlere bölündü ve maliyet dengeleri, yardımcı denklemlerle birlikte uygulandı. Sonuçta, her ürünün maliyeti hesaplandı. Değişik konfigürasyonların performans belirleyici parametreleri ve maliyetleri ile karşılaştırılması da bu tezde verilmiştir.

Anahtar Kelimeler: Kombine Çevrim, Kojenerasyon, Enerji, Ekserji, Termoekonomi

To My Family

ACKNOWLEDGEMENTS

The author wishes to express his deepest gratitude to his supervisor Prof. Dr. Tülay Yeşin for her invaluable supervision, advice, encouragements and insight throughout the research. Besides, the author gratefully thanks to her for creating an opportunity for submitting papers to ECOS 2005, Norway and ATC 2005, Istanbul conferences which caused great motivation in advancing the thesis.

The author would also like to express his sincere thanks to Prof. Dr. Yalçın A. Göğüş for his important contributions to this study. His invaluable guidance and support is gratefully acknowledged.

The author would like to thank to all faculty members of the Mechanical Engineering Department for their instruction and advice during undergraduate and graduate studies.

The author would also like to thank Bilenerji A.Ş. managers and engineers, especially Aygün Anlı and Mustafa Tuygun, for their cooperation in supplying data for Bilkent Combined Cycle Cogeneration Plant.

The author gratefully thanks to his parents Melih and Nesrin Çolpan and his sister Aslı Çolpan for their invaluable support in his entire life.

TABLE OF CONTENTS

LIST OF TABLES

TABLES

LIST OF FIGURES

FIGURES

LIST OF SYMBOLS

SYMBOLS

c	Cost per unit of exergy [$/GJ]
$\dot{C}$	Cost rate associated with exergy [$/h]
e	Specific exergy [kJ/kg]
E	Exergy [kJ]
$\dot{E}$	Exergy flow rate [kW]
g	Acceleration due to gravity [m/s^2]
h	Specific enthalpy [kJ/kg]
$\dot{H}$	Enthalpy flow rate [kW]
i_{eff}	Effective annual cost-of-money rate
$\dot{m}$	Mass flow rate [kg/s]
P	Pressure [bar]
$\dot{Q}$	Heat rate [kW]
$\overline{R}$	Universal gas constant [kJ/kmol-K]
s	Specific entropy [kJ/kg-K]
$\overline{s}$	Specific entropy [kJ/kmol-K]
T	Temperature [°C]
x	Mole fraction
x'	Mole fraction of the gas phase
X	Value of a cost component [$]
V	Velocity [m/s]
$\dot{W}$	Power [kW]
y_D	Exergy destruction as a percentage of the total exergy supplied to the plant
y_D^*	Exergy destruction as a percentage of the total exergy destruction within the plant

y_L	Exergy loss as a percentage of the total exergy supplied to the plant
z	Elevation [m]
$\dot{Z}^{CI}$	Cost rate associated with capital investment [$/h]
$\dot{Z}^{OM}$	Cost rate associated with operating and maintenance expenses [$/h]
$\dot{Z}$	Cost rate associated with the capital and operating and maintenance expenses [$/h]

Abbreviations

BFW	Boiler feed water
CC	Carrying charges
CRF	Capital recovery factor
ER	Exchange rate
EXC	Expenditure costs
FC	Fuel costs
FUE	Fuel utilization efficiency
GT	Gas turbine
HHV	Higher heating value
HL	Heat loss from heat recovery steam generator in terms of heat absorbed. (Taken as 0.02 in this thesis)
HP	High pressure
HRSG	Heat recovery steam generator
IP	Intermediate pressure
ISO	International standards organization
LHV	Lower heating value
LP	Low pressure
OMC	Operating and maintenance costs
PEC	Purchased equipment costs
PHR	Power-to-heat ratio
PURPA	Public utility regulatory policy act
RWC	Raw water costs
SPECO	Specific exergy costing

ST	Steam turbine
TRR	Total revenue requirement

Subscripts

ap	Approach
D	Destruction
Dest	Destruction
e	Exit
El	Electrical
EX	Expenditure
F	Fuel
gen	Generator
gt	Gas turbine
i	Inlet
L	Levelized
liq	Liquid
mix	Mixture
o	Ambient
p	Pump
pp	Pinch point
P	Product
ref	Reference
RW	Raw water
sat	Saturated
st	Steam turbine
tot	Total
v	Vapor

Superscripts

PH	Physical
KN	Kinetic

PT	Potential
CH	Chemical

Greek Letters

ε	Exergetic efficiency
η	Efficiency
λ	Fuel-air ratio on mass basis
$\overline{\lambda}$	Fuel-air ratio on molar basis
ν	Specific volume [m^3/kg]
ρ	Density [kg/m^3]
τ	Total annual number of hours of system operation at full load. [h]
ϕ	Relative humidity

CHAPTER 1

INTRODUCTION

1.1 THE OBJECTIVES OF THE THESIS

Thermal systems design and analysis involve principles from many fields of mechanical engineering such as; thermodynamics, heat transfer, fluid mechanics, manufacturing and mechanical design. In this thesis, thermodynamics aspect of the design is handled.

Among the thermal systems, combined cycle cogeneration systems are analyzed by advanced thermodynamic topics. These topics include exergy and thermoeconomics. Exergy analysis, which is the combination of first law and second law of thermodynamics, helps to highlight the thermodynamic inefficiencies of a system. It is clear that improving a system thermodynamically without considering economics is misleading. Hence, many researchers have started to develop links between exergy and economics. As a result, a new area called thermoeconomics or exergoeconomics has been formed. Some researchers use these terms as synonyms; whereas others indicate the difference between them. There are different approaches of thermoeconomics. Among them, SPECO method is selected to be used in combined cycle cogeneration systems in this thesis. So, the main objective of this thesis is to analyze combined cycle cogeneration systems thermodynamically and economically.

Different configurations of combined cycle cogeneration systems are introduced and compared with each other in terms of energetic, exergetic and thermoeconomic concepts. Performance assessment parameters are used for thermodynamic comparison and cost or cost per unit exergy of system products are used for thermoeconomic comparison.

1.2 LITERATURE SURVEY

The book 'Thermal Design & Optimization' by Bejan, Tsatsaronis and Moran (1996) provides a comprehensive and rigorous introduction to thermal system design and optimization from a contemporary perspective. The book includes current developments in engineering thermodynamics, heat transfer, and engineering economics relevant to design. The use of exergy analysis and entropy generation minimization is featured. A detailed description of engineering economics and thermoeconomics are also presented. Moreover, a case study is considered throughout the book for continuity of the presentation. The case study involves the design of a gas turbine cogeneration system.

The paper 'On the Calculation of Efficiencies and Costs in Thermal Systems' by Lazzaretto and Tsatsaronis (1999) represents an extension, a further generalization, and a more systematic presentation of the contents of the previous papers by the same authors. This paper describes SPECO method for calculating exergy-related costs in thermal systems. General rules are formulated for defining fuel and product and for calculating the auxiliary costing equations (based on the F and P rules).

The paper 'Selection of Cycle Configurations for Combined Cycle Cogeneration Power Plants' by Tawney, Ehman and Brown (2000) focuses on several ranges of process steam flows and conditions in order to provide a basis for comparison of the most common cycle configurations in combined cycle applications. Plant design, cycle performance, and economics of each configuration are evaluated based on requirements of flexibility and process steam flows. Rather than self-establishing the energy balances, GateCycle^{TM} Heat Balance software developed by GE Enter Software, Inc. is used to build thermal models. Additionally, a financial software tool developed within Bechtel is used to construct an economic model for each cycle configuration. It is concluded that, the selection of a cogeneration facility type and the economic parameters are very much site specific and are based on numerous variables such as site ambient conditions, the level of desired power output and steam demand, capacity factor, flexibility, power purchase agreement and steam

purchase agreement requirements, and owner's economic parameters for return on equity.

The paper 'Performance Assessment Parameters of a Cogeneration System' by Huang (1996) describes ten parameters for investigating the performance of cogeneration systems. Additionally, usefulness of each parameter is presented. In conclusion, it is shown that second-law efficiency (exergetic efficiency) and power-to-heat ratio are the most appropriate and useful ones for a decision-maker to use to compare the performance of alternate designs.

The paper 'Exergetic and Engineering Analyses of Gas Turbine Based Cogeneration Systems' by Bilgen (2000) presents exergetic and engineering analyses as well as a simulation of gas turbine-based cogeneration plants. Two cogeneration cycles, one consisting of a gas turbine and the other of a gas turbine and steam turbine has been analyzed. The results showed good agreement with the reported data.

The paper 'First-and Second-Law Analysis of Steam-Turbine Cogeneration Systems' by Habib (1994) presents an analysis of a cogeneration system. The analysis quantifies the irreversibilities of the different components of each plant. Additionally, the influence of the heat-to-power ratio and the process pressure on the thermal efficiency and utilization factor is presented. The results show that the total irreversibility of the cogeneration plant is 38 percent lower compared to the conventional plant. This reduction in the irreversibility is accompanied by an increase in the thermal efficiency and utilization factor by 25 and 24 percent, respectively. The results show that the exergy destruction in the boiler is the highest.

The paper 'Performance Evaluation of a Combined-Cycle Cogeneration System' by Huang and Naumowicz (1999) presents a methodology for performance evaluation of a combined-cycle cogeneration system. Energy balances and performance assessment parameters of that system are given. Results for such a system using an advanced gas turbine as the prime mover show that it is a very versatile system. It

can produce a large power-to-heat ratio together with high second-law efficiency over a wide range of process steam pressures.

The paper 'Performance Simulation of Heat Recovery Steam Generators in a Cogeneration System' by Karthikeyan et al. (1998) gives energy balances for a one pressure level heat recovery steam generator. Effects of pinch and approach points on steam generation and also on temperature profiles across heat recovery steam generator are investigated. The effects of operating conditions on steam production and also on exit gas temperature from the heat recovery steam generator are discussed. It is concluded that low pinch point results in improved heat recovery steam generator performance due to reduced irreversibilities. Additionally, the supplementary firing enhances the steam production.

The book 'Handbook for Cogeneration and Combined Cycle Power Plants' by Boyce (2002) covers all major aspects of power plant design, operation, and maintenance. It covers cycle optimization and reliability, technical details on sizing, plant layout, fuel selection, types of drives, and performance characteristics of all major components in a cogeneration or combined cycle power plant. Comparison of various energy systems, latest cycles and power augmentation techniques, reviews and benefits of latest codes, detailed analysis of available equipment, techniques for improving plant reliability and maintainability, testing and plant evaluation techniques, and advantages and disadvantages of fuel are also included in this book.

1.3 OUTLINE OF THE THESIS

The following chapter overviews cogeneration technologies. Main emphasis is given to combined cycle cogeneration configurations and their main components. Case studies analyzed through the rest of the thesis are also described in this chapter.

The third chapter includes energy analyses of case studies. Performance assessment parameters related to energy concept are described and analyzed for their change with steam demand, pressure of high pressure steam drum and pinch point.

The fourth chapter discusses exergy analysis, and its application to case studies. This analysis includes formulation of exergy terms, exergy destructions within plant, exergy losses to environment, exergetic efficiency of the plants and ratios related with exergy destruction and exergy loss.

In the fifth chapter, SPECO method used for thermoeconomic analysis is discussed. Engineering economics analysis is studied. General methodology used in such analysis is given. Thermoeconomic analysis of case studies is discussed and comparisons of case studies in terms of costs are given.

Sixth chapter is devoted to an existing plant, Bilkent combined cycle cogeneration plant. Its analysis is accomplished through energy, exergy, economic and thermoeconomic analyses. The results of these analyses are discussed in this chapter.

Seventh chapter includes discussions on some important points about the studies in the thesis. These include reasons for selection of the gas turbine system for case studies and influence of aggregation level in thermoeconomic analysis.

Eighth chapter includes conclusions related to studies in this thesis.

CHAPTER 2

COMBINED CYCLE COGENERATION SYSTEMS

2.1 INTRODUCTION

2.1.1 Cogeneration

Cogeneration is the production of electrical energy and useful thermal energy from the same energy source. In conventional electricity generation, only a small portion of fuel energy is converted into electricity and the remaining is lost as waste heat. Cogeneration reduces this loss by recovering part of this. Principal applications of cogeneration include industrial sites, district heating and buildings.

Cogeneration systems are generally classified according to their prime movers. Currently available systems include; steam turbines, gas turbines, combined cycle and reciprocating engines. There are also new technologies which are expected to become economically available in the next ten years. These include; fuel cells, Stirling engine and micro-turbines. [13]

2.1.2 Combined Cycle Cogeneration Systems

The most widely used combined cycle system consists of primer movers as gas turbine and steam turbine. In these systems, topping cycle (gas turbine) produces electrical energy and rejects heat; whereas bottoming cycle (steam turbine) recovers and uses that waste heat to produce electrical energy and process heat.

It is also possible to combine Diesel cycle with Rankine cycle. The difference is gas turbine unit is replaced by a Diesel engine. Medium to high power engines may make the addition of the Rankine cycle economically feasible. [12]

2.2 CONFIGURATIONS

Combined cycle cogeneration systems can be quite complex as there are different configurations that can be selected and optimized to provide the desired flexibility, reliability and rate of return for the owner [10]. Main configuration differences arise due to using different types of steam turbines and heat recovery steam generators.

Steam turbines may be condensing or back-pressure (non-condensing) type. In back-pressure steam turbines, steam exits the turbine at a pressure greater than or equal to the atmospheric pressure, the pressure depending on the needs of the thermal load. In condensing steam turbines, steam for the thermal load is obtained by extraction from one or more intermediate stages at the appropriate pressure and temperature. The remaining steam is exhausted at the pressure of the condenser. In comparison to the back-pressure system, the condensing one has a higher capital cost and, in general, a lower total efficiency. However, it can control the electrical power independently, to a certain extent, of the thermal load by proper regulation of the steam flow rate through the turbine. [12]

Heat recovery steam generators mainly differ in circulation type, number of pressure levels and supplementary firing. According to its circulation type, HRSGs can be of natural or forced circulation design. In forced circulation type, HRSGs are vertical. The steel structure of the HRSG supports the drums. The water is circulated through tubes using pumps. In natural circulation type, there is no need for the pumps. HRSGs are horizontal type. Circulation is established by the density difference between the down comer and riser circuits and their hydraulic resistances. According to their pressure levels, HRSGs can be single pressure or multi-pressure types. Using multi-pressure level increases the usage of energy from exhaust gas of gas turbine; thus decreasing the energy loss from system. Depending on the steam requirements,

HRSGs can take three forms: unfired, supplementary-fired and exhaust-fired. In unfired HRSGs, the energy from the exhaust is used as such, while in supplementary-fired and exhaust-fired HRSGs, additional fuel is inputted to the exhaust gas to increase steam production. [11]

2.3 DESCRIPTION OF CASE STUDIES

Three different configurations of combined cycle cogeneration systems are chosen to be studied in this thesis. They are shown in Figures 1-3.

Each of the cases has the same gas turbine system. The gas turbine system is taken same as that of CGAM system (i.e. Air compressor, air preheater, combustion chamber and gas turbine of that system). Reasons of this selection are discussed in Section 7.1 Description and analysis of CGAM system is given in Appendix C. In addition to the gas turbine and auxiliary systems, case-1 consists of a two-pressure HRSG and a back-pressure steam turbine. Case-2 consists of a two-pressure HRSG and a condensing steam turbine. Case-3 consists of a three-pressure HRSG and a condensing steam turbine. In each of them, one of the steam generators supply steam to the integral deaerator to heat up the condensate to the saturation temperature corresponding to the pressure of its drum and degas that condensate.

For controlling the steam turbine inlet temperature, a desuperheater may be used between first and second superheater stages. Additionally, some of the steam needed to deaerate the condensate could be sent from a higher pressure steam drum to control stack temperature. Stack temperature should be controlled due to corrosion considerations. A typical limit for stack temperature may be taken as 400 K. These security components are shown with dotted lines in Figures 1-3.

The systems used in this study can cope with their steam demand change. A dump condenser is used with the back pressure steam turbine in case-1 for this purpose. Extraction-condensing steam turbine is used for that in case-2 and case-3. The cooling water of the condensers is considered to be pumped from sea or lake.

The operation data used in the case studies are given in Table 1. Data for the gas turbine system and environmental conditions are taken same as the CGAM system, which is given in Appendix C.

Table 1: Operation Data of Case Studies

HP Steam Drum Pressure	40 bar
LP Steam Drum Pressure	1.2 bar
Pinch Point and Approach Temp.	10 °C
Steam Turbine Inlet Temp.	475 °C
Steam Export (Sat. vapor) Pressure	10 bar
Condenser Pressure	0.07 bar
Dump Condenser Pressure	1 bar
Cooling Water Temp. Difference	10 °C
Condensate Return Temperature	60 °C
Steam Turbine Isentropic Efficiency	0.8
Pumps Isentropic Efficiency	0.8
Electric Generator Efficiency	0.98

In addition to the assumptions for the gas turbine system given in Appendix C, the assumptions done for the analyses of case studies are as follows: Heat loss from HRSG is assumed to be 2% of heat absorbed. Pressure drop on the gas side of HRSG is 5% and that of on the water side is neglected. Blow down requirements and deaerator vent flows are not taken into account. All the steam export from the system returns as condensate.

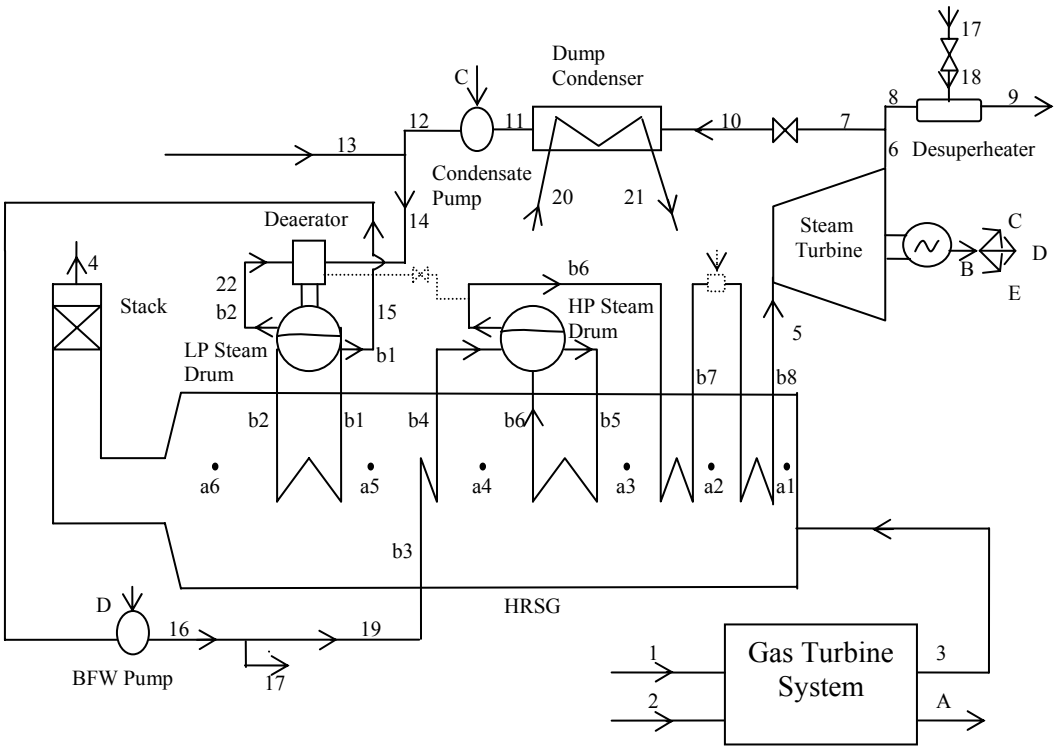

Figure 1: Schematic Drawing of Case-1

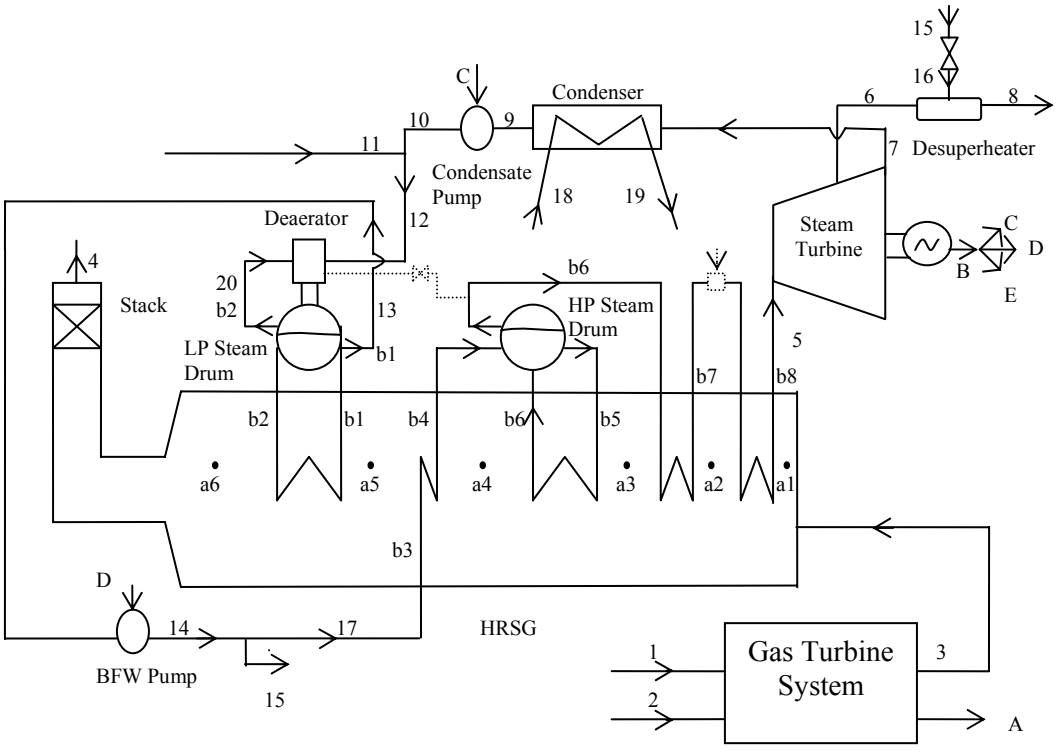

Figure 2: Schematic Drawing of Case-2

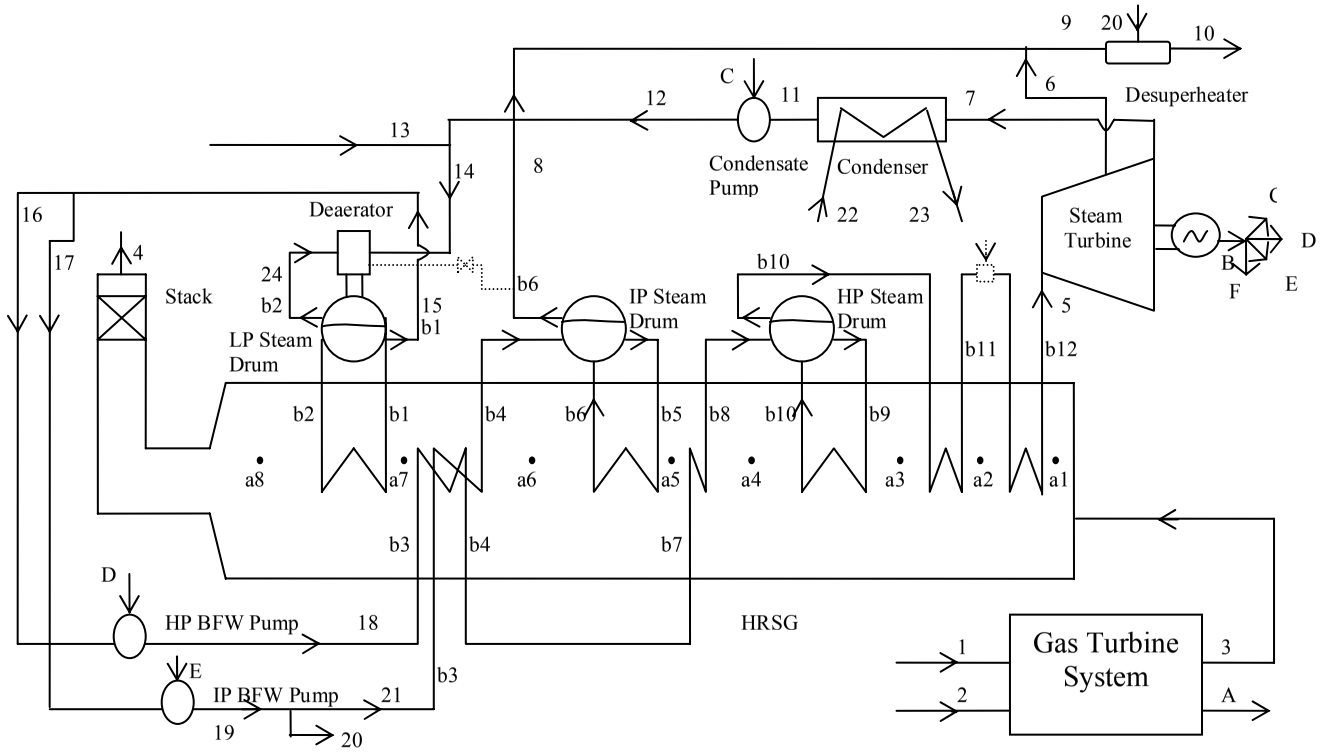

Figure 3: Schematic Drawing of Case-3

CHAPTER 3

ENERGY ANALYSIS

3.1 INTRODUCTION

Basic thermodynamics, which is briefly discussed in Appendix B, is applied to case studies to find the mass flow rate of steam generated at the drums, thermodynamic properties of each state, the electrical output of the system and thermal energy of process. Effect of steam demand, pressure of high pressure steam drum and pinch point on performance assessment parameters are also discussed.

In the analyses, processes are considered to be steady state steady flow. Additionally, kinetic and potential energy effects are ignored. For ideal gases, formulations in Appendix A are used which take into account the variation of enthalpy and absolute entropy with temperature for various substances. For water, steam tables at [9] are used.

3.2 ENERGY BALANCES

Since case-3 is the most complex configuration among the case studies, its energy balances are presented in this section. Equations for other cases may be written in similar way.

Energy balances for gas turbine system are given in Appendix C.

HRSG temperature profile for case-1 and case-2 is given in Figure 4. That for case-3 is given in Figure 5. In these figures, pinch point is defined as the difference between the temperature of exhaust gas exiting the evaporator and saturation temperature of

the steam corresponding to the related pressure level. Approach temperature is defined as the difference between the saturation temperature and water temperature entering evaporator. In these figures, a and b denote gas side and water side states, respectively. Some states within HRSG may correspond to states represented by numerical numbers in Figures 1-3; i.e. states a1, a8, b12 in Figure 5 correspond to 3, 4 and 5 in Figure 3, respectively.

From Figure 5, mass flow rate of the steam generated at the HP steam drum is calculated by applying an energy balance for the control volume around the HP evaporator and the HP superheater stages.

$$\dot{m}_5 = \dot{m}_3 \cdot \left[(1 - HL) \cdot (h_{a1} - h_{a4}) / (h_{b12} - h_{b8})\right] \quad (1)$$

Mass flow rate of saturated steam generated at the IP steam drum is calculated by using an energy balance for the control volume around the IP evaporator.

$$\dot{m}_8 = \dot{m}_3 \cdot \left[(1 - HL) \cdot (h_{a5} - h_{a6}) / (h_{b6} - h_{b4})\right] \quad (2)$$

where h_{a5} is calculated from an energy balance for the control volume around the HP 2nd economizer:

$$h_{a5} = h_{a4} - \left[\dot{m}_5 \cdot (h_{b8} - h_{b7})\right] / \left[(1 - HL) \cdot \dot{m}_3\right] \quad (3)$$

Stack gas should be calculated due to corrosion considerations. From the energy balance for the control volume around the LP evaporator, we have

$$h_{a8} = h_{a7} - \left[\dot{m}_{24} \cdot (h_{b2} - h_{b1})\right] / \left[(1 - HL) \cdot \dot{m}_3\right] \quad (4)$$

where h_{a7} is calculated from the energy balance for the control volume around the HP 1st economizer and the IP economizer, $\dot{m}_{24}$ may be calculated from an energy

balance for the control volume around the deaerator as follows. It should be noted that a single temperature profile is assumed at this section of HRSG.

$$h_{a7} = h_{a6} - \left[(\dot{m}_5 + \dot{m}_8)\cdot(h_{b4} - h_{b3})\right] / \left[(1 - HL)\cdot \dot{m}_3\right] \quad (5)$$

$$\dot{m}_{24} = \dot{m}_{14}\cdot(h_{b1} - h_{14})/(h_{b2} - h_{b1}) \quad (6)$$

After calculating h_{a8}, T_{a8} is calculated by iteration. It should be checked whether stack gas temperature is greater than 400 K.

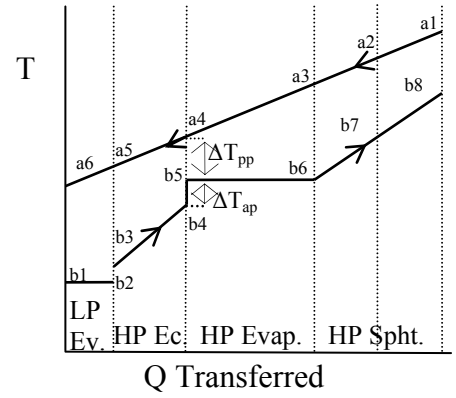

Figure 4: HRSG Temperature Profile for Case-1 and Case-2

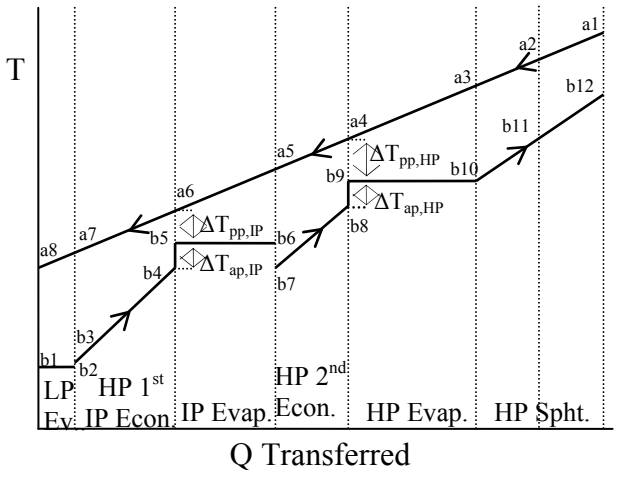

Figure 5: HRSG Temperature Profile for Case-3

Enthalpy of states 6 and 7 may be written as

$$h_6 = h_5 - \eta_{st} \cdot (h_5 - h_{6s}) \quad (7)$$

$$h_7 = h_5 - \eta_{st} \cdot (h_5 - h_{7s}) \quad (8)$$

From energy balances for the control volumes around desuperheater and between points 6, 8 and 9, mass flow rate of 9 may be written as

$$\dot{m}_9 = \left[\dot{m}_{10} \cdot (h_{10} - h_{20}) + \dot{m}_8 \cdot (h_6 - h_8)\right] / (h_6 - h_{20}) \quad (9)$$

Enthalpy of state 12 may be written as

$$h_{12} = h_{11} + v_{11} \cdot (P_{12} - P_{11}) / \eta_p \quad (10)$$

Enthalpy of states 18 and 19 may be written similar to Equation (10).

Enthalpy of states of 9 and 14 may be given as

$$h_9 = (\dot{m}_6 \cdot h_6 + \dot{m}_8 \cdot h_8) / \dot{m}_9 \quad (11)$$

$$h_{14} = (\dot{m}_{12} \cdot h_{12} + \dot{m}_{13} \cdot h_{13}) / \dot{m}_{14} \quad (12)$$

Mass flow rate of cooling water may be written by using an energy balance for the control volume around condenser

$$\dot{m}_{22} = \dot{m}_7 \cdot (h_7 - h_{11}) / (h_{23} - h_{22}) \quad (13)$$

Mass flow rate and enthalpy of other states may be written with respect to the results of Equations (1-13). Entropy of the states which have substance as water may be found from steam tables by using two thermodynamic properties; i.e. pressure and temperature or pressure and enthalpy.

Electrical output of steam turbine (State B) is given as

$$(\dot{W}_{el})_{ST} = (\dot{m}_5 \cdot h_5 - \dot{m}_6 \cdot h_6 - \dot{m}_7 \cdot h_7) \cdot \eta_{gen} \quad (14)$$

Electrical input needed for condensate pump (State C) is given as

$$(\dot{W}_{el})_{con.pump} = \dot{m}_{11} \cdot (h_{12} - h_{11}) \quad (15)$$

Electrical input needed for other pumps may be written similarly. If other consumptions are ignored, total power consumption of the plant is the summation of electrical inputs to the pumps. Bottoming cycle power output may be given as

$$\dot{W}_{bottoming} = (\dot{W}_{el})_{ST} - (\dot{W}_{el})_{consumption} \quad (16)$$

Hence, net power output of the plant may be given as

$$(\dot{W}_{net})_{plant} = \dot{W}_{GT} + \dot{W}_{bottoming} \quad (17)$$

Enthalpy difference of the process may be given as

$$\Delta\dot{H}_{process} = \dot{m}_{10} \cdot (h_{10} - h_{13}) \quad (18)$$

3.3. PERFORMANCE ASSESSMENT PARAMETERS

There are several performance assessment parameters of cogeneration systems in literature. Huang (1999) describes ten of these parameters. These are; fuel-utilization efficiency, efficiency of power generation, fuel chargeable to power, power-to-heat ratio, energy saving index, fuel energy saving ratio, fuel saving rate, second law efficiency, economic efficiency and PURPA efficiency.

Among these parameters, fuel utilization efficiency is the most widely used parameter. However, power-to-heat ratio and second-law efficiency (exergetic efficiency) are stated to be the most useful parameters by Huang. Moreover, exergetic efficiency is the most meaningful and logical parameter. Exergetic efficiency is discussed in Section 4.5.

Only energy accounting is considered in fuel utilization efficiency. Its definition may be given as

$$FUE = \frac{(\dot{W}_{net})_{plant} + \Delta\dot{H}_{process}}{\dot{m}_{fuel} \cdot LHV} \tag{19}$$

The cost effectiveness of a cogeneration system is directly related to the amount of electric power it can produce for a given amount of process heat. Hence, power-to-heat ratio becomes one of the key parameters in cogeneration systems. Its definition may be given as

$$PHR = \frac{(\dot{W}_{net})_{plant}}{\Delta\dot{H}_{process}} \tag{20}$$

3.4 RESULTS OF ENERGY ANALYSIS

Energy balances are applied to case studies for the operation data given in Table 1. The results of these balances and performance assessment parameters are given below. Since cogeneration systems are required to be able to cope efficiently with their steam demand change [18], the results are given for different process steam demands. It is assumed that steam demand changes between 2 and 10 kg/s.

Calculations for thermodynamic properties of ideal gases are accomplished by the help of MathCAD 7 Professional. Formulations given in Appendix A are arranged

according to the required format of that software. Microsoft® Office Excel 2003 is used to cope with different situations of the case studies.

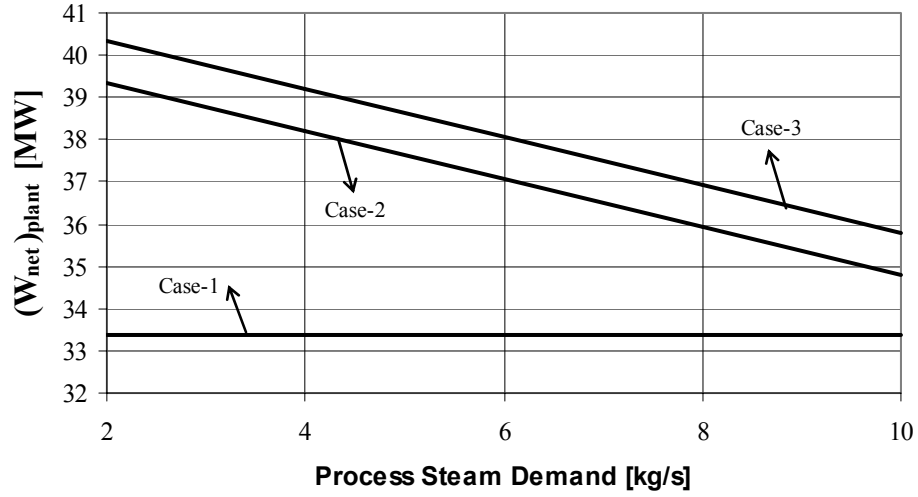

Figure 6: Change of Net Power Output of Plant with Process Steam Demand

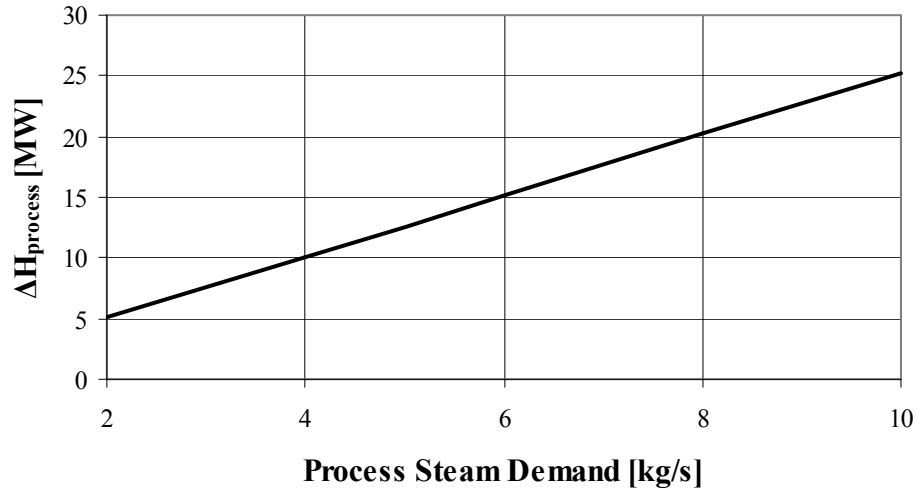

Figure 7: Change of Enthalpy Difference Rate of Process with Process Steam Demand

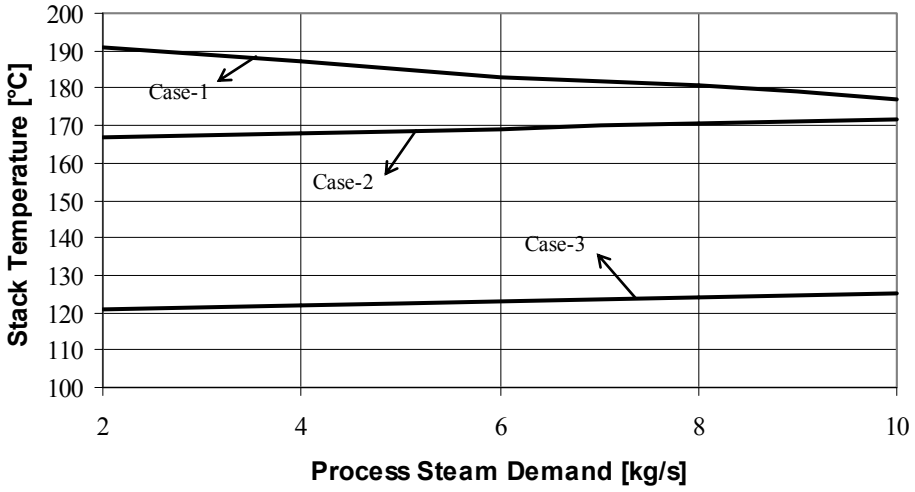

Figure 8: Change of Stack Temperature with Process Steam Demand

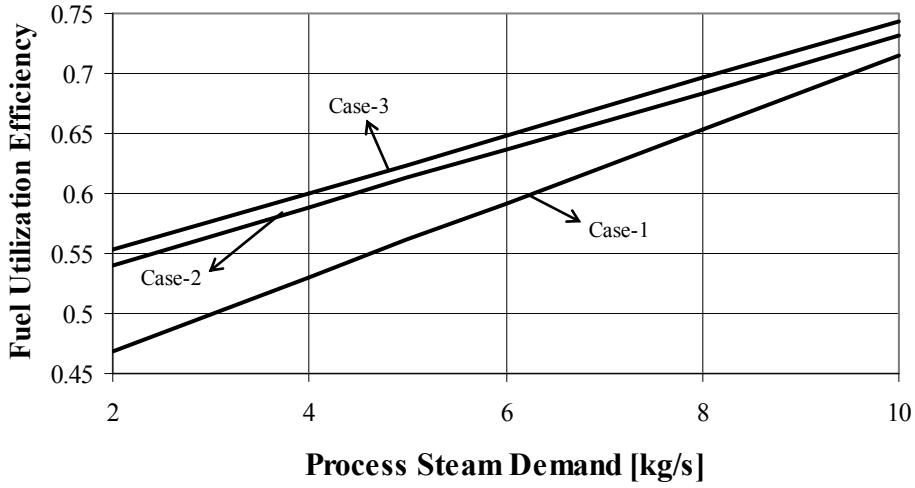

Figure 9: Change of Fuel Utilization Efficiency with Process Steam Demand

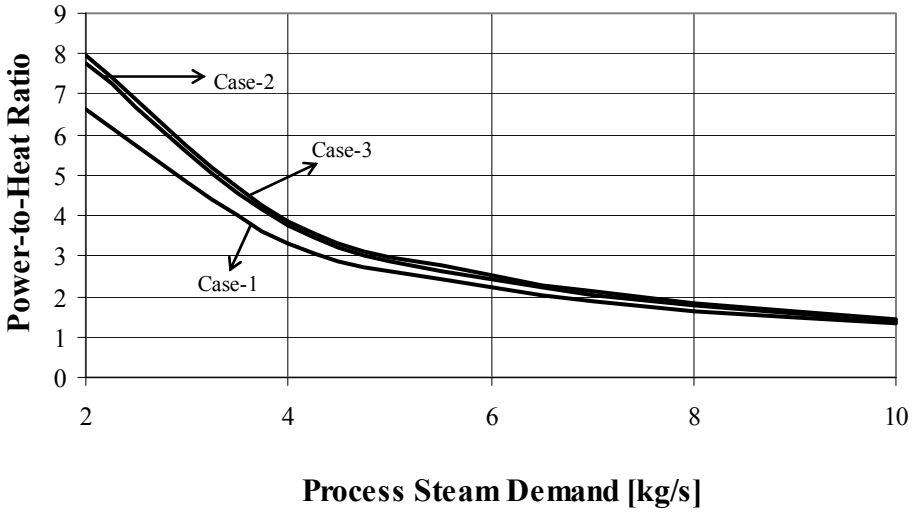

Figure 10: Change of Power-to-Heat Ratio with Process Steam Demand

After several energy balances in HRSG, steam mass flow rate generated at the steam drums are calculated. Hence, it is found that in each of the cases, 11.1 kg/s steam is produced at the HP steam drums. In the third case, 1.78 kg/s steam is produced at the IP steam drum. Steam generated at the LP drums change with steam demand. It changes between 0.257 kg/s and 0.858 kg/s, 1.310 kg/s and 1.107 kg/s, 1.505 kg/s and 1.302 kg/s for case-1, case-2 and case-3, respectively, as steam demand changes between 2 kg/s and 10 kg/s.

Electrical output of steam turbine does not change with steam demand in case-1. However, bottoming cycle electrical output changes very slightly due to variations in electrical inputs to pumps. Nevertheless, this change is so little that it is not noticeable in Figure 6. Additionally, this case has the lowest electricity production because of the high exit pressure of steam turbine. For cases 2 and 3, the electrical output of steam turbine decreases as steam demand increases. For the same steam demand, case-3 has a higher electrical output because extraction of steam from steam turbine is less in this case due to steam going to process from the IP steam drum. Since the power output of gas turbine is fixed for all cases, the trend of change of bottoming cycle electrical output with steam demand is same as Figure 6. Its values

may be found by subtracting the value of gas turbine output (30 MW) from the values given in Figure 6.

For all the cases, process steam and condensate return from process conditions, i.e. temperature and pressure, are taken as same. Hence, for the same steam demand, all cases have the same enthalpy difference rate of process, which is shown in Figure 7.

Stack temperature changes with steam demand in a small range as can be seen from Figure 8. Average stack temperatures for the case-1, case-2 and case-3 are 184°C, 169 °C and 123 °C, respectively. A higher stack temperature means a higher energy loss from stack and more air pollution. Hence, case-3 is more advantageous in terms of energy savings and environmental considerations. However, for this case, the stack gas temperature is very near to the limit for corrosion considerations. If needed, a little amount of steam may be extracted from HP steam drum in case-1 and case-2, and IP steam drum in case-3 as shown in Figures 1-3.

Trend of fuel utilization efficiency and power-to-heat ratio can be seen from Figures 9 and 10. FUE increases whereas PHR decreases as steam demand increases. Case-3 has the highest FUE and PHR for a given steam demand; case-2 and case-1 follow it, respectively. For higher steam demands, FUE and PHR of case-1 get closer to those of case-2 and case-3 due to the fact that $(\dot{W}_{net})_{plant}$ for case-2 and case-3 decreases as steam demand increases while $(\dot{W}_{net})_{plant}$ for case-1 changes very slightly.

Effects of some important parameters of operating data given in Table 1 are discussed below.

In unfired HRSGs, characteristically, steam conditions range from 10.3 bars saturated to approximately 100 bars, 510 °C. Steam temperatures are usually 10 °C or more below the turbine exhaust gas temperature [31]. Due to these facts, a study has been carried out to investigate the effect of HP steam drum pressure. Its effect on fuel utilization efficiency for each case for the same process steam demand are given

in Figure 11. Its effect on power-to-heat ratio is similar to Figure 11, because enthalpy difference of process is same for same steam demand for different HP steam drum pressures. Hence, both of the performance assessment parameters are proportional to net power output of the plant. When Figure 11 is observed, it is seen that trend is different for each cases. For case-1, as HP steam drum pressure increases, FUE sharply decreases and then increases slightly. For case-2, it changes in a small range. For case-3, it increases as HP steam drum pressure increases.

Another important parameter in HRSG design is pinch point. It is clear that lowering the pinch point increases the heat recovery. However this increases the cost of the HRSG. Effect of pinch point on fuel utilization efficiency is given in Figure 12. It may be seen that as pinch point increases, FUE decreases for each case as expected. The trend of PHR is similar to this figure due to the reasons explained in the above paragraph.

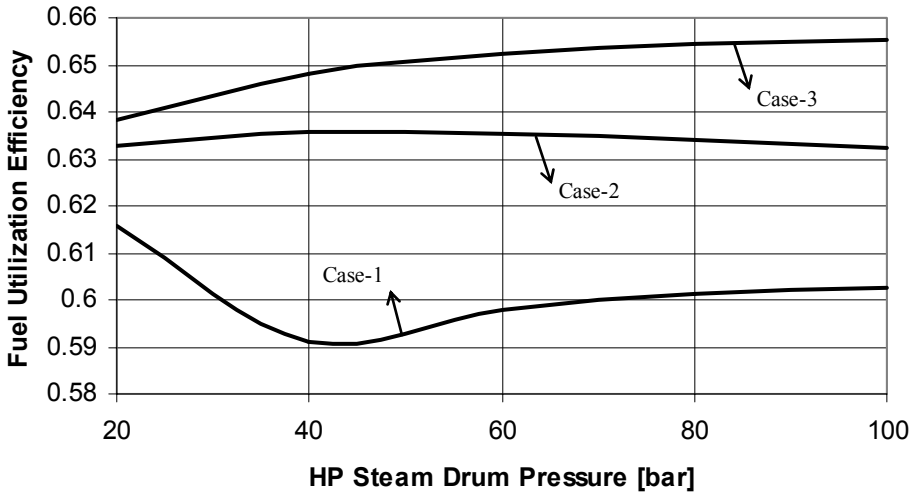

Figure 11: Change of Fuel Utilization Efficiency with HP Steam Drum Pressure for 6 kg/s Steam Demand

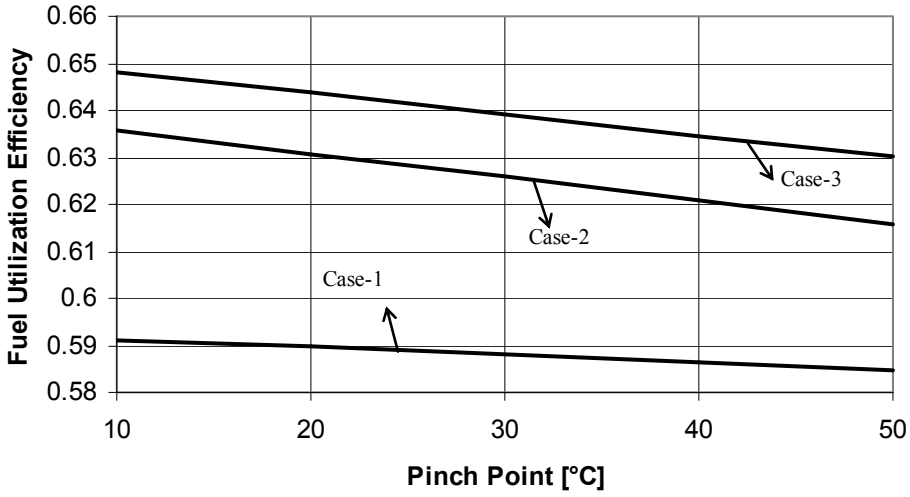

Figure 12: Change of Fuel Utilization Efficiency with Pinch Point for 6 kg/s Steam Demand

CHAPTER 4

EXERGY ANALYSIS

4.1 INTRODUCTION

Exergy is defined as the maximum work that may be achieved by bringing a system into equilibrium with its environment. Every system not in equilibrium with its environment has some quantity of exergy, while a system that is in equilibrium with its environment has, by definition, zero exergy since it has no ability to do work with respect to its environment. [14]

Exergy analysis is a method that uses the conservation of mass and conservation of energy principles together with the second law of thermodynamics for the analysis, design and improvement of energy systems. The exergy method is a useful tool for furthering the goal of more efficient energy-resource use, for it enables the locations, types, and true magnitudes of wastes and losses to be determined. Many engineers and scientists suggest that the thermodynamic performance of a process is best evaluated by performing an exergy analysis in addition to or in place of conventional energy analysis because exergy analysis appears to provide more insights and to be more useful in furthering efficiency improvement efforts than energy analysis. [30]

4.2 EXERGY COMPONENTS

In the absence of nuclear, magnetic, electrical, and surface tension effects, the total exergy of a system E can be divided into four components: physical exergy E^{PH}, kinetic exergy E^{KN}, potential exergy E^{PT}, and chemical exergy E^{CH} [1]:

$$E = E^{PH} + E^{KN} + E^{PT} + E^{CH} \tag{21}$$

Equation (21) can be expressed on unit-of-mass basis

$$e = e^{PH} + e^{KN} + e^{PT} + e^{CH} \tag{22}$$

Kinetic exergy and potential exergy are as follows

$$e^{KN} = \tfrac{1}{2} \cdot V^2 \tag{23}$$

$$e^{PT} = g \cdot z \tag{24}$$

Physical flow exergy for simple compressible pure substances is given as

$$e^{PH} = (h - h_o) - T_o(s - s_o) \tag{25}$$

In evaluating physical exergy of ideal gases, some special considerations should be taken into account. When an ideal gas mixture containing $H_2O_{(g)}$, is cooled at constant pressure below the dew point temperature, some condensation of the water vapor would occur: Suppose that an ideal gas mixture, at a temperature higher than the dew point temperature, consists of N_2, O_2, and CO_2, and $H_2O_{(g)}$ and their mole fractions are $x_{N_2}, x_{O_2}, x_{CO_2}, x_{H_2O(g)}$, respectively. At atmospheric conditions, the mixture could consist of N_2, O_2, and CO_2, together with saturated water vapor in equilibrium with saturated liquid. The partial pressure of water vapor would be equal to the saturation pressure. The amount of water vapor after condensation process, x_v, can be found as below

$$P_{sat}(T_o) = \frac{x_v}{x_{N_2} + x_{O_2} + x_{CO_2} + x_v} \cdot P_o \tag{26}$$

Rearranging Equation (26);

$$x_v = \frac{(1 - x_{H_2O(g)}) \cdot P_{sat}(T_o)}{P_o - P_{sat}(T_o)} \tag{27}$$

So, the new composition would consist of N_2, O_2, CO_2, $H_2O_{(g)}$ and $H_2O_{(l)}$, with their mole fractions $x_{N_2}, x_{O_2}, x_{CO_2}, x_v$ and $(1 - x_{N_2} - x_{O_2} - x_{CO_2} - x_v)$, respectively.

Then, h_o may be calculated using the new composition as follows

$$h_o = \frac{x_{N_2}\bar{h}_{N_2} + x_{O_2}\bar{h}_{O_2} + x_{CO_2}\bar{h}_{CO_2} + x_v\bar{h}_{H_2O(g)} + (1 - x_{N_2} - x_{O_2} - x_{CO_2} - x_v)\bar{h}_{H_2O(l)}}{M_{mix}} \tag{28}$$

In Equation (28), enthalpy terms are calculated at atmospheric temperature.

The mole fractions of the components of the gas phase are

$$x'_{N_2} = \frac{x_{N_2}}{x_{N_2} + x_{O_2} + x_{CO_2} + x_v} \tag{29}$$

$$x'_{O_2} = \frac{x_{O_2}}{x_{N_2} + x_{O_2} + x_{CO_2} + x_v} \tag{30}$$

The mole fractions of CO_2 and $H_2O_{(g)}$ of the gas phase may be written similarly. The contribution of N_2 to $\bar{s}_o$ is evaluated at T_o and the partial pressure $x'_{N_2} P_o$

$$\bar{s}_{N_2}(T_o, x'_{N_2} \cdot P_o) = \bar{s}^o_{N_2}(T_o) - \bar{R} \cdot \ln \frac{x'_{N_2} \cdot P_o}{P_{ref}} \tag{31}$$

Contributions of other components may be written similarly. Hence, s_o may be calculated using the same composition used in the calculation of h_o, result of Equation (31), similar results of other components and molecular weight of ideal gas mixture.

$$s_o = \frac{x_{N_2}\bar{s}_{N_2} + x_{O_2}\bar{s}_{O_2} + x_{CO_2}\bar{s}_{CO_2} + x_v\bar{s}_{H_2O(g)} + (1 - x_{N_2} - x_{O_2} - x_{CO_2} - x_v)\bar{s}_{H_2O(l)}}{M_{mix}} \tag{32}$$

Chemical exergy is the exergy component associated with the departure of the chemical composition of a system from that of environment. Standard molar chemical exergy tables are available in literature. For example, table at [38] gives values for atmospheric conditions at 298.15 K and 1 atm. Also, table at [37] gives values for that at 298.15 K and 1.019 atm. According to [1], if the environmental conditions of a system is slightly different than the conditions used in these tables, the tables still may be used.

For water, standard chemical exergy tables may be used for standard atmospheric conditions. For other atmospheric conditions, the following formulation may be used:

$$\bar{e}^{CH} = \bar{R} \cdot T_o \cdot \ln \frac{P_{sat}(T_o)}{x_{o,H_2O(g)} \cdot P_o} \tag{33}$$

For an ideal gas mixture, the following formulation may be used:

$$\bar{e}^{CH} = -\bar{R} \cdot T_o \cdot \sum x_k \cdot \ln \frac{x_{o,k}}{x_k} \tag{34}$$

Equation (34) may be expressed as [1]:

$$\bar{e}^{CH} = \sum x_k \cdot \bar{e}_k^{CH} + \bar{R} \cdot T_o \cdot \sum x_k \cdot \ln x_k \tag{35}$$

In cases when the condensation considerations mentioned above are taken into account, x_k term of Equations (34) and (35) should be replaced with x'_k to find the contribution of the gas phase to the chemical exergy. The contribution of water phase

to chemical exergy may be calculated from Equation (33) or tables. Hence, chemical exergy may be calculated by adding these contributions as follows:

$$\bar{e}^{CH} = (x_{N_2} + x_{O_2} + x_{CO_2} + x_v)\cdot \bar{e}^{CH}_{gas} + (1 - x_{N_2} - x_{O_2} - x_{CO_2} - x_v)\cdot \bar{e}^{CH}_{liq} \tag{36}$$

For a hydrocarbon fuel, C_aH_b, standard chemical exergy tables may be used. The most accurate relation for chemical exergy of that fuel can be defined as below [32]

$$\begin{aligned}\bar{e}^{CH}_F = &\left[\bar{h}_F + (a+\frac{b}{4})\cdot\bar{h}_{O_2} - a\cdot\bar{h}_{CO_2} - \frac{b}{2}\cdot\bar{h}_{H_2O(g)}\right](T_o, P_o)\\ &- T_o\cdot\left[\bar{s}_F + (a+\frac{b}{4})\cdot\bar{s}_{O_2} - a\cdot\bar{s}_{CO_2} - \frac{b}{2}\cdot\bar{s}_{H_2O(g)}\right](T_o, P_o)\\ &+ \bar{R}\cdot T_o\cdot\ln\left[\frac{(x_{o,O_2})^{a+b/4}}{(x_{o,CO_2})^a\cdot(x_{o,H_2O(g)})^{b/2}}\right]\end{aligned} \tag{37}$$

An approximate formulation for chemical exergy of gaseous hydrocarbon fuels is given as [33]

$$\frac{\bar{e}^{CH}_F}{LHV} \cong 1.033 + 0.0169\frac{b}{a} - \frac{0.0698}{a} \tag{38}$$

If the fuel is methane, a simpler relation may be given as [4]

$$\frac{\bar{e}^{CH}_F}{HHV} \approx 0.94 \tag{39}$$

4.3 EXERGY BALANCE

The steady state form of control volume exergy balance [1]

$$0 = \sum_j\left(1 - \frac{T_o}{T_j}\right)\cdot\dot{Q}_j - \dot{W}_{cv} + \sum_i \dot{m}_i\cdot e_i - \sum_e \dot{m}_e\cdot e_e - \dot{E}_D \tag{40}$$

The last term in Equation (40), $\dot{E}_D$, is equal to $T_o \cdot \dot{S}_{gen}$ from Guoy-Stodola theorem. Additionally, exergy losses are included in the fourth term of Equation (40).

4.4 EXERGY DESTRUCTION AND EXERGY LOSS

Unlike energy, exergy is not conserved but destroyed by irreversibilities within a system. These irreversibilities may be classified as internal and external irreversibilities. Main sources of internal irreversibilities are friction, unrestrained expansion, mixing and chemical reaction. External irreversibilities arise due to heat transfer through a finite temperature difference. Exergy is lost when the energy associated with a material or energy stream is rejected to the environment.

The rate of exergy destruction in a system component can be compared to the exergy rate of the fuel provided to the overall system, $\dot{E}_{F,tot}$, giving the exergy destruction ratio

$$y_D = \frac{\dot{E}_D}{\dot{E}_{F,tot}} \tag{41}$$

Alternatively, the component exergy destruction rate can be compared to the total exergy destruction rate within the system, $\dot{E}_{D,tot}$ giving the ratio

$$y_D^* = \frac{\dot{E}_D}{\dot{E}_{D,tot}} \tag{42}$$

The exergy loss ratio is defined similarly by comparing the exergy loss to the exergy of the fuel provided to the overall system

$$y_L = \frac{\dot{E}_L}{\dot{E}_{F,tot}} \tag{43}$$

4.5 EXERGETIC EFFICIENCY

In defining the exergetic efficiency, it is necessary to identify both a product and a fuel for the thermodynamic system being analyzed. The product represents the desired result produced by the system. Accordingly, the definition of the product must be consistent with the purpose of purchasing and using the system. The fuel represents the resources expended to generate the product, and is not necessarily restricted to being an actual fuel such as natural gas, oil or coal. Both the product and the fuel are expressed in terms of exergy [1]. Exergetic efficiency of a component or system may be given as

$$\varepsilon = \frac{\dot{E}_P}{\dot{E}_F} = 1 - \frac{\dot{E}_D + \dot{E}_L}{\dot{E}_F} \tag{44}$$

Overall exergetic efficiency of the system can be defined in terms of exergy destruction ratio and exergy loss ratio.

$$\varepsilon = 1 - \sum y_D - \sum y_L \tag{45}$$

4.6 EXERGY ANALYSIS OF CASE STUDIES

Exergy components of each state of the cases shown in Figures 1-3 are calculated for different process steam demands, HP steam drum pressure and pinch point. Kinetic and potential exergy effects are ignored. For physical exergy, Equation (25) is used for water, methane and ideal gas mixtures. For chemical exergy, standard tables are used for water and methane. Equation (35) is used together with tables for chemical exergy of ideal gas mixtures. Additionally, condensation considerations and the related equations due to these considerations which are described in Section 4.2 are used.

Exergy balances and exergetic efficiencies for the components of case-3 are given below. Balances and efficiencies for other cases may be written with similar efforts.

System, shown in Figure 3, is seperated into several subsystems. Exergy balances for the components of the gas turbine are given in Appendix C.

For case 3, for the control volume around HRSG, including deaerator,

$$\dot{E}_{Dest} = (\dot{E}_3 - \dot{E}_4) + (\dot{E}_{18} - \dot{E}_5) + (\dot{E}_{21} - \dot{E}_8) + (\dot{E}_{14} - \dot{E}_{15}) \tag{46}$$

$$\varepsilon = \frac{(\dot{E}_5 - \dot{E}_{18}) + (\dot{E}_8 - \dot{E}_{21}) + (\dot{E}_{15} - \dot{E}_{14})}{(\dot{E}_3 - \dot{E}_4)} \tag{47}$$

It should be noted that exergy transfer due to heat loss from HRSG is taken as zero by considering a large enough control volume so that heat transfer occurs at the ambient temperature. For the control volume around steam turbine, including electric generator

$$\dot{E}_{Dest} = (\dot{E}_5 - \dot{E}_6 - \dot{E}_7) - \dot{E}_B \tag{48}$$

$$\varepsilon = \frac{\dot{E}_B}{(\dot{E}_5 - \dot{E}_6 - \dot{E}_7)} \tag{49}$$

For the control volume around condenser, condensate pump and related junction point,

$$\dot{E}_{Dest} = \dot{E}_7 + \dot{E}_{13} - \dot{E}_{14} + (\dot{E}_{22} - \dot{E}_{23}) + \dot{E}_C \tag{50}$$

There are several discussions to define the exergetic efficiency of condensers in literature. A new definition by the suggestion of Professor Yalçın A. Göğüş is applied to the control volume including condenser, condensate pump and related junction point. This definition is based on the fact that the aim of the condenser is to reject heat.

$$\varepsilon = 1 - \frac{\dot{E}_7 + \dot{E}_{13} - \dot{E}_{14} + (\dot{E}_{22} - \dot{E}_{23}) + \dot{E}_C}{Q_{7\to 11}} \tag{51}$$

For the control volume around desuperheater and the related junction point

$$\dot{E}_{Dest} = \dot{E}_8 + \dot{E}_6 + \dot{E}_{20} - \dot{E}_{10} \tag{52}$$

$$\varepsilon = \frac{\dot{E}_{10}}{\dot{E}_8 + \dot{E}_6 + \dot{E}_{20}} \tag{53}$$

For the control volume around HP BFW pump

$$\dot{E}_{Dest} = (\dot{E}_{16} - \dot{E}_{18}) + \dot{E}_D \tag{54}$$

$$\varepsilon = \frac{\dot{E}_{18} - \dot{E}_{16}}{\dot{E}_D}$$

For the control volume around IP BFW pump

$$\dot{E}_{Dest} = (\dot{E}_{17} - \dot{E}_{19}) + \dot{E}_E \tag{55}$$

$$\varepsilon = \frac{\dot{E}_{19} - \dot{E}_{17}}{\dot{E}_E} \tag{56}$$

In the case studies, exergy rate of stream exiting HRSG and exergy rate difference of condenser cooling water inlet and outlet streams are exergy losses. The exergy loss due to heat loss in the gas turbine and the HRSG may be taken as zero by considering large enough control volume, so that heat loss occurs at the ambient temperature.

Exergetic efficiency of the plants for the case studies may be given as

$$\varepsilon_{plant} = \frac{(\dot{W}_{net})_{plant} + \Delta\dot{E}_{process}}{\dot{E}_f} \quad (57)$$

4.6.1 Results of Exergy Analysis of Case Studies

To illustrate, values of exergy components, exergy destructions, exergy losses and the relevant ratios for one of the conditions, i.e. case-3 for operating data given in Table 1 and 6 kg/s steam demand, are tabulated in Table 2. Other results are shown with figures in this section.

The exergy destruction in the gas turbine system, which is equal to 33242.30 kW, remains constant with the change of steam demand, HP steam drum pressure and pinch point. Hence, this is not shown in the figures. Additionally, this destruction has the largest magnitude of all cases. The destructions inside the gas turbine system are shown in Table C.4 and Figure C.2.

Figure 13 shows that as steam demand increases exergetic efficiency of the plant increases for each cases. For a given steam demand, case-3 has the highest efficiency, and case-2 and case-1 follow it, respectively. Figures 14-17 highlight the reasons of the changes in Figure-13. For example, the reason for low exergetic efficiency in case-1 is, mainly, the high exergy destruction in dump condenser and also, the high total exergy loss. For case-1, at low demands, y_D^* for dump condenser is the highest, whereas, at high demands, y_D^* for HRSG is the highest among the bottoming cycle components. The destruction in HRSG and steam turbine is lower in case-1 when compared to other cases. For case-2 and case-3, the exergy destruction in HRSG is the highest among the bottoming cycle components, steam turbine, condenser, desuperheater and BFW pumps follow it, respectively. It may also seen that, the main reason of having a higher exergetic efficiency for case-3 than case-2 is that the total exergy loss in case-3 is considerably lower than case-2. On the other hand, in all cases, exergy destruction in desuperheater and BFW pumps are very low and their effect are unnoticeable.

Table 2: Exergy components for 6 kg/s steam demand for Case-3

State	Substance	$\dot{m}$ [kg/s]	P (kPa)	T (°C)	$\dot{E}_{PH}$ [kW]	$\dot{E}_{CH}$ [kW]	$\dot{E}$ [kW]
1	Air	91.276	101.33	25.00	0.00	0.00	0.00
2	Fuel	1.642	1200.00	25.00	627.10	84366.80	84993.90
3	Comb.Gases	92.918	106.66	506.63	21385.10	366.50	21751.60
4	Comb.Gases	92.918	101.33	123.00	1599.59	366.50	1966.09
5	Water	11.087	4000.00	475.00	14429.35	27.69	14457.04
6	Water	3.747	1000.00	309.03	3528.65	9.36	3538.01
7	Water	7.340	7.00	38.97	753.01	18.34	771.34
8	Water	1.785	1000.00	179.91	1461.75	4.46	1466.21
9	Water	5.532	1000.00	265.43	4966.88	13.82	4980.69
10	Water	6.000	1000.00	179.91	4913.97	14.99	4928.96
11	Water	7.340	7.00	38.97	9.94	18.34	28.27
12	Water	7.340	120.00	39.01	9.89	18.34	28.22
13	Water	6.000	120.00	60.00	47.81	14.99	62.80
14	Water	13.340	120.00	48.45	49.09	33.32	82.42
15	Water	13.340	120.00	104.72	509.81	33.32	543.13
16	Water	11.087	120.00	104.72	423.70	27.69	451.39
17	Water	2.253	120.00	104.72	86.11	5.63	91.74
18	Water	11.087	4000.00	105.93	435.37	27.69	463.07
19	Water	2.253	1000.00	105.00	86.62	5.63	92.25
20	Water	0.468	1000.00	105.00	18.01	1.17	19.18
21	Water	1.785	1000.00	105.00	68.61	4.46	73.07
22	Water	396.290	101.33	25.00	0.00	989.90	989.90
23	Water	396.290	101.33	35.00	271.50	989.90	1261.41
24	Water	1.403	120.00	104.72	718.26	3.51	721.77

State	A	B	C	D	E	F
$\dot{E}$ [kW]	30000	8127.03	1.05	56.30	2.60	8067.09

Table 3: Exergy Destruction, Its Relevant Ratios and Exergetic Efficiency of Subsystems for 6 kg/s Steam Demand for Case-3

Component	$\dot{E}_D$ [kW]	y_D^*	y_D	ε
Gas turbine system	33242.30	0.8348	0.3911	0.6089
HRSG and deaerator	3937.68	0.0989	0.0463	0.8010
Steam Turbine and its electric generator	2020.67	0.0507	0.0238	0.8009
Condenser, condensate pump and junction point	481.26	0.0121	0.0057	0.9709
Desuperheater and junction point	94.44	0.0024	0.0011	0.9812
HP BFW pump	44.63	0.0011	0.0005	0.2074
IP BFW pump	2.08	0.0001	0.0000	0.1975
Overall Plant	39823.06	1.0000	0.4685	0.5051

Table 4: Exergy Loss and Its Relevant Ratio of Streams for 6 kg/s Steam Demand for Case-3

Exergy Loss		
Stream	$\dot{E}_L$ [kW]	y_L
Stack gas	1966.09	0.0231
Condenser cooling water	271.50	0.0032
Overall plant	2237.59	0.0263

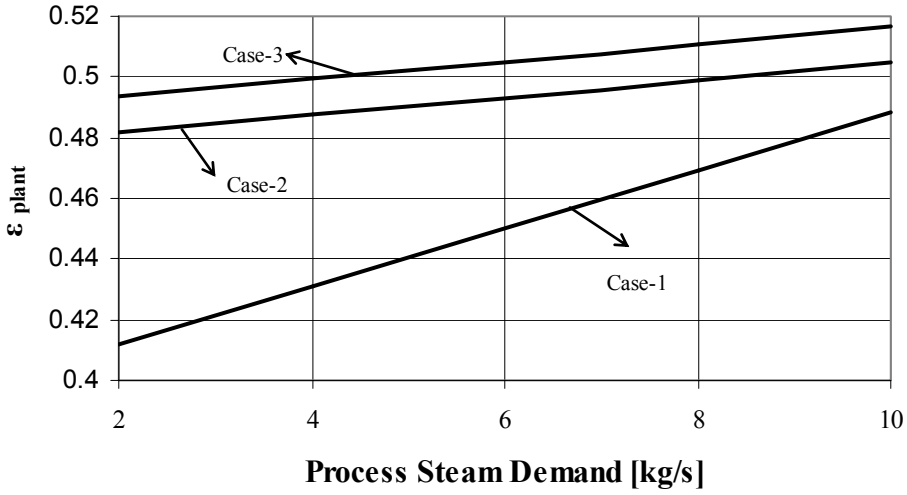

Figure 13: Change of Exergetic Efficiency of the Plant with Process Steam Demand

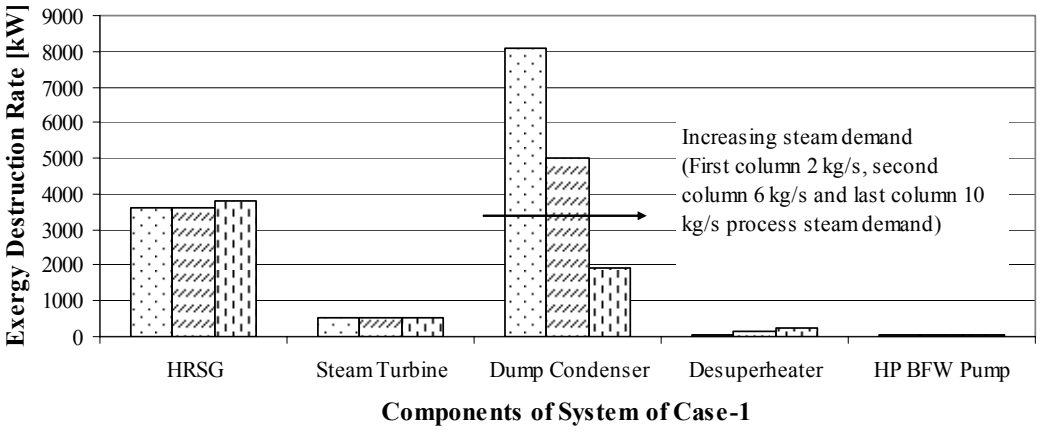

Figure 14: Exergy Destruction Rates in Case-1 for Different Steam Demands

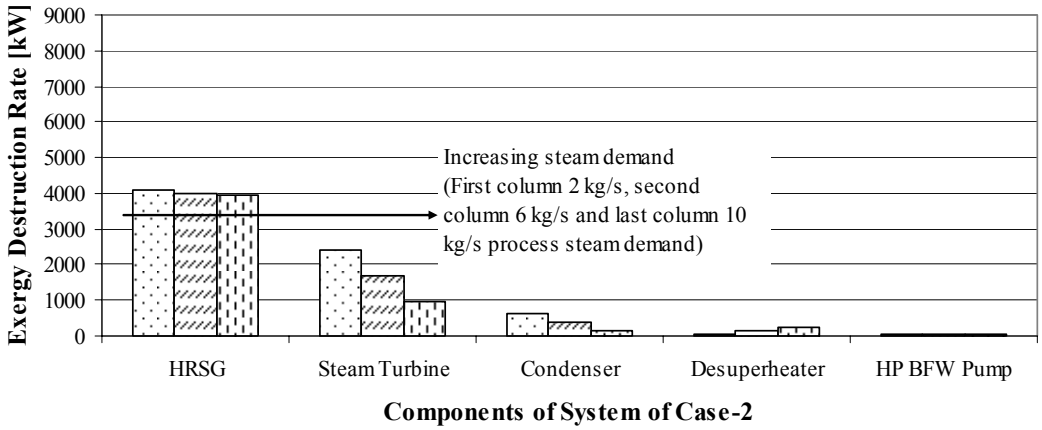

Figure 15: Exergy Destruction Rates in Case-2 for Different Steam Demands

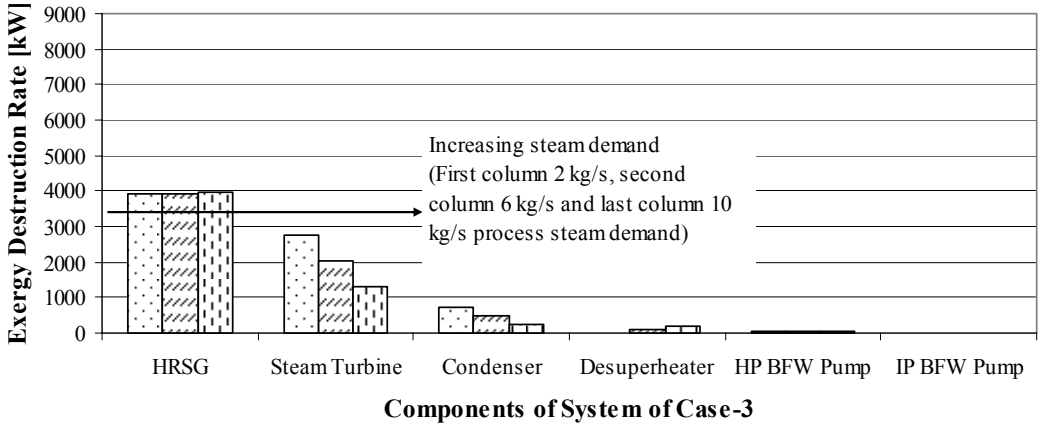

Figure 16: Exergy Destruction Rates in Case-3 for Different Steam Demands

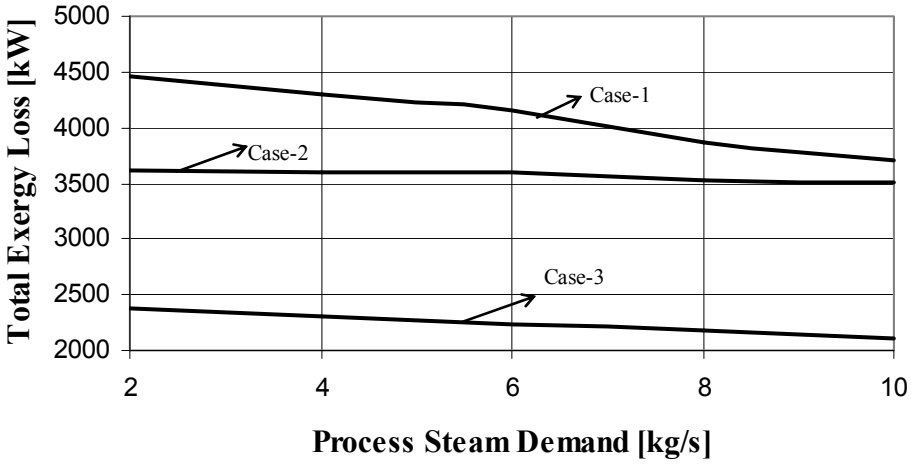

Figure 17: Change of Total Exergy Loss in Cases with Process Steam Demand

The effect of HP steam drum pressure is discussed below.

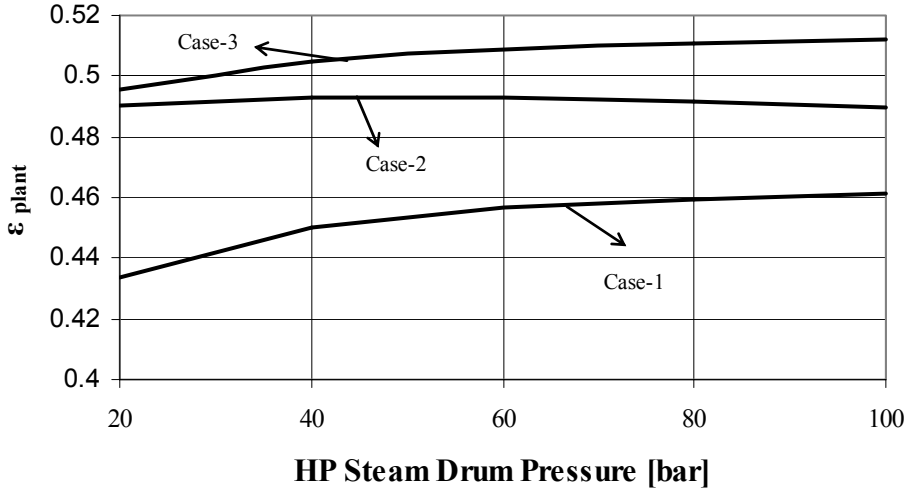

Figure 18: Change of Exergetic Efficiency of the Plant in Cases with HP Steam Drum Pressure at 6 kg/s Steam Demand

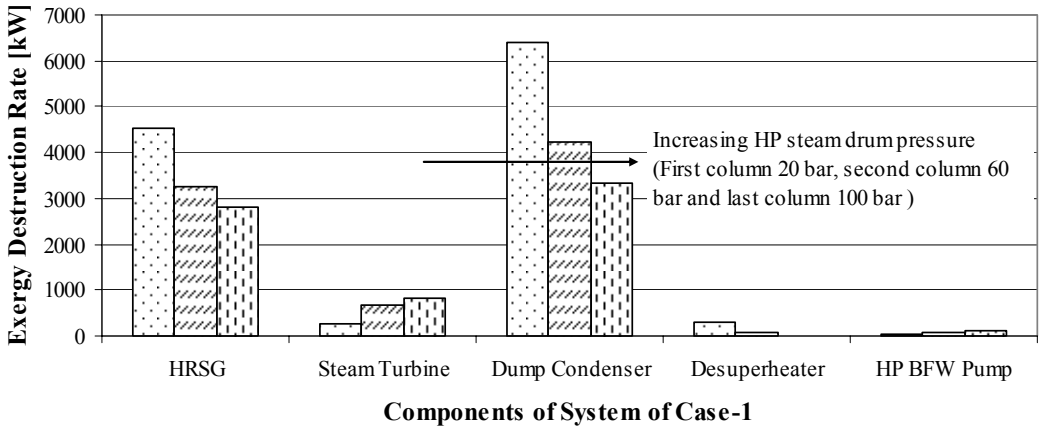

Figure 19: Exergy Destruction Rates in Case-1 for Different HP Steam Drum Pressure at 6 kg/s Steam Demand

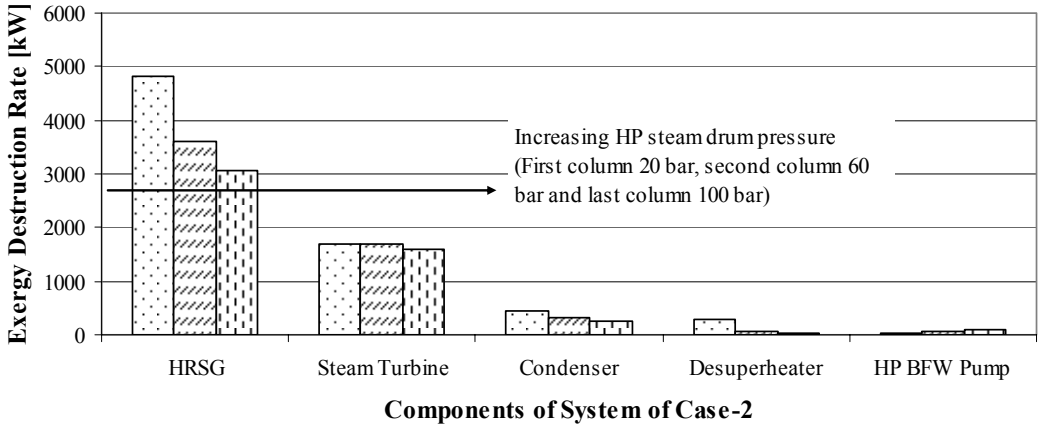

Figure 20: Exergy Destruction Rates in Case-2 for Different HP Steam Drum Pressure at 6 kg/s Steam Demand

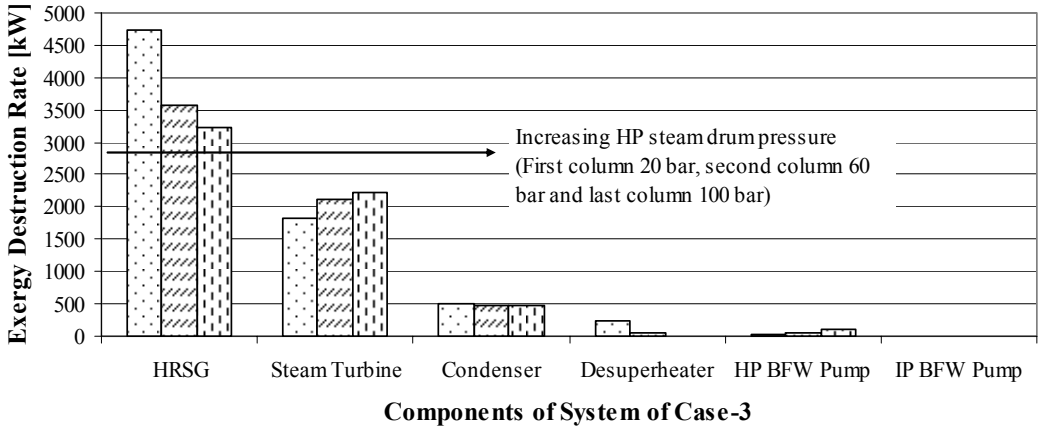

Figure 21: Exergy Destruction Rates in Case-3 for Different HP Steam Drum Pressure at 6 kg/s Steam Demand

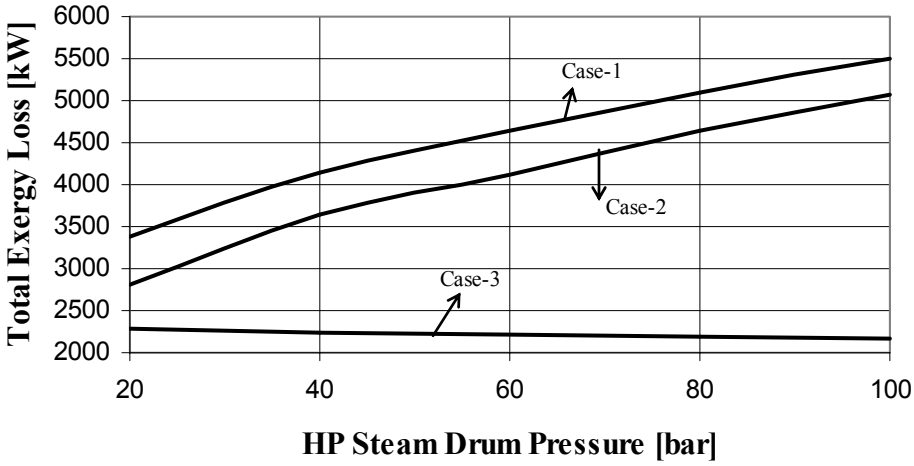

Figure 22: Change of Total Exergy Loss in Cases with HP Steam Drum Pressure at 6 kg/s Steam Demand

Figure 18 shows that, exergetic efficiency of case-1 and case-3 increases with HP steam drum pressure, whereas that of case-2 is not very sensitive to HP steam drum pressure. In all cases, the exergy destruction in HRSG, dump condenser or condenser and desuperheater decreases, whereas exergy destruction in BFW pumps increase as

HP steam drum pressure increases. For steam turbine, exergy destruction in case-1 and case-3 increases whereas that in case-2 decreases as HP steam drum pressure increases. When Figure 22 is observed, exergy loss in case-1 is the highest and that in case-2 and case-3 follow it, respectively, for a given HP steam drum pressure. It may also be seen that exergy loss in case-3 is not very sensitive to HP steam drum pressure, whereas that in case-1 and case-2 increase.

The effect of pinch point is discussed below.

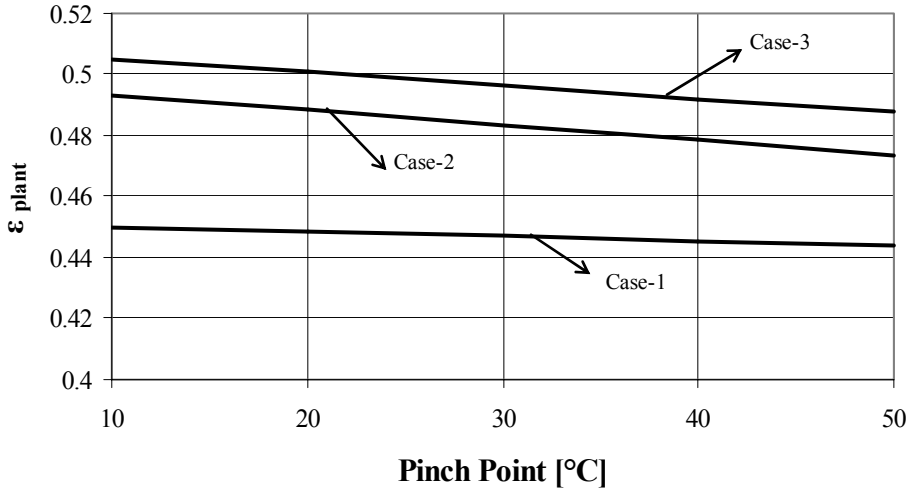

Figure 23: Change of Exergetic Efficiency of the Plant in Cases with Pinch Point at 6 kg/s Steam Demand

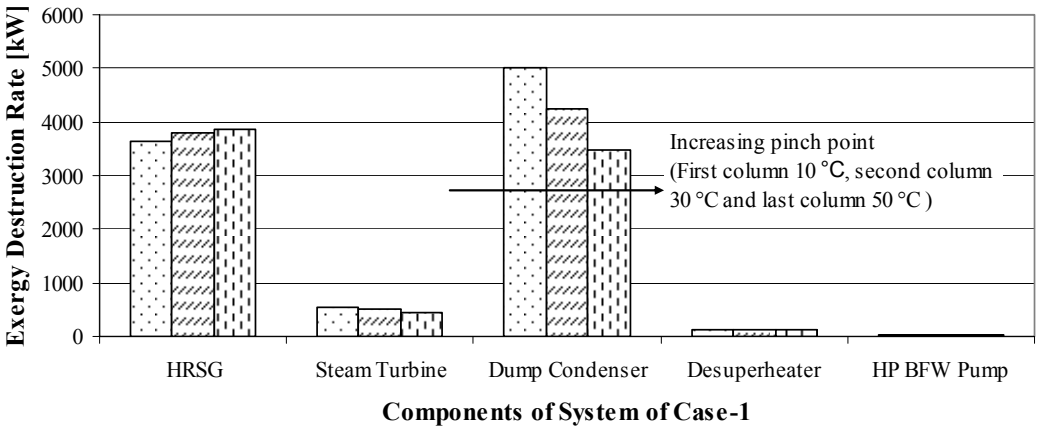

Figure 24: Exergy Destruction Rates in Case-1 for Different Pinch Point at 6 kg/s Steam Demand

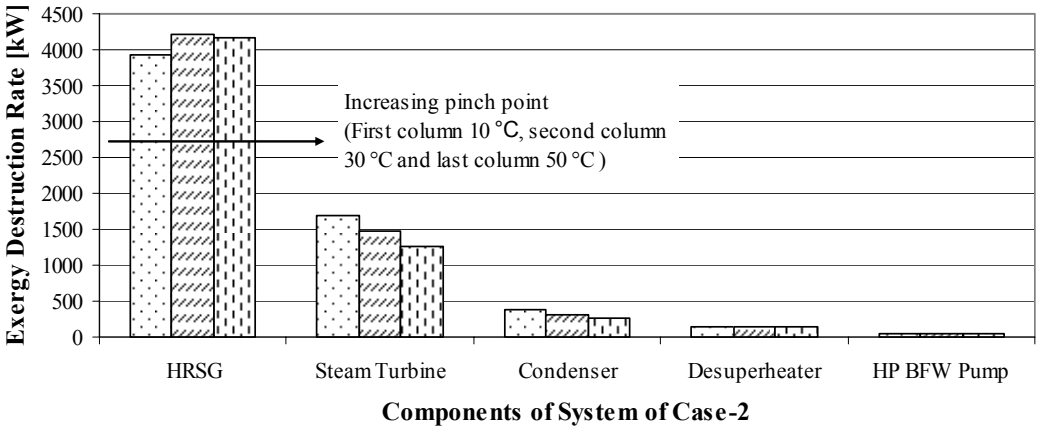

Figure 25: Exergy Destruction Rates in Case-2 for Different Pinch Point at 6 kg/s Steam Demand

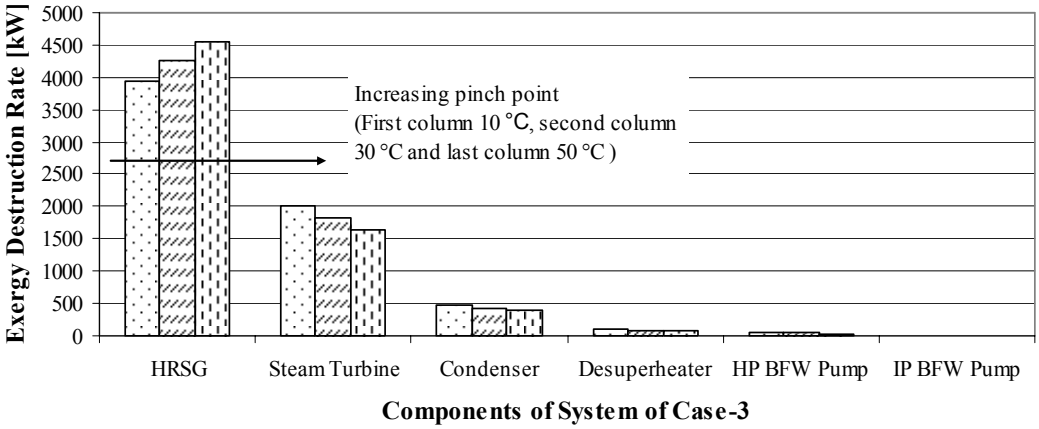

Figure 26: Exergy Destruction Rates in Case-3 for Different Pinch Point at 6 kg/s Steam Demand

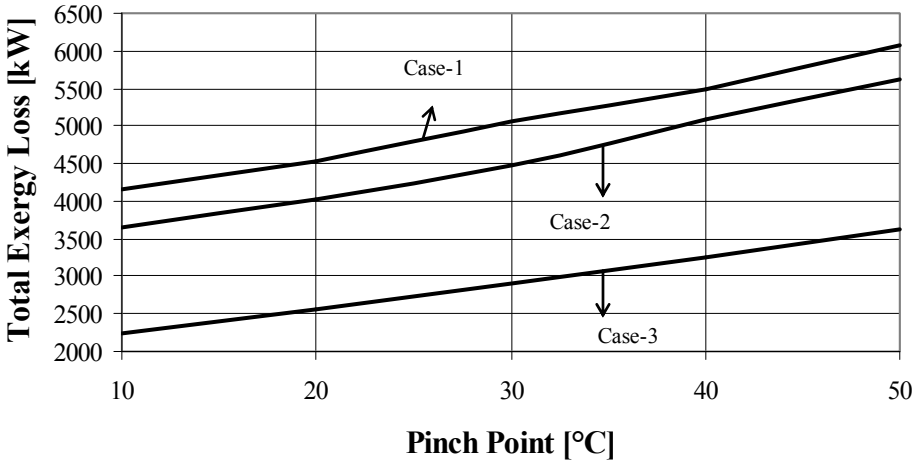

Figure 27: Change of Total Exergy Loss in Cases with Pinch Point at 6 kg/s Steam Demand

Pinch point effects the temperature of some states inside HRSG. As a result of this effect, the mass flow rate of steam generated at the drums, and stack temperature change. Hence, exergy flow rates of the states change. When Figure 23 is observed, it may be seen that exergetic efficiency of each state decreases, whereas total exergy loss increases as pinch point increases, as expected. From Figures 24-26, the exergy destruction within bottoming cycle components may be investigated. It is seen that exergy destruction in HRSG increases as pinch point increases in case-1 and case-3. However, exergy desruction in HRSG in case-2 increases, then decreases as pinch point increases. Exergy destruction in steam turbine, dump condenser or condenser for all cases decrease as pinch point increases. The effect of exergy destruction in remaining components is not very significant.

CHAPTER 5

THERMOECONOMIC ANALYSIS

5.1 INTRODUCTION

Thermoeconomics combines exergy analysis and economic principles to provide the system designer or operator with information not available through conventional energy analysis and economic evaluations, but crucial to the design and operation of a cost-effective system. Thermoeconomics can be considered as exergy-aided cost minimization. The objective of a thermoeconomic analysis might be: (a) to calculate separately the cost of each product generated by a system having more than one product; (b) to understand the cost formation process and the flow of costs in the system; (c) to optimize specific variables in a single component; or (d) to optimize the overall system. [21]

The aim of the thermoeconomic analysis in this thesis is to calculate the cost of each product of the systems and investigate the cost formation process in the systems.

5.2 HISTORY OF THERMOECONOMICS

In the 60'es, Wolfgang Fratscher, Jan Szargut and Valeriy Brodyanskii published their first papers on the "economic value of the concept of exergy". Then, Myron Tribus, Yehia El-Sayed and Robert Evans published a series of papers on a mathematical cost-optimization procedure based on "availability". The name "Thermo-Economics" made its first appearance in Tribus' MIT course notes of 1960 and in Evans' doctoral thesis of 1961. The concept was well developed in academic circles thanks to the efforts of Yehia El-Sayed, Richard Gaggioli, Tadeusz Kotas and

Michael Moran in the early 80's and of Antonio Valero and George Tsatsaronis in the late 80'es. Valero, in a series of papers in 1986-89, derived a general and completely formalized costing theory to calculate the exergetic cost of a product from the exergetic input into the process and the structure of the production process. In the 90'es, Thermo-Economics was extended (mostly by Christos Frangopoulos and Michael Von Spakovsky) by adapting it to off-design conditions and time-dependent problems and by including environmental effects. In more recent years, the literature on thermoeconomics is abundant. [20]

Essentially, there are two thermoeconomic techniques proposed in literature: the Thermoeconomic Functional Analysis (T.F.A.) and the Exergetic Cost Theory. The first, proposed by El-Sayed and Evans (1970) and El-Sayed and Tribus (1983) and subsequently developed by Frangopoulos (1983, 1991, 1992) and Von Spakovsky and Evans (1990, 1993), is an optimization methodology that provides marginal costs. The second, introduced by Tsatsaronis and Winhold (1985) and then developed by Valero et al. (1986), is a cost accounting methodology, which provides average costs. [19]

Among the different approaches in literature, SPECO method [3, 36] is used in this study. The basic principle of the SPECO method is initially suggested by Tsatsaronis and Lin (1990). Then, it is developed by Tsatsaronis and his coworkers.

5.3 SPECO METHOD

Specific exergy costing method (SPECO) consists of the following three steps. [3]

First step is the identification of exergy streams. All material and energy streams crossing the boundaries of the components being considered should be first identified. This is accomplished by inspection of the process flow diagram. The exergy streams associated with the entering and exiting material and energy streams are known from the exergy analysis. At this point, a decision must be made with respect to whether the analysis of the components should be conducted using total

exergy or separate forms of the total exergy of a material stream. Considering separate exergy forms usually improves the accuracy of the results. However, this improvement is often marginal and not necessary for extracting the main conclusions from the thermoeconomic evaluation.

Second step is the definition of fuel and product. In evaluating the performance of a component it is, in general, meaningful and appropriate to operate with exergy differences associated with each material stream between inlet and outlet. For example, in defining the product of a heat exchanger operating above ambient temperature we consider only the exergy addition to the cold stream and not the sum of the exergies associated with material streams at the outlet. Similarly, for defining the fuel of a heat exchanger we consider only the exergy removal from the hot stream and not the sum of the exergies associated with the material streams at the inlet. Exergy differences (exergy additions to or removals from a stream) should be applied to all exergy streams associated with a change of physical exergy and to some exergy streams associated with the conversion of chemical exergy. In many cases involving conversion of chemical exergy (e.g., conversion of the chemical exergy of a solid fuel in to chemical and thermal exergy through a gasification process), the purpose of owning and operating the component dictates that the chemical exergy at the outlet is considered on the product side and the chemical exergy at the inlet on fuel side.

Third step is writing the cost balances and auxiliary equations. Exergy costing usually involves cost balances formulated for each system component separately. A cost balance applied to the kth component shows that the sum of cost rates associated with all exiting exergy streams equals the sum of cost rates of all entering exergy streams plus the appropriate charges due to capital investment ($\dot{Z}_k^{CI}$) and operating and maintenance expenses ($\dot{Z}_k^{OM}$). The sum of the last two terms is denoted by $\dot{Z}_k$

$$\dot{Z}_k = \dot{Z}_k^{CI} + \dot{Z}_k^{OM} \tag{53}$$

The steady-state form of control volume cost balance is

$$\sum_{j=1}^{n} \dot{C}_{j,k,in} + \dot{Z}_k = \sum_{j=1}^{m} \dot{C}_{j,k,out} \tag{54}$$

Equation (54) states that the total cost of the exiting exergy streams equals to the total expenditure to obtain them: the cost of the entering exergy streams plus the capital and other costs. The total cost of a stream may be defined as:

$$\dot{C}_j = c_j \cdot \dot{E}_j \tag{55}$$

The term c_j in Equation (55) is the levelized cost per unit of exergy. In analyzing a component, we may assume that the costs per exergy unit are known for all entering streams. These costs are known from the components they exit or, if a stream enters the overall system consisting of all components under consideration, from the purchase cost of this stream. Consequently, the unknown variables that need to be calculated with the aid of the cost balance for the kth component are the costs per unit exergy of the exiting streams. This is shown in Figure 28.

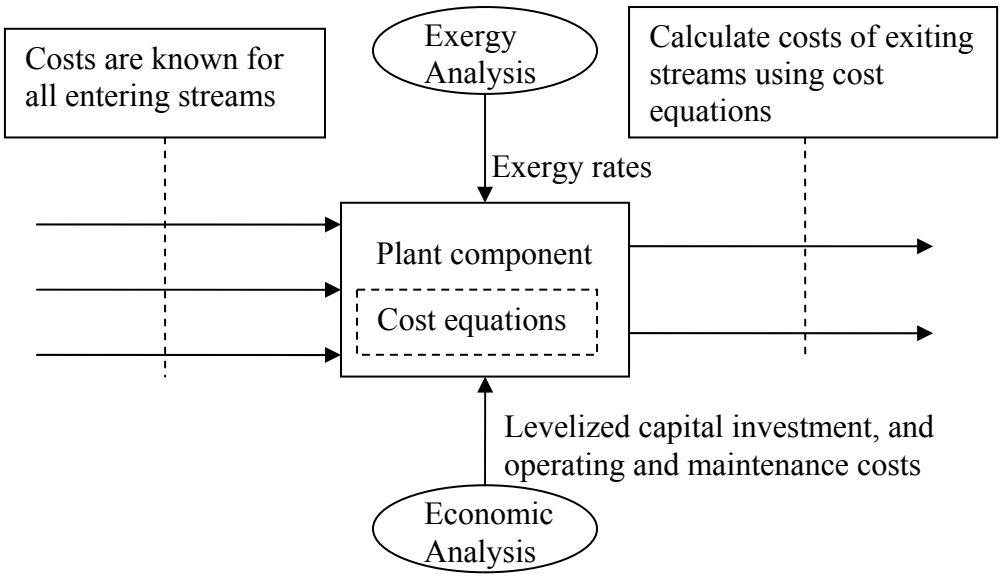

Figure 28: Schematic of SPECO Method Description [5]

In general, if there are N_e exergy streams exiting the component being considered, we have N_e unknowns and only one equation, the cost balance. Therefore, we need to formulate N_e-1 auxiliary equations. This is accomplished with the aid of the F and P rules.

The F rule (Fuel rule) refers to the removal exergy from an exergy stream within the component being considered when for this stream the exergy difference between inlet and outlet is considered in the definition of the fuel. The F rule states that the total cost associated with this removal of exergy must be equal to the cost at which the removed exergy was supplied to the same stream in upstream components.

The P rule (Product rule) refers to the supply of exergy to an exergy stream within the component being considered. The P rule states that each exergy unit is supplied to any stream associated with the products at the same average cost c_p. This cost is calculated from the cost balance and the equations obtained by applying the F rule.

5.4 ECONOMIC ANALYSIS

The aim of economic analysis in this thesis is to provide sufficient inputs to be used in thermoeconomic analysis. These inputs are levelized cost rates associated with capital and operation and maintenance expenses for components of the plant and levelized cost rates of the expenditures (i.e. fuel costs, raw water costs) supplied to the overall system.

The following steps should be applied in this kind of economic analysis [4]:

1. Purchased equipment costs should be estimated: There are several ways to obtain purchased equipment costs (PEC) of components. The best source is vendors' quotations. The other ways are: cost estimates from past purchased orders, quotations from experienced professional cost estimators, cost databases maintained by engineering companies, commercial computer

programs and literature (e.g. cost-estimating charts, Gas Turbine World Handbook)

2. Year-by-year analysis should be done: In this analysis, carrying charges and expenses should be estimated for each year within the plant economic life.

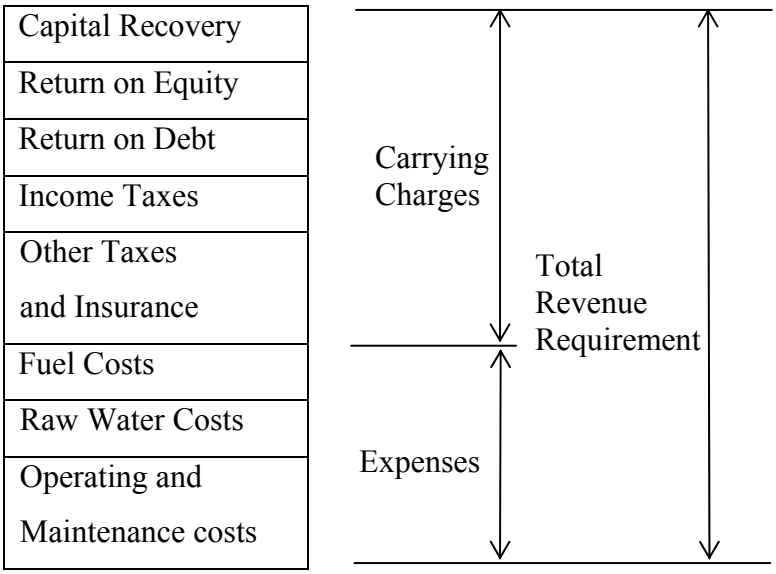

Figure 29: Cost Components Used in Economic Analysis

$$TRR_j = CC_j + FC_j + RWC_j + OMC_j \tag{56}$$

Fuel costs and raw water costs are usually part of the operating and maintenance costs. However, it is considered seperately from the O&M costs due to the fact that these costs are needed as inputs in thermoeconomic analysis.

3. Levelized costs should be calculated: Costs components vary significantly within the economic life of the plant. In general, carrying charges decrease while fuel, raw water and O&M costs increase with increasing years of

operation. Therefore, levelized annual values for all cost components should be used to simplify thermoeconomic analysis.

Levelized annual values for cost components: If money transactions occur at the end of each year within the plant economic life, for any cost component, X (i.e. Total revenue requirement, carrying charges, fuel cost, etc.), levelized cost can be shown as

$$X_L = CRF \cdot \sum_{j=1}^{n} \frac{X_j}{(1+i_{eff})^j} \tag{57}$$

Where, CRF is the capital recovery factor, i_{eff} is the effective annual cost-of-money and X_j is the value of X in the jth year.

Capital recovery factor:

$$CRF = \frac{i_{eff} \cdot (1+i_{eff})^n}{(1+i_{eff})^n - 1} \tag{58}$$

If cost escalation is applied to an expenditure (e.g., fuel costs, raw water costs, O&M costs) which results in a geometrically increasing series, levelized cost of that expenditure can be shown as

$$Y_L = Y_o \cdot CELF = Y_o \cdot \frac{k_Y \cdot (1-k_Y^n)}{(1-k_Y)} \cdot CRF \tag{59}$$

With

$$k_Y = \frac{1+r_Y}{1+i_{eff}} \text{ and } r_Y = \text{constant} \tag{60}$$

Where, Y_o is the value of expenditure at the beginning of the first year, r_Y is the average nominal escalation rate of the expenditure Y.

Cost rate associated with capital and operation and maintenance expenses for the kth component:

$$\dot{Z}_k^{CI} = \frac{CC_L}{\tau} \cdot \frac{PEC_k}{\sum_k PEC_k} \tag{61}$$

$$\dot{Z}_k^{OM} = \frac{OMC_L}{\tau} \cdot \frac{PEC_k}{\sum_k PEC_k} \tag{62}$$

Levelized cost rate of fuel supplied to the overall system

$$\dot{C}_F = \frac{FC_L}{\tau} \tag{63}$$

Levelized cost rate of raw water supplied to the overall system

$$\dot{C}_{RW} = \frac{RWC_L}{\tau} \tag{64}$$

Where τ is the total annual number of hours of system operation at full load.

5.5 THERMOECONOMIC ANALYSIS OF CASE STUDIES

Thermoeconomic analysis has been carried out to investigate the effect of steam demand on the cost of system products. The effect of HP steam drum pressure and pinch point are not discussed due to inadequate economic models in literature.

5.5.1 Economic Modeling of Case Studies

Purchased equipment costs of components of gas turbine system, total annual number of hours of system operation at full load and levelized fuel costs are taken same as CGAM system.

Levelized carrying charges and O&M costs should be greater than that of the CGAM system due to increase in plant components. So, for simplicity, it is assumed that summation of carrying charges and O&M costs of combined cycle cogeneration systems change such that $\dot{Z}_k$ of gas turbine components remain constant. Hence, cost of exhaust gas and power of gas turbine system remains constant for all cases.

Purchased equipment cost of HRSG is calculated by using the same formula given in Appendix C. However, the formula is extended for other HRSG sections and coefficients of the formula and unit costs are assumed to be the same also for other sections. There is no formula given for other plant equipments; i.e., steam turbine, desuperheater, etc. Thus, back-pressure steam turbine price is taken for two values ($\$1000\times10^3$ and $\$2000\times10^3$), extraction-condensing steam turbine price is also taken for two values ($\$3000\times10^3$ and $\$4000\times10^3$). For other plant components, since their prices are lower, reasonable values are taken.

In Table 5, superscripts show the cases that the values are valid for.

5.5.2 Cost Balances

Each system is divided into several subsystems and cost balance is applied to each subsystem. Auxiliary equations are applied by using fuel and product rules. Hence, a set of linear equations are formed and solved.

For illustration, cost balances and auxiliary equations for case-2 are given below. Cost balances for the gas turbine system are given in Appendix C.

Table 5: Purchased Equipment Costs and Costs Associated with Levelized Capital and O&M Costs of Plant Components

Component	PEC (Thousand $)	$\dot{Z}$ ($/h)
HRSG	1720[1,2] 2360[3]	347[1,2] 476[3]
Steam Turbine	1000[1] 2000[1] 3000[2,3] 4000[2,3]	202[1] 403[1] 605[2,3] 807[2,3]
Desuperheater	100[1,2,3]	20[1,2,3]
Dump Condenser	300[1]	60[1]
Condenser	500[2,3]	101[2,3]
Condensate Pump	50[1] 100[2,3]	10[1] 20[2,3]
HP BFW Pump	200[1,2,3]	40[1,2,3]
IP BFW Pump	150[3]	30[3]
Other Plant eq.	1000[1,2,3]	202[1,2,3]

For the control volume around HRSG (including deaerator),

$$(\dot{C}_3 - \dot{C}_4) + (\dot{C}_{17} - \dot{C}_5) + (\dot{C}_{12} - \dot{C}_{13}) + \dot{Z}_{HRSG} = 0 \tag{65}$$

$$\frac{\dot{C}_3}{\dot{E}_3} = \frac{\dot{C}_4}{\dot{E}_4} \qquad \text{(F rule)} \tag{66}$$

$$\frac{\dot{C}_5 - \dot{C}_{17}}{\dot{E}_5 - \dot{E}_{17}} = \frac{\dot{C}_{13} - \dot{C}_{12}}{\dot{E}_{13} - \dot{E}_{12}} \qquad \text{(P rule)} \tag{67}$$

For the control volume around steam turbine (including electric generator),

$$(\dot{C}_5 - \dot{C}_6 - \dot{C}_7) - \dot{C}_B + \dot{Z}_{ST} = 0 \tag{68}$$

$$\frac{\dot{C}_5}{\dot{E}_5} = \frac{\dot{C}_6}{\dot{E}_6} = \frac{\dot{C}_7}{\dot{E}_7} \qquad \text{(F rule)} \tag{69}$$

The electricity generated in the steam turbine splits into three streams. Two streams are sent to pumps. Remaining is the net power output of the bottoming cycle. If cost balance is applied around this splitting point and from product rule, it may be shown that

$$\frac{\dot{C}_B}{\dot{W}_B} = \frac{\dot{C}_C}{\dot{W}_C} = \frac{\dot{C}_D}{\dot{W}_D} = \frac{\dot{C}_E}{\dot{W}_E} \tag{70}$$

For the control volume around desuperheater,

$$\dot{C}_{15} + \dot{C}_6 - \dot{C}_8 + \dot{Z}_{Dsph} = 0 \tag{71}$$

For the control volume around condenser and condensate pump,

$$(\dot{C}_7 - \dot{C}_{10}) + (\dot{C}_{18} - \dot{C}_{19}) + \dot{C}_c + \dot{Z}_{con.} + \dot{Z}_{c.pump} = 0 \tag{72}$$

$$\frac{\dot{C}_{18}}{\dot{E}_{18}} = \frac{\dot{C}_{19}}{\dot{E}_{19}} \text{ (F rule)} \tag{73}$$

It's assumed that $\dot{C}_{18}$=0, so, from Equation (73) $\dot{C}_{19}$=0. Additionally, cost rate of condensate return is assumed to be zero. Hence,

$$\dot{C}_{12} = \dot{C}_{10} \tag{74}$$

For the control volume around BFW pump,

$$\dot{C}_{13} + \dot{C}_D - \dot{C}_{14} + \dot{Z}_{BFW\,Pump} = 0 \tag{75}$$

For the control volume around splitting point after BFW pump,

$$\frac{\dot{C}_{14}}{\dot{E}_{14}} = \frac{\dot{C}_{15}}{\dot{E}_{15}} = \frac{\dot{C}_{17}}{\dot{E}_{17}} \tag{76}$$

Solving linear Equations (65)-(76), cost formation within the system and cost of products may be found.

Cost of other plant equipment and the monetary loss associated with exergy lost should be apportioned between products. One assumption may be apportioning them between products according to their exergy rate.

$$\dot{C}_{8-final} = \dot{C}_8 + (\dot{Z}_{other} + \dot{C}_4) \cdot \frac{(\dot{E}_8 - \dot{E}_{11})}{\dot{W}_A + \dot{W}_E + (\dot{E}_8 - \dot{E}_{11})} \tag{77}$$

$$\dot{C}_{E-final} = \dot{C}_E + (\dot{Z}_{other} + \dot{C}_4) \cdot \frac{\dot{W}_E}{\dot{W}_A + \dot{W}_E + (\dot{E}_8 - \dot{E}_{11})} \tag{78}$$

$$\dot{C}_{A-final} = \dot{C}_A + (\dot{Z}_{other} + \dot{C}_4) \cdot \frac{\dot{W}_A}{\dot{W}_A + \dot{W}_E + (\dot{E}_8 - \dot{E}_{11})} \tag{79}$$

Cost balances and auxiliary equations for case-1 and case-3 may be written with similar efforts.

5.5.3 Results of Thermoeconomic Analysis

For the same process steam demand; exergy rate of process steam, exergy rate of condensate return from process, electrical output of gas turbine are the same for all cases. However, electrical power output of bottoming cycle is different. So; to make comparison between cases, cost per unit exergy of products is selected rather than selecting cost of products.

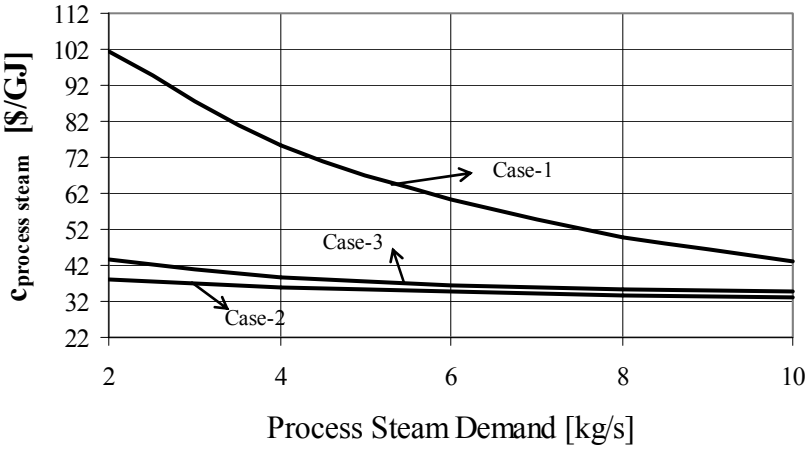

Figure 30: Change of Cost per Unit of Exergy of Process Steam with Process Steam Demand

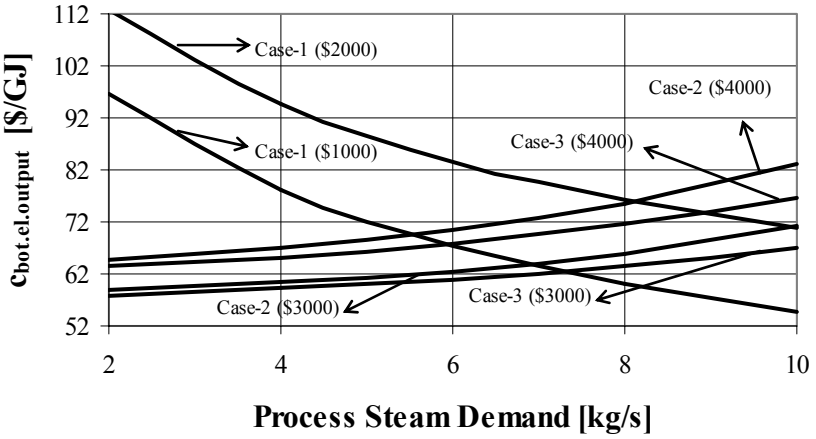

Figure 31: Change of Cost per Unit of Exergy of Bottoming Cycle Electrical Output with Process Steam Demand

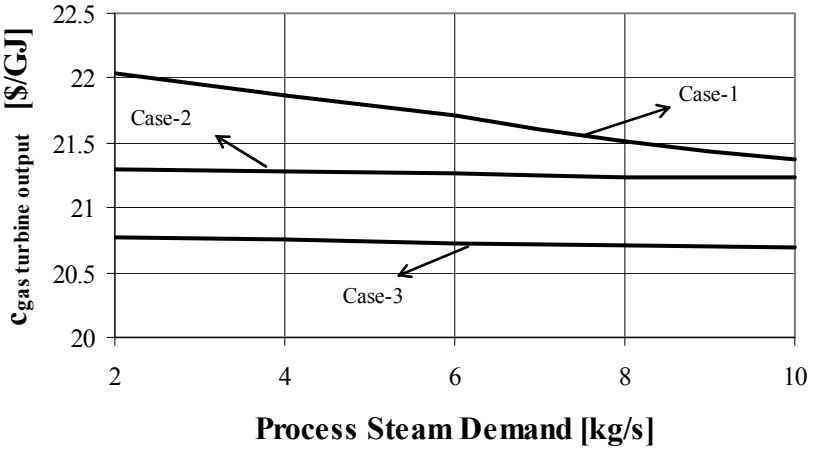

Figure 32: Change of Cost per Unit of Exergy of Gas Turbine Electrical Output with Process Steam Demand

It is seen from Figure 30 that for the same process steam demand, case-1 has the highest specific cost of process steam and case-2 is slightly lower than case-3. In the case of bottoming cycle electrical output cost, cost of it for case-1 decreases while cost of it for case-2 and case-3 increases as steam demand increases. For case-1, it has lower cost only for high steam demands. When overall steam demand range is considered, it may be seen that case-3 has the lowest specific cost for bottoming cycle electrical output. Case-2 and case-1 follow it, respectively.

In the case of cost of electrical output of the gas turbine system, cost of it found after cost balances and auxiliary equations are same in all cases due to the economic assumptions described in economic analysis section. However, when the cost associated with exergy loss is apportioned between products, case-1 has the highest cost of it. Case-2 and case-3 follow it, respectively, as it can be seen from Figure 32.

Cost formation for 6 kg/s steam demand is given in Tables 6-8. Some cost values are not given, i.e. shown with dashed line. This is because these are internal parameters of the subsystems, i.e. they are not inflows or outflows to the subsystem.

Table 6: Exergy Rate, Cost Rate, Cost per Unit Exergy of States of Case-1 for $\$1000\times10^3$ Steam Turbine and 6 kg/s Process Steam Demand.

State (Case-1)	Substance	$\dot{E}$ [kW]	$\dot{C}$ [$/h]	c [$/GJ]
1	Air	0	0	0.00
2	Fuel	84994	1398	4.57
3	Combustion Gases	21752	1137	14.52
4	Combustion Gases	3899	204	14.52
5	Water	14457	2162	41.54
6	Water	10469	1566	41.54
7	Water	5434	813	41.54
8	Water	5035	753	41.54
9	Water	4929	828	46.64
10	Water	3626	-	-
11	Water	209	-	-
12	Water	209	883	1175.81
13	Water	63	0	0.00
14	Water	248	883	987.49
15	Water	479	904	524.47
16	Water	491	957	541.70
17	Water	28	54	541.70
18	Water	28	-	-
19	Water	463	903	541.70
20	Water	912	0	0.00
21	Water	1163	0	0.00
22	Water	287	-	-
A	Net power output of gas turbine sys.	30000	2026	18.76
B	Power output of steam turbine	3448	798	64.32
C	Power input to condensate pump	0	0	64.32
D	Power input to BFW pump	60	14	64.32
E	Net power output of bottoming cycle	3388	785	64.32

Table 7: Exergy Rate, Cost Rate, Cost per Unit Exergy of States of Case-2 for $\$3000\times10^3$ Steam Turbine and 6 kg/s Steam Demand.

State (Case-2)	Substance	$\dot{E}$ [kW]	$\dot{C}$ [$/h]	c [$/GJ]
1	Air	0	0	0.00
2	Fuel	84994	1398	4.57
3	Combustion Gases	21752	1137	14.52
4	Combustion Gases	3380	177	14.52
5	Water	14457	1530	29.40
6	Water	5035	533	29.40
7	Water	605	64	29.40
8	Water	4929	568	32.03
9	Water	22	-	-
10	Water	22	185	2324.49
11	Water	63	0	0.00
12	Water	77	185	665.03
13	Water	479	222	128.63
14	Water	491	275	155.31
15	Water	28	16	155.31
16	Water	28	-	-
17	Water	463	259	155.31
18	Water	776	0	0.00
19	Water	989	0	0.00
20	Water	622	-	-
A	Net power output of gas turbine sys.	30000	2026	18.76
B	Power output of steam turbine	7116	1538	60.04
C	Power input to condensate pump	1	0	60.04
D	Power input to BFW pump	60	13	60.04
E	Net power output of bottoming cycle	7056	1525	60.04

Table 8: Exergy Rate, Cost Rate, Cost per Unit Exergy of States of Case-3 for $\$3000\times10^3$ Steam Turbine and 6 kg/s Steam Demand.

State (Case-3)	Substance	$\dot{E}$ [kW]	$\dot{C}$ [$/h]	c [$/GJ]
1	Air	0	0	0.00
2	Fuel	84994	1398	4.57
3	Combustion Gases	21752	1137	14.52
4	Combustion Gases	1966	103	14.52
5	Water	14457	1593	30.61
6	Water	82	9	30.61
7	Water	771	85	30.61
8	Water	1466	190	36.08
9	Water	4981	-	-
10	Water	4929	616	34.69
11	Water	28	-	-
12	Water	28	206	2029.75
13	Water	63	0	0.00
14	Water	2802	206	20.45
15	Water	543	250	127.93
16	Water	451	208	127.93
17	Water	92	42	127.93
18	Water	463	260	155.86
19	Water	92	73	219.21
20	Water	19	15	219.21
21	Water	73	58	219.21
22	Water	990	0	0.00
23	Water	1261	0	0.00
24	Water	722	-	-
A	Net power output of gas turbine sys.	3000	2026	18.76
B	Power output of steam turbine	8127	1724	58.92
C	Power input to condensate pump	1	0	58.92
D	Power input to HP BFW pump	56	12	58.92
E	Power input to IP BFW pump	3	1	58.92
F	Net power output of bottoming cycle	8067	1711	58.92

When the Table 6 is observed, it is seen that the highest cost rate is achieved at state 5 in case-1, which is the entry to steam turbine. Cost of net power output of gas turbine system, steam turbine exit, and others follow it, respectively. The highest cost per unit exergy is seen at state 12, which is the exit of subsystem including expansion valve, dump condenser and condensate pump. This is due to the low exergy at this state.

It is seen from Table 7 that the highest cost rate is achieved at state A in case-2, which is the net power output of gas turbine system. Cost of power output of steam turbine, steam turbine inlet, and others follow it, respectively. The highest cost per unit exergy is seen at state 10, which is the exit of subsystem including condenser and condensate pump.

From Table 8, it may be seen that the highest cost rate is achieved at state A in case-3, which is the net power output of gas turbine system. Cost rate of states B, F, 5 and others follow it, respectively. The highest cost per unit exergy is also achieved at the exit of subsystem including condenser and condensate pump.

CHAPTER 6

BILKENT COMBINED CYCLE COGENERATION PLANT

6.1 INTRODUCTION

This chapter is devoted to an existing plant, Bilkent combined cycle cogeneration plant. First, a detailed description of this plant is given. Then, energy, exergy analyses are applied to investigate the cycle thermodynamically. Finally, a thermoeconomic analysis is applied to calculate the cost of products of the system and observe the cost formation within the system.

6.2 DESCRIPTON OF THE PLANT

6.2.1 General Description

Bilkent combined cycle cogeneration plant is located in Bilkent University complex, Ankara, Turkey. The plant produces electrical energy and steam for the adjacent paper mill and the nearby Bilkent University complex; the electrical surplus is sold. Additionally, there is also an old system next to this plant, consisting of a gas turbine and a waste heat recovery boiler which is used only to produce process steam. However, this system is not taken into account in this study.

The plant consists of a gas turbine package, a heat recovery steam generator (HRSG), a steam turbine with relevant generator and a main steam condenser. Furthermore, auxiliary systems common to the combined cycle are provided. The schematic drawing of the plant is shown in Figure 34. Additionally, there is a dump steam condenser, which is needed during start-up and shut-down of the unit, or in case of steam turbine outage.

Fuel of the plant is natural gas supplied by local supplier Botaş. Natural gas is seperated from oil and humidity in dedicated seperators and compressed by the electrically driven natural gas compressors.

Raw water is supplied by municipality. It is used as the make-up of the condensate return from the process. Also, it is supplied to the cooling tower basin.

A hybrid cooling tower system which operates as a wet/dry cooling tower during the entire year, provides cooling water for steam condensing and for machinery cooling purposes. This system is mainly constituted by a cooling tower, divided into two cells, a cooling tower basin, collecting cooled water from the towers and cooling tower circulating pumps, which supplies cooling water to the steam condenser and to other users. The ambient air which serves as cooling air is conveyed through the dry section and the wet section in parallel flows by force using the induced draught fans.

Steam export is either only steam from the intermediate pressure steam generator (in case of no extraction from the steam turbine) or a mixture of steam from the intermediate pressure steam generator and steam from the controlled extraction of the steam turbine.

6.2.2 Process Description and Operation Conditions

In this paper, the performance of the plant is investigated at ISO day condition (15°C, 101.325 kPa, 60% relative humidity). The conditions of natural gas supplied at plant battery limit are 16 bar and 15°C. It is compressed by the fuel compressor to 40 bar. After cooling to 35°C and throttling, it enters the combustion chamber.

The aeroderivative gas turbine consists of a gas generator, a power turbine and an electrical generator. The exhaust gas of the power turbine is used as the waste heat source of the HRSG which is an unfired, natural circulation, three pressure level type.

Exhaust gas from gas turbine flow into HRSG meeting in sequence the following coils:

- HP steam superheater, first stage
- HP steam superheater, second stage
- HP steam evaporator
- HP 1st economizer
- IP steam evaporator
- HP 2nd economizer
- IP economizer
- LP steam evaporator with integral deaerator

Exhaust gases are discharged to the atmosphere through the relevant stack.

The superheated high pressure steam is delivered to the steam turbine which produces power by expansion up to vacuum conditions permitted by the water cooled steam condenser. Some of that steam is extracted to IP level according to the process steam demand and mixed with steam produced in IP steam drum, the remaining steam is diverted to the condenser. The return condensate from the paper mill has very low quality, hence it is sent to the old system. The return condensate from university (60°C) and raw water enters the demineralisation unit to be treated. It is accepted that approximately 70% of the steam export from combined cycle cogeneration plant returns as condensate. These streams are mixed with the condensate from condenser and the mixture enters the deaerator where it is heated up to the saturation temperature corresponding to the pressure of the LP steam drum and degassed by means of the saturated steam produced in the LP evaporator. The heated feedwater in the LP drum is removed by the feedpumps and sent to relevant economizers.

In addition to the descriptions above, the plant data used in this study are given in Table 9.

Table 9: Operation Data of Bilkent Plant at ISO Ambient Conditions

Gas turbine	
Gas Generator[1]	
Exhaust Temperature	1006.75 K
Exhaust Pressure	359.21 kPa
Power Turbine Isentropic Eff.[2]	0.91
Electric Generator Efficiency	0.98
HRSG[3]	
HP Steam Drum Pressure	46 bar
IP Steam Drum Pressure	16 bar
LP Steam Drum Pressure	1.7 bar
HP Pinch Point	11 °C
HP Evaporator Approach Temp.	9 °C
IP Pinch Point	11 °C
IP Evaporator Approach Temp.	9 °C
Steam Turbine	
Inlet Temperature	450 °C
Isentropic Efficiency of Stages	0.70
Electric Generator Efficiency	0.98
Condenser Pressure	0.07 bar
Pumps Isentropic Efficiency[2]	0.80
Steam Export Pressure (Sat. Vap.)	13 bar
Raw Water Temperature	15 °C
Make-up Tank Outlet Temperature	32 °C

[1] Data are obtained from a performance test of the gas generator at ISO ambient conditions.
[2] The values that are assumed.
[3] Pressure drop across HRSG is assumed to be 5%, heat loss to environment is assumed to be 2% of heat absorbed and blow down requirements are not taken into account. Pinch and approach temperature values are obtained from the manufacturer of HRSG which is Desa-Otak Engineering.

Rolls-Royce RB211 gas turbine package is used in the plant. The gas turbine is an aeroderivative type. It consists of a RB211-24G gas generator and a 4865 RPM Power turbine. The gas generator is a twin spool gas generator.

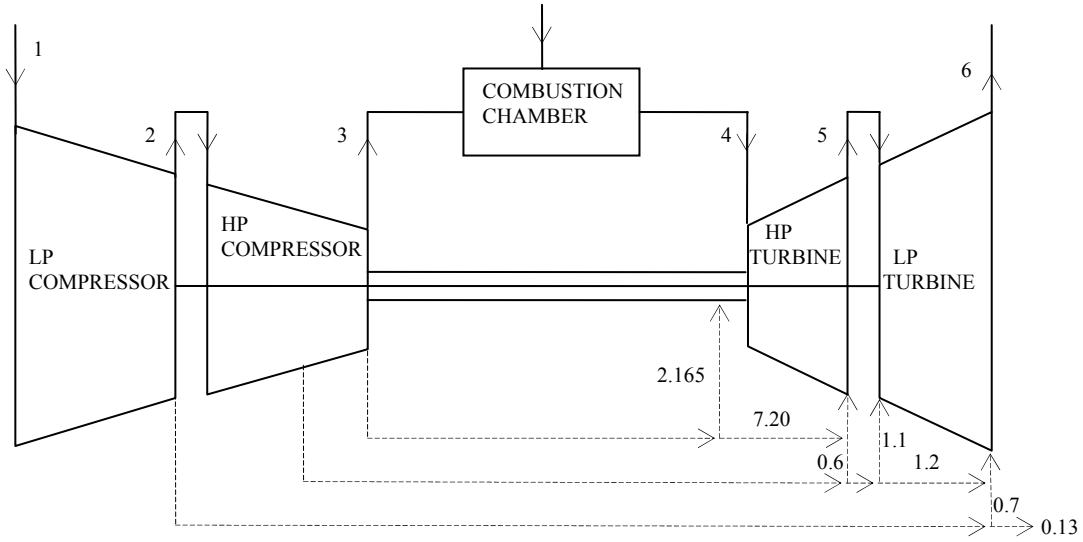

Figure 33: Schematic of Gas Generator of Bilkent Plant

Table 10: Properties of Bleeding and Cooling Flows of Gas Generator of Bilkent Plant

Bleed offtake	Bleed Returns	% $\dot{m}_1$ Flow
LP Compressor	Overboard Dump	0.13
LP Compressor	LP Turbine Rotor Delivery	0.7
HP Compressor	LP Turbine Rotor Entry	1.1
HP Compressor	LP Turbine Rotor Delivery	1.2
HP Compressor	HP Turbine Rotor Delivery	0.6
HP Compressor	HP Turbine Nozzle Cooling	2.165
HP Compressor	HP Turbine Rotor Delivery	7.2

Figure 33 shows the schematic of gas generator and bleeding and cooling flows to this generator. Table 10 gives the ratios of these flows in terms of mass flow rate entering LP compressor which is published by the manufacturer. Table 11 gives test values of the gas generator of Bilkent plant which gives mass flow rate, temperature and pressure of several states within the gas generator. Hence, approximate values for bleeding and cooling flows of gas generator of Bilkent plant are generated depending on the available data. These values are used to calculate the molar composition of gas generator exit.

Table 11: Test Values of Gas Generator of Bilkent Plant for ISO Day Conditions and Natural Gas as Fuel

Station	Mass Flow(kg/s)	Pressure(kPa)	Temperature (K)
LP Comp. Entry	84.43	101.33	288.16
LP Comp. Delivery	83.73	464.56	460.32
HP Comp. Entry	83.73	464.56	460.32
HP Comp. Delivery	73.46	2069.32	717.99
Comb. Outlet	74.91	1953.91	1450.68
HP Turb. Ent.	76.73	1953.91	1434.29
HP Turb. Del.	83.27	N/A	1165.71
LP Turb. Del.	85.79	359.21	1006.75

6.3. ENERGY ANALYSIS

6.3.1 Modeling Environment

Atmospheric air may be considered as being consisting of dry air and water vapor. Dry air composition may be taken as 78.98% N_2, 20.99% O_2, 0.03% CO_2. $H_2O_{(g)}$ concentration depends on environment temperature, pressure and relative humidity.

$$x_{o,H_2O(g)} = \frac{\phi_o \cdot P_{sat(T_o)}}{P_o} \tag{80}$$

Hence, air composition at ISO day (15°C ambient temperature, 101.325 kPa ambient pressure and 60% relative humidity) is: 78.18% N_2, 20.78% O_2, 0.03% CO_2, 1.01% $H_2O_{(g)}$

6.3.2 Calculation of Gas Turbine Exit Composition

Combustion equation of natural gas (Taken as CH_4) for λ theoretical air in ISO environmental conditions may be shown as

$$CH_4 + 2\lambda(0_2+3.7627N_2+0.0014CO_2)+0.0972\lambda\ H_2O_{(g)} \longrightarrow$$
$$(1+0.0028\lambda)CO_2 + (2+0.0972\lambda)\ H_2O_{(g)} +7.5254\lambda N_2+ 2(\lambda-1)O_2$$

λ then may be given as

$$\frac{\dot{m}_{fuel}}{\dot{m}_{air}} = \frac{\dot{n}_{CH_4} \cdot M_{CH_4}}{\dot{n}_{air} \cdot M_{air}} = \frac{1 \times 16.043}{9.6254 \times \lambda \times 28.745} \tag{81}$$

$$\lambda = \frac{0.058 \times \dot{m}_{air}}{\dot{m}_{fuel}} \tag{82}$$

Exhaust gas composition of combustion chamber may be calculated by using combustion equation and the theoretical air.

$$x_{N_2} = \frac{7.5254 \cdot \lambda}{1 + 9.6254 \cdot \lambda} \tag{83}$$

$$x_{O_2} = \frac{2 \cdot (\lambda - 1)}{1 + 9.6254 \cdot \lambda} \tag{84}$$

$$x_{CO_2} = \frac{1 + 0.0028 \cdot \lambda}{1 + 9.6254 \cdot \lambda} \tag{85}$$

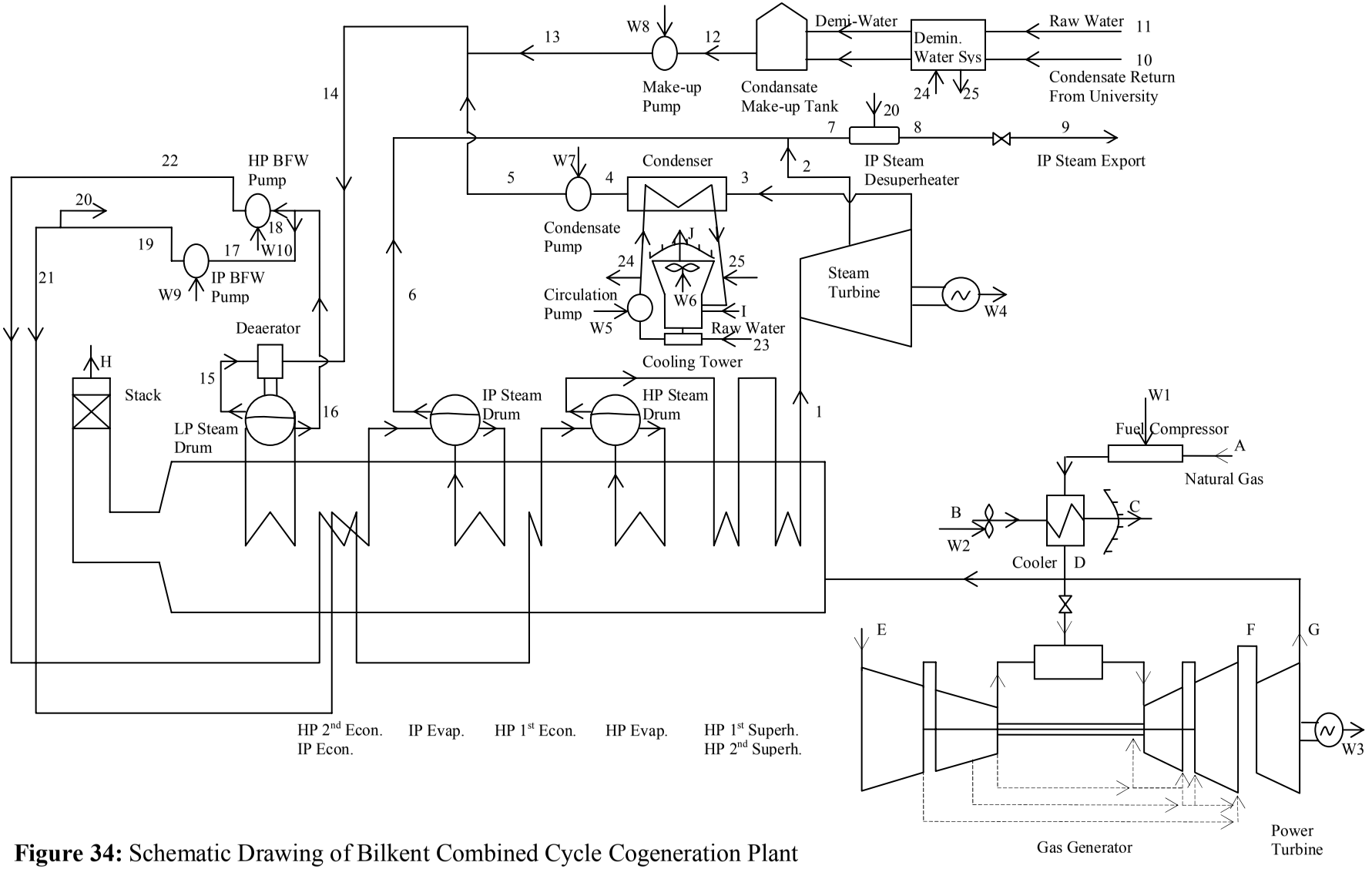

Figure 34: Schematic Drawing of Bilkent Combined Cycle Cogeneration Plant

$$x_{H_2O} = \frac{2 + 0.0972 \cdot \lambda}{1 + 9.6254 \cdot \lambda} \tag{86}$$

In this thesis, gas generator is treated as a single unit. The molar composition of gas turbine exit is calculated as follows: The mass flow rate of combustion chamber inlet, 73.46 kg/s; the mass flow rate of fuel, 1.45 kg/s and Equation (82) are used and λ is found as 2.9384. From Equations (83)-(86), molar composition at combustion chamber exit is calculated as 75.51% N_2, 13.24% O_2, 7.81% $H_2O_{(g)}$, and 3.44% CO_2. Combustion gases exiting combustion chamber, 74.91 kg/s mix with the air coming from compressors, 10.88 kg/s. Since this reaction is not chemical, moles of each component; i.e. N_2, is conserved. Hence, the moles of each component leaving gas generator and molar composition of gas generator exit may be calculated. Molar composition of power turbine exit is the same as this composition. So, molar composition of the gas turbine exit is found as: 75.85% N_2, 14.19% O_2, 6.95% $H_2O_{(g)}$, 3.01% CO_2.

6.3.3 Energy Balances

Inlet conditions of gas generator are 101.33 kPa, 288.16 K and 84.43 kg/s, with the molar composition: 78.18% N_2, 20.78% O_2, 0.03% CO_2, 1.01% $H_2O_{(g)}$. Exit conditions of gas generator are 359.21 kPa, 1006.75 K and 85.79 kg/s, with the molar composition: 75.85% N_2, 14.19% O_2, 6.95% $H_2O_{(g)}$, 3.01% CO_2. Using the exit conditions of gas generator, isentropic efficiency of power turbine, electrical generator efficiency and pressure drop across HRSG, electrical output of power turbine and temperature of power turbine exit may be found as follows:

$$P_G = P_H / 0.95 \tag{87}$$

For the isentropic expansion, $\bar{s}_F = \bar{s}_{Gs}$ so it may be written that

$$\bar{s}^{\circ}(T_{Gs}) = \bar{s}^{\circ}(T_F) + \bar{R} \cdot \ln \frac{P_G}{P_F} \tag{88}$$

From Equation (88), T_{Gs} may be found by iteration. Then, $\bar{h}_{Gs}$ may be calculated.

Using the isentropic efficiency definition, $\bar{h}_G$ is calculated as follows

$$\bar{h}_G = \bar{h}_F - \eta_{pt} \cdot (\bar{h}_F - \bar{h}_{Gs}) \tag{89}$$

After finding $\bar{h}_G$, T_G may be found by iteration. Then, electrical output of the power turbine, or the whole gas turbine system, may be calculated.

$$(\dot{W}_{el})_{GT} = \eta_{el.gen} \cdot \dot{m}_F \cdot \left(\frac{\bar{h}_F - \bar{h}_G}{M_{mix}} \right) \tag{90}$$

HRSG energy balances should be applied in the same order as described in Section 2.1. Hence, mass flow rate generated in steam drums and stack temperature may be found.

The electrical output of the steam turbine may be given as

$$(\dot{W}_{el})_{ST} = (\dot{m}_1 \cdot h_1 - \dot{m}_2 \cdot h_{2a} - \dot{m}_3 \cdot h_{3a}) \cdot \eta_{gen} \tag{91}$$

Where

$$h_{2a} = h_1 - \eta_{st1} \cdot (h_1 - h_{2s}) \tag{92}$$

$$h_{3a} = h_1 - \eta_{st2} \cdot (h_1 - h_{3s}) \tag{93}$$

To find $\dot{m}_2$ and $\dot{m}_3$, energy balances for the control volumes around IP steam desuperheater and connection point between points 2,6 and 7 are used. From these balances:

$$(\dot{m}_7 - \dot{m}_6) \cdot h_{2a} + \dot{m}_6 \cdot h_6 = \dot{m}_7 \cdot h_7 \quad (94)$$

$$\dot{m}_7 \cdot h_7 + (\dot{m}_8 - \dot{m}_7) \cdot h_{20} = \dot{m}_8 \cdot h_8 \quad (95)$$

From Equations (94) and (95), $\dot{m}_7$ can be written as

$$\dot{m}_7 = \frac{\dot{m}_8 \cdot (h_8 - h_{20}) + \dot{m}_6 \cdot (h_{2a} - h_6)}{h_{2a} - h_{20}} \quad (96)$$

Where

$$h_{20} = h_{19} = h_{15} + v_{15} \cdot (P_{19} - P_{15}) / \eta_p \quad (97)$$

$\dot{m}_2$ and $\dot{m}_3$ can be calculated after finding $\dot{m}_7$ from Equation (96)

$$\dot{m}_2 = \dot{m}_7 - \dot{m}_6 \quad (98)$$

$$\dot{m}_3 = \dot{m}_1 - \dot{m}_2 \quad (99)$$

Then, h_7 may be calculated from (94) or (95). h_{14} is calculated from the energy balance for the control volume around the related junction point,

$$h_{14} = (\dot{m}_5 \cdot h_5 + \dot{m}_{13} \cdot h_{13}) / \dot{m}_{14} \quad (100)$$

Power consumptions in the plant are due to power input to following components: natural gas compressor, natural gas cooler fan, cooling tower circulating pump, cooling tower fan, condensate pump, make-up pump, HP BFW pump, IP BFW

pump. Other losses are ignored. Among these components, the values of power input to natural gas cooler and cooling tower fan are taken from design case studies of the plant. That for natural gas compressor may be calculated from an energy balance around it since inlet and exit conditions of it are known. Power input to remaining components may be calculated as below. To illustrate, power input to condensate pump is given.

$$\dot{W}_{con.pump} = \dot{m}_4 \cdot (h_5 - h_4) \tag{101}$$

$$h_5 = h_4 + \nu_4 \cdot (P_5 - P_4) / \eta_p \tag{102}$$

Enthalpy difference of the process may be given as

$$\Delta\dot{H}_{process} = \dot{m}_9 \cdot h_9 - \dot{m}_{10} \cdot h_{10} - \dot{m}_{11} \cdot h_{11} \tag{103}$$

6.3.4 Results of Energy Balances

Although kinetic and potential energy effects are ignored and some assumptions are done, the results are compared with that of the monitoring system of the plant which gives mass flow rate, temperature, electrical output, etc. of some key points and it is found that the results are in $\pm 3\,\%$ error range.

The electrical power output of gas turbine is found as 23719 kW and it does not vary with steam demand. Work inputs to fuel compressor, natural gas cooler fan, cooling tower fan, and cooling tower circulation pump assumed not to vary with steam demand and their values are taken as 468 kW, 40 kW, 140 kW, and 282 kW, respectively.

The steam produced in HP steam drum and IP steam drum is calculated as 9.53 kg/s and 1.38 kg/s, respectively. Steam produced in LP steam drum changes from 1.59 kg/s to 1.86 kg/s as steam demand changes from 1.5 kg/s to 10 kg/s.

Stack temperature is about 130°C and this does not vary significantly with the steam demand. Also, this is a safe value when corrosion effects are considered. Other results are given in Figure 35 and Figure 36.

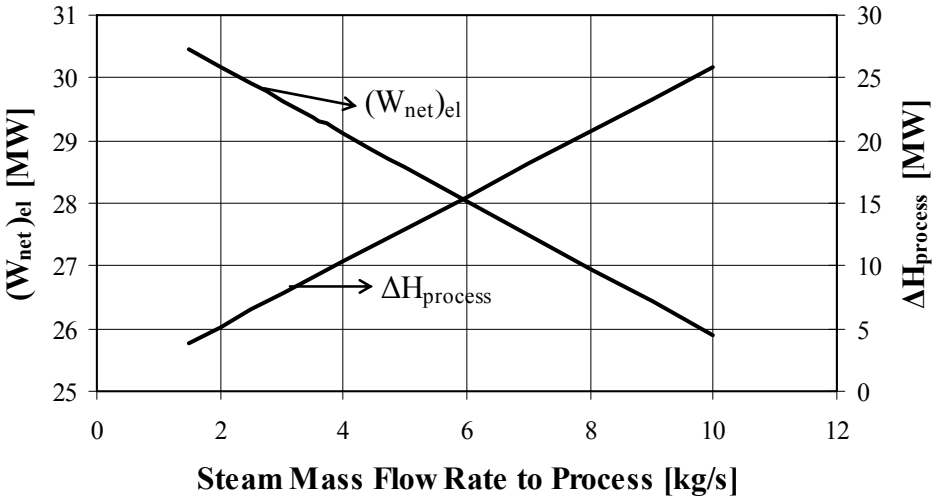

Figure 35: Change of Energetic Outputs of the Plant with Mass Flow Rate to Process

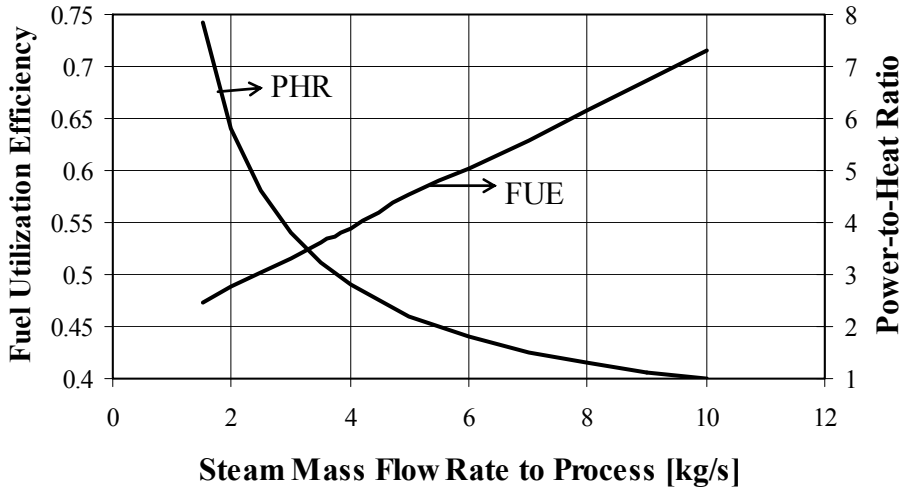

Figure 36: Changes of FUE and PHR with Steam Mass Flow Rate to Process

From Figure 35, it is seen that as steam mass flow rate to process increases from 1.5 kg/s to 10 kg/s, $(\dot{W}_{net})_{el}$ decreases steadily from 30.45 MW to 25.89 MW, whereas $\Delta\dot{H}_{process}$ increases steadily from 3.89 MW to 25.93 MW

From Figure 36, it may be concluded that as steam mass flow rate to process increases, fuel utilization efficiency increases steadily from 0.473 to 0.715 whereas power-to-heat ratio decreases from 7.828 to 0.998. Hence, in terms of energy concepts, high steam mass flow rate to process conditions are more efficient since FUE is higher, however lower steam mass flow rate to process conditions are economically more feasible since PHR is higher.

To illustrate, mass flow rate and thermodynamic properties for a chosen steam mass flow rate to process, 15 t/h, are given in Table 12.

6.4 EXERGY ANALYSIS

6.4.1 Exergy Components and Exergy Balances

The plant is seperated into ten subsystems. Exergy inflows and outflows to these subsystems, exergy destruction in these subsystems and exergy losses to the environment are calculated. Schematic of these subsystems and exergy balances for them may be found in Table 14.

Physical exergy for natural gas states (states A and D) may be calculated as follows

$$\dot{E}_D^{PH} = \dot{m}_D \cdot \frac{(\bar{h}_D - \bar{h}_o) - T_o \cdot (\bar{s}_D - \bar{s}_o)}{M_{CH_4}} \qquad \text{or} \qquad (104)$$

$$\dot{E}_D^{PH} = \dot{m}_D \cdot \frac{(\bar{h}_D - \bar{h}_o) - T_o \cdot (\bar{s}^\circ(T_D) - \bar{s}^\circ(T_o) - \bar{R} \cdot \ln \frac{P_D}{P_o})}{M_{CH_4}} \qquad (105)$$

Table 12: Mass flow rate and thermodynamic properties of Bilkent plant for 15 t/h steam to process

State	Substance	$\dot{m}$ (kg/s)	P (kPa)	T (°C)	h (kJ/kg)	s (kJ/kgK)
A	Natural gas	1.45	1600.00	15.00	-4688.626	
B	Air	n.a.	101.33	15.00	-99.280	
C	Air	n.a.	101.33	15.00	-99.280	
D	Natural gas	1.45	4000.00	35.00	-4644.937	
E	Air	84.43	101.33	15.00	-99.280	
F	Comb. gases	85.79	359.21	733.60	-212.707	
G	Comb. gases	85.79	106.39	494.65	-494.832	
H	Comb. gases	85.79	101.33	130.00	-899.655	
I	Air	n.a.	101.33	15.00	-99.280	
J	Air	n.a.	101.33	15.00	-99.280	
1	Water	9.53	4600.00	450.00	3321.880	6.8634
2	Water	2.44	1600.00	335.70	3112.680	7.0147
3	Water	7.09	7.00	38.97	2488.470	8.0076
4	Water	7.09	7.00	38.97	163.270	0.5587
5	Water	7.09	650.00	39.17	164.080	0.5613
6	Water	1.38	1600.00	201.30	2793.880	6.4227
7	Water	3.82	1600.00	283.72	2997.151	6.8156
8	Water	4.17	1600.00	201.30	2787.600	6.4095
9	Water	4.17	1300.00	191.64	2787.600	6.4953
10	Water	2.92	300.00	60.00	251.130	0.8312
11	Water	1.25	350.00	15.00	62.990	0.2245
12	Water	4.17	n.a.	32.00	134.140	0.4644
13	Water	4.17	650.00	32.16	134.830	0.4666
14	Water	11.26	650.00	36.58	153.258	0.5265
15	Water	1.68	170.00	115.12	2699.200	7.1820
16	Water	11.26	170.00	115.12	483.010	1.4746
17	Water	1.73	170.00	115.12	483.010	1.4746
18	Water	9.53	170.00	115.12	483.010	1.4746
19	Water	1.73	1600.00	115.57	484.900	1.4795
20	Water	0.35	1600.00	115.57	484.900	1.4795
21	Water	1.38	1600.00	115.57	484.900	1.4795
22	Water	9.53	4600.00	116.50	488.860	1.4897
23	Water	12.50	350.00	15.00	62.990	0.2245
24	Water	6.02	390.00	15.12	63.500	0.2262
25	Water	6.02	390.00	25.12	105.390	0.3690

Table 13: Electrical Outputs of Bilkent Plant for 15 t/h Steam to Process

$\dot{W}_{W1}$	68 kW	$\dot{W}_{W6}$	140 kW
$\dot{W}_{W2}$	40 kW	$\dot{W}_{W7}$	6 kW
$\dot{W}_{W3}$	23719 kW	$\dot{W}_{W8}$	3 kW
$\dot{W}_{W4}$	6294 kW	$\dot{W}_{W9}$	3 kW
$\dot{W}_{W5}$	282 kW	$\dot{W}_{W10}$	56 kW

Formulations to calculate enthalpy and absolute entropy for methane may be found in Appendix A. For state A, since the temperature of this state is same as that of the environment, physical exergy may be written as

$$\dot{E}_A^{PH} = \dot{m}_A \cdot \frac{\overline{R} \cdot T_o \cdot \ln \frac{P_A}{P_o}}{M_{CH_4}} \tag{106}$$

Temperature and pressure of states B, C, E, I and J are same with those of the environment. Hence, physical exergy of these states are zero.

Physical exergy for combustion products (states F,G, and H) as follows

$$\dot{E}_F^{PH} = \dot{m}_F \cdot \frac{\overline{h}_F - \overline{h}_o - T_o \cdot (\overline{s}_D - \overline{s}_o)}{M_{mix}} \tag{107}$$

Formulations to calculate enthalpy and absolute entropy for ideal gas components may be found in Appendix A. In calculating $\overline{s}_D$, contributions of each component should be calculated using the following formula. To illustrate, entropy of nitrogen for the temperature and partial pressure at state F is shown. Entropy of other components may be written similarly. Then, using the molar composition and entropy of each component, $\overline{s}_D$ may be found.

$$\bar{s}_{N_2}(T_F, x_{N_2} \cdot P_F) = \bar{s}^{\circ}_{N_2}(T_F) - \bar{R} \cdot \ln \frac{x_{N_2} \cdot P_F}{P_{ref}} \quad (108)$$

P_{ref} is the reference pressure defined in the absolute entropy table.

Condensation considerations are taken into account, as described in Section 4.2 and $\bar{h}_o$ and $\bar{s}_o$ should be calculated using the formulations in that section.

For water states, physical exergy (state 1,2, etc.) may be calculated as below. All enthalpy and entropy values may be taken from steam tables.

$$\dot{E}_1^{PH} = \dot{m}_1 \cdot [h_1 - h_o - T_o \cdot (s_1 - s_o)] \quad (109)$$

Chemical exergy for natural gas states (states A and D) is calculated from Equation (37), that for water states (1,2, etc.) is calculated from Equation (33) and that for combustion products (states F,G, and H) are calculated by using Equations (34) and (36). Since the composition of states B, C, E, I and J is same with the composition of ambient air, the chemical exergy of these states is zero.

Exergetic efficiency of the plant may be given as

$$\varepsilon_{plant} = \frac{(\dot{W}_{net})_{el} + (\dot{E}_9 - \dot{E}_{10} - \dot{E}_{11})}{\dot{E}_A + \dot{E}_{11} + \dot{E}_{23}} \quad (110)$$

6.4.2 Results of Exergy Analysis

Exergy components of the plant are calculated using the formulations given in Section 6.4.1. After applying exergy balances, exergy destructions and its relevant ratios in the subsystems are calculated. To illustrate, exergy flow rates for 15 t/h steam to process are given in Table 15, exergy destructions and its relevant ratios for that process steam mass flow rate are given in Table 16.

Table 14: Exergy Balances for the Subsystems of Bilkent Plant

No	Control Volume	Exergy Balance
1	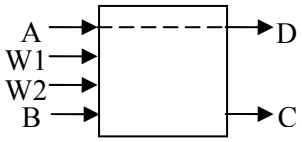	$\dot{E}_{DEST} = (\dot{E}_A - \dot{E}_D) + (\dot{E}_B - \dot{E}_C) + \dot{E}_{W1} + \dot{E}_{W2}$
2	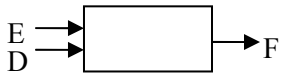	$\dot{E}_{DEST} = \dot{E}_E + \dot{E}_D - \dot{E}_F$
3	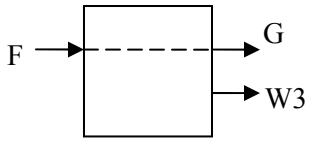	$\dot{E}_{DEST} = (\dot{E}_F - \dot{E}_G) - \dot{E}_{W3}$
4	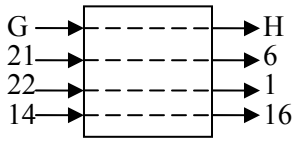	$\dot{E}_{DEST} = (\dot{E}_G - \dot{E}_H) + (\dot{E}_{21} - \dot{E}_6) + (\dot{E}_{22} - \dot{E}_1) + (\dot{E}_{14} - \dot{E}_{16})$
5	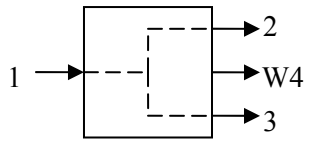	$\dot{E}_{DEST} = (\dot{E}_1 - \dot{E}_2 - \dot{E}_3) - \dot{E}_{W4}$
6	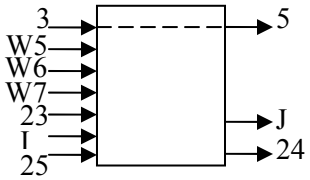	$\dot{E}_{DEST} = (\dot{E}_3 - \dot{E}_5) + \dot{E}_{W5} + \dot{E}_{W6} + \dot{E}_{W7} + \dot{E}_{23} + \dot{E}_I + \dot{E}_{25} - \dot{E}_J - \dot{E}_{24}$
7		$\dot{E}_{DEST} = \dot{E}_2 + \dot{E}_6 + \dot{E}_{20} - \dot{E}_9$
8	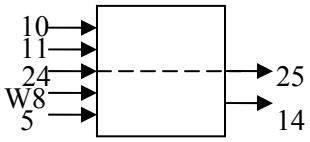	$\dot{E}_{DEST} = \dot{E}_{10} + \dot{E}_{11} + (\dot{E}_{24} - \dot{E}_{25}) + \dot{E}_{W8} + \dot{E}_5 - \dot{E}_{14}$
9	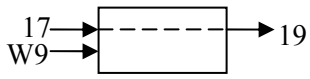	$\dot{E}_{DEST} = (\dot{E}_{17} - \dot{E}_{19}) + \dot{E}_{W9}$
10	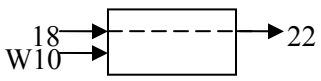	$\dot{E}_{DEST} = (\dot{E}_{18} - \dot{E}_{22}) + \dot{E}_{W10}$

Table 15: Exergy Flow Rates of Bilkent Plant for 15 t/h Steam to Process

State	Substance	$\dot{E}_{PH}$ (kW)	$\dot{E}_{CH}$ (kW)	$\dot{E}$ (kW)
A	Natural Gas	598	75452	76050
B	Air	0	0	0
C	Air	0	0	0
D	Natural Gas	798	75452	76250
E	Air	0	0	0
F	Comb. gases	44585	1075	45660
G	Comb. gases	19472	1075	20547
H	Comb. gases	1979	1075	3054
I	Air	0	0	0
J	Air	0	0	0
1	Water	12826	647	13474
2	Water	2662	165	2827
3	Water	1297	482	1779
4	Water	28	482	510
5	Water	29	482	511
6	Water	1308	94	1402
7	Water	3953	259	4212
8	Water	3927	283	4210
9	Water	3824	283	4107
10	Water	39	198	237
11	Water	0	85	85
12	Water	8	283	291
13	Water	9	283	292
14	Water	37	765	802
15	Water	1058	114	1172
16	Water	673	765	1439
17	Water	104	118	221
18	Water	570	647	1217
19	Water	104	118	222
20	Water	21	24	45
21	Water	83	94	177
22	Water	584	647	1232
23	Water	0	849	849
24	Water	0	409	409
25	Water	4	409	414

$\dot{E}_{W1}$	468 kW	$\dot{E}_{W5}$	282 kW	$\dot{E}_{W9}$	3 kW
$\dot{E}_{W2}$	40 kW	$\dot{E}_{W6}$	140 kW	$\dot{E}_{W10}$	56 kW
$\dot{E}_{W3}$	23719 kW	$\dot{E}_{W7}$	6 kW		
$\dot{E}_{W4}$	6294 kW	$\dot{E}_{W8}$	3 kW		

Table 16: Exergy destruction and its relevant ratios of Bilkent plant at 15 t/h steam to process

Control Volume#	$\dot{E}_D$ [kW]	y_D [%]	y_D^* [%]
1	307	0.40	0.75
2	30590	39.74	74.53
3	1394	1.81	3.40
4	3390	4.40	8.26
5	2574	3.34	6.27
6	2549	3.31	6.21
7	167	0.22	0.41
8	30	0.04	0.07
9	2	0.00	0.01
10	41	0.05	0.10

It is seen from Table 16 that the largest portion of exergy destruction occurs in control volume 2 (gas generator), mainly because of combustion process. Exergy destructions in control volume 4 (HRSG); control volume 5 (steam turbine), control volume 6 (condenser + cooling tower + condensate pump), control volume 3 (power turbine) and others follow it, respectively.

Steam mass flow rate to process does not effect the exergy destructions in control volume 1 (natural gas compressor), control volume 2 (gas generator), and control volume 3 (power turbine). Its effect on bottoming cycle components is given in Figure 37.

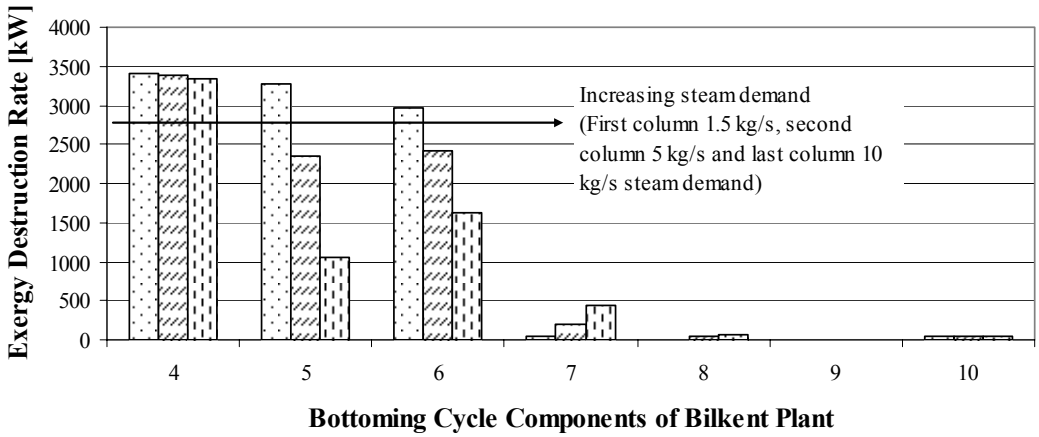

Figure 37: Exergy Destruction Rates in the Bottoming Cycle Components of Bilkent Plant for Different Steam Demand

From Figure 37, it is seen that exergy destruction in control volume 5 and control volume 6 decreases, whereas exergy destruction in control volume 7, control volume 8 and control volume 9 increases as steam flow rate to process increases. Exergy destruction in 4 and control volume 10 is not very sensitive to process steam change.

Exergy losses due to heat losses in the gas generator and the HRSG, and exergy losses due to the cooling tower and the natural gas cooler exit streams are considered as zero by taking the control volumes large enough so that the heat losses occur at the ambient temperature and the exit streams mix with the ambient air. Hence, the only exergy loss is due to the HRSG exit. For 15 t/h steam to process, the exergy loss is 3054 kW which is 3.96% of the exergy supplied to the plant. Additionally, exergy loss does not change significantly with steam to process.

Exergetic efficiency of the plant changes between 0.413 and 0.454 as steam demand increases between 1.5 kg/s and 10 kg/s, as can be seen from Figure 38. From the results of exergy destruction and exergy loss analyses described above, the main reason for the increase in exergetic efficiency with steam demand is the exergy destruction decrease in the control volumes 5 and 6.

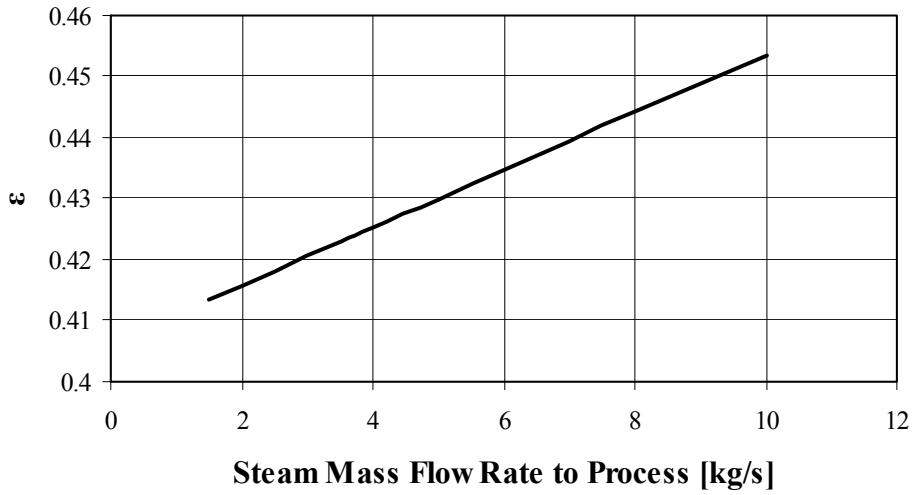

Figure 38: Change of Exergetic Efficiency of Bilkent Plant with Steam Mass Flow Rate to Process

6.5 ECONOMIC ANALYSIS

6.5.1 Economical Data of Bilkent Plant

The economical data of Bilkent plant, which is started its commerical operation at the beginning of 2000, is obtained from Bilenerji A.Ş., the company that operates the plant. Additionally, fuel costs are obtained from local natural gas supplier, BOTAŞ, for the years between 2000-2004 by making necessary unit conversions (i.e., TL/M^3 to \$/kg by using exchange rates of years supplied by Central Bank of the Republic of Turkey and using density of Turkish natural gas). Raw water costs are obtained from raw water supplier, ASKI, for the year 2004 since the data for previous years are not available. These data are presented in the following section.

Other economical data of the plant are as follows: For operating and maintenance costs, there is an extra overhaul cost which is 0.85 M\$ in the third year and 1.75 M\$ in the sixth year in every six year periods. Nominal escalation rates of costs are taken

as the estimated average general inflation within plant economic life, which is 3% in U.S. Dollars. Effective annual cost-of-money rate is taken as 10%. Total number of hours of system operating at full load is taken as 8200 hours. Plant economic life is 25 years. Total capital investment of the plant is 27.8 Million U.S.$.

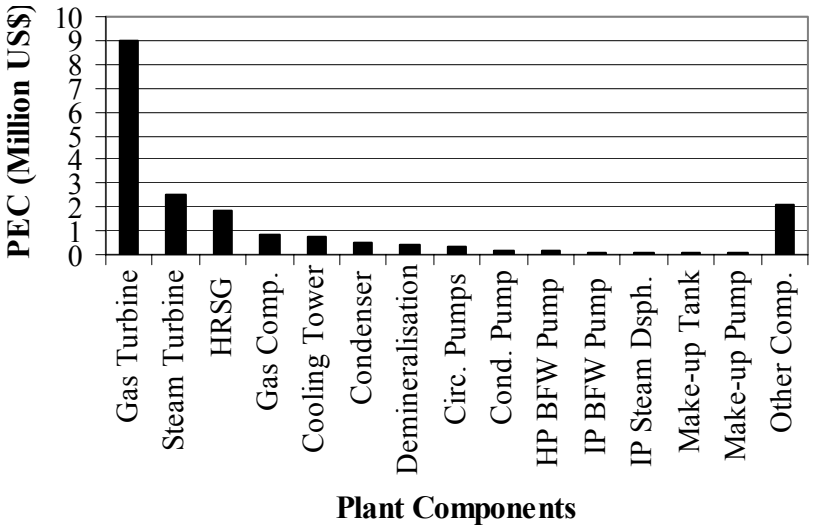

Figure 39: Distribution of Purchased-Equipment Cost of Plant Components

6.5.2 Year-by-Year Analysis

Data for carrying charges for entire life of the plant, operating & maintenance cost for the first year and overhaul costs that are mentioned in the previous section are obtained from the company that operates the plant. For future year costs of O&M, the costs are escalated with the given nominal escalation rate. After escalation, overhaul costs are added.

From BOTAS website [39], the price of natural gas (TL/m^3) is obtained for the desired month and year. From Central Bank of the Republic of Turkey website [41], exchange rate (TL/$) for the desired date is obtained. Taking the money transactions

at the end of each year (i.e. December), fuel cost for years 2000-2004 are calculated using the formulation given below. Results are given in Table 17.

$$FC = \frac{P_{N.Gas} \times \dot{m}_{Fuel} \times \tau \times 3600}{\rho_{N.Gas} \times ER} \tag{111}$$

In Equation (111), $P_{N.Gas}$ and ER stand for price of natural gas and exchange rate, respectively, and their values for the years 2000-2004 are given in Table 17. Please note that values are given in terms of TL. The new Turkish currency is YTL which is 10^{-6} times of TL. Mass flow rate of fuel, $\dot{m}_{Fuel}$ is taken as 1.45 kg/s from gas turbine data. Total number of hours of system operating at full load, τ, is taken as 8200 hours which is given in economical data section. Density of Turkish natural gas, $\rho_{N.Gas}$, is taken as 0.717 kg/m^3 [8].

From Table 17, it is seen that due to uncertanities in World economy and other reasons, fuel costs fluctuated between 2000-2004. However, for future years, it is assumed that fuel costs are escalated with the nominal escalation rate, which is 3%.

Table 17: Fuel Costs of Bilkent Plant for The Years Between 2000-2004

Year	Price of Natural Gas (TL/m^3)	Exchange Rate (TL/\$)	Fuel Cost (10^3 \$)
2000	116283	684316	10144
2001	280990	1489445	11262
2002	268733	1519967	10555
2003	234460	1454169	9625
2004	288692	1426523	12082

The price of raw water (TL/m^3) is obtained from the ASKI website [40] for the date of last price change. The date of last price change is 04.12.2004 (end of 2004). Price of water is given as 2978475 TL/m^3. The exchange rate at that date is 1396800 TL/$. The density of raw water may be taken as 997 kg/m^3.

Raw water is supplied to the demineralisation water system and to the cooling tower basin in the plant. If it is assumed that average steam demand is 15 t/h, the mass flow rate of make-up water is 1.25 kg/s. Additionally, approximately 12.5 kg/s raw water is supplied to cooling tower basin. Hence, 13.75 kg/s raw water is supplied to the plant.

So, raw water cost for the year 2004 may be calculated by using the data described above and the following formulation. It is calculated that raw water cost at that year is $\$868\times10^3$

$$RWC = \frac{P_{R.Water} \times \dot{m}_{R.Water} \times \tau \times 3600}{\rho_{R.Water} \times ER} \tag{112}$$

For previous and future costs, an escalation and deescalation ratio of 3% is used.

All cost components are shown in Table 18 for the entire life of the plant. Total revenue requirement for a given year is the summation of carrying charge, operating & maintenance cost, fuel cost and raw water cost for that year.

6.5.3 Cost Levelization

Since the costs change year by year, costs should be levelized to be used as inputs in thermoeconomic analysis. Levelization for 25 years is done by using the formulations given in Section 5.4. After applying formulas, levelized costs are calculated, the results are given in Table 19 and Table 20.

Table 18: Year-by-Year Analysis (All values are round numbers given in thousand dollars) of Bilkent Plant

Year	Carrying Charges	Operating & Maintenance Costs	Fuel Costs	Raw Water Costs	Total Revenue Requirement
2000	4950	1950	10144	771	17824
2001	4950	2009	11262	794	19024
2002	4800	2919	10555	818	19101
2003	4600	2131	9625	843	17208
2004	4400	2195	12082	868	19555
2005	4200	4011	12444	894	21559
2006	4200	2328	12818	921	20277
2007	5200	2398	13202	948	21759
2008	4300	3320	13598	977	22206
2009	4300	2544	14006	1006	21867
2010	4500	2621	14427	1036	22596
2011	4500	4449	14859	1068	24887
2012	3000	2780	15305	1100	22197
2013	2600	2864	15764	1133	22373
2014	2600	3800	16237	1167	23816
2015	2600	3038	16724	1202	23577
2016	2700	3129	17226	1238	24306
2017	2700	4973	17743	1275	26705
2018	2600	3320	18275	1313	25522
2019	2700	3419	18823	1352	26309
2020	2600	4372	19388	1393	27768
2021	2600	3628	19970	1435	27649
2022	2600	3736	20569	1478	28399
2023	2600	3848	21186	1522	29173
2024	2600	3964	21821	1568	29970

Table 19: Values of Levelized Cost Components of Bilkent Plant

Levelized Costs	CC_L	OMC_L	FC_L	RWC_L	TRR_L
$10^3 \times \$$	4139	2826	13362	1023	21350

.

Gas turbine system is sold as one unit, and prices of its subcomponents are not available. However, to obtain more accurate results from thermoeconomic analysis, gas generator and power turbine are considered seperately. Hence, it is assumed that power turbine and its electricity generator has a price of 2 M$ and gas generator 7 M$, respectively. Levelized costs are shared according to this assumption.

Table 20: Cost Rate Associated With Capital and O&M Costs for Components of Bilkent Plant

Component	PEC (M$)	$\dot{Z}_k^{CI}$ ($/h)	$\dot{Z}_k^{OM}$ ($/h)	$\dot{Z}_k$ ($/h)
Gas Turbine Package	9.00	238	163	401
Steam Turbine	2.50	66	45	111
HRSG	1.85	49	33	82
Gas Compressor	0.85	23	15	38
Cooling Tower	0.75	20	14	33
Condenser	0.50	13	9	22
Demineralization sys.	0.40	11	7	18
Circ. Pumps	0.35	9	6	16
Condensate Pump	0.20	5	4	9
HP BFW Pump	0.20	5	4	9
IP BFW Pump	0.10	3	2	4
IP Steam Desuperh.	0.10	3	2	4
Make-up Tank	0.10	3	2	4
Make-up Pump	0.05	1	1	2
Other Components	2.10	56	38	94

Levelized cost rate of fuel is calculated as $1629/h and that of raw water as $119/h.

6.6 THERMOECONOMIC ANALYSIS

The objective of the thermoeconomic analysis in this study is to understand the cost formation process and to calculate the cost of each product generated by the plant.

Aggregation level influences the accuracy of the results, hence it is taken low enough. Importance of aggregation level is discussed in Chapter 8.

Cost balances are applied to each subsystem. Auxiliary equations are applied by using fuel and product rules. Hence, a set of linear equations, which are shown in Table 21, are formed and solved. Additionally, the following balances should be used together with the balances given in Table 21.

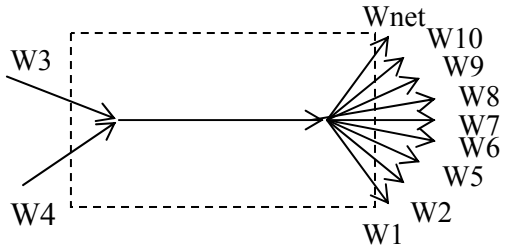

Figure 40: Control Volume Showing the Distribution of Electric Streams of Bilkent Plant

From the cost balance around the control volume shown in Figure 40

$$\dot{C}_{W3} + \dot{C}_{W4} = \dot{C}_{W1} + \dot{C}_{W2} + \dot{C}_{W5} + \dot{C}_{W6} + \dot{C}_{W7} + \dot{C}_{W8} + \dot{C}_{W9} + \dot{C}_{W10} + \dot{C}_{Wnet} \qquad (113)$$

From P rule

$$\frac{\dot{C}_{W1}}{\dot{E}_{W1}} = \frac{\dot{C}_{W2}}{\dot{E}_{W2}} = \frac{\dot{C}_{W5}}{\dot{E}_{W5}} = \frac{\dot{C}_{W6}}{\dot{E}_{W6}} = \frac{\dot{C}_{W7}}{\dot{E}_{W7}} = \frac{\dot{C}_{W8}}{\dot{E}_{W8}} = \frac{\dot{C}_{W9}}{\dot{E}_{W9}} = \frac{\dot{C}_{W10}}{\dot{E}_{W10}} = \frac{\dot{C}_{Wnet}}{\dot{E}_{Wnet}} = c_{p1} \quad (114)$$

From Equations (113) and (114),

$$\dot{C}_{W3} + \dot{C}_{W4} = c_{p1}(\dot{E}_{W1} + \dot{E}_{W2} + \dot{E}_{W5} + \dot{E}_{W6} + \dot{E}_{W7} + \dot{E}_{W8} + \dot{E}_{W9} + \dot{E}_{W10} + \dot{E}_{Wnet}) \quad (115)$$

The right hand side of Equation (115) is equal to $c_{p1}\left(\dot{E}_{W3} + \dot{E}_{W4}\right)$. So,

$$c_{p1} = \frac{\dot{C}_{W3} + \dot{C}_{W4}}{\dot{E}_{W3} + \dot{E}_{W4}} \quad (116)$$

Hence, all the products of the control volume given in Figure 40 may be written in terms of c_{p1} by using Equations (114) and (116).

Cost formation in the plant for 15 t/h process steam flow is given in Table 22. It can be observed that the highest cost is achieved at state F, which is the exit of gas generator. Costs of states D, A, W3, 1, G, and others follow it, respectively. On the other hand, the highest cost per unit exergy is seen at state 5.

Cost rate of products, $\dot{C}_9$ and $\dot{C}_{Wnet}$ are calculated by cost balances. Then, cost rate associated with other plant equipment and exergy loss in the plant should be apportioned between products. An assumption may be to divide the cost rate associated with other plant equipment equally between steam and net power, and the monetary loss associated with the exergy loss according to their exergy values.

Figure 41 shows the final cost rates of products for different process steam flows. It is seen from Figure 41 that as steam mass flow rate to process increases from 1.5 kg/s to 10 kg/s, cost of process steam increases from \$210/h to \$890/h, whereas cost of electrical power output decreases from \$2399/h to \$1700/h.

Table 21: Cost Balances for the Subsystems of Bilkent Plant

No	Control Volume	Cost Balance
1	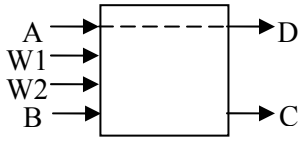	$(\dot{C}_A - \dot{C}_D) + \dot{C}_{W1} + \dot{C}_{W2} +$ $\dot{C}_B - \dot{C}_C + \dot{Z}_1 = 0$ $\dot{C}_B = \dot{C}_C = 0\ (\dot{E}_B = \dot{E}_C = 0)$
2	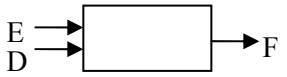	$\dot{C}_E + \dot{C}_D + \dot{Z}_2 = \dot{C}_F$
3	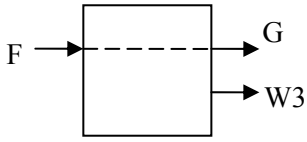	$(\dot{C}_F - \dot{C}_G) + \dot{Z}_3 = \dot{C}_{W3}$ $\frac{\dot{C}_F}{\dot{E}_F} = \frac{\dot{C}_G}{\dot{E}_G}$ (F Rule)
4	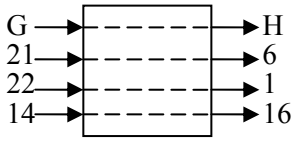	$(\dot{C}_G - \dot{C}_H) + (\dot{C}_{21} - \dot{C}_6) +$ $(\dot{C}_{22} - \dot{C}_1) + (\dot{C}_{14} - \dot{C}_{16}) + \dot{Z}_4 = 0$ $\frac{\dot{C}_G}{\dot{E}_G} = \frac{\dot{C}_H}{\dot{E}_H}$ (F Rule) $\frac{\dot{C}_6 - \dot{C}_{21}}{\dot{E}_6 - \dot{E}_{21}} = \frac{\dot{C}_1 - \dot{C}_{22}}{\dot{E}_1 - \dot{E}_{22}} = \frac{\dot{C}_{16} - \dot{C}_{14}}{\dot{E}_{16} - \dot{E}_{14}} = c_{p2}$ (P Rule)
5	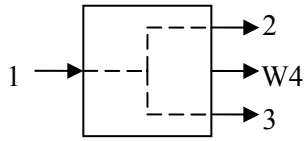	$(\dot{C}_1 - \dot{C}_2 - \dot{C}_3) + \dot{Z}_5 = \dot{C}_{W4}$ $\frac{\dot{C}_1}{\dot{E}_1} = \frac{\dot{C}_2}{\dot{E}_2} = \frac{\dot{C}_3}{\dot{E}_3}$ (F Rule)
6	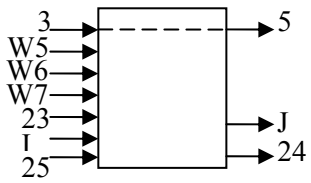	$(\dot{C}_3 - \dot{C}_5) + \dot{C}_{W5} + \dot{C}_{W6} + \dot{C}_{W7} +$ $\dot{C}_{23} + \dot{C}_I + \dot{C}_{25} + \dot{Z}_6 - \dot{C}_J - \dot{C}_{24} = 0$ $\dot{C}_{25}$=0 (Assumption) $\dot{C}_I = \dot{C}_J = 0\ (\dot{E}_I = \dot{E}_J = 0)$
7		$\dot{C}_2 + \dot{C}_6 + \dot{C}_{20} + \dot{Z}_7 = \dot{C}_9$
8	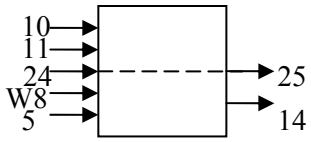	$\dot{C}_{10} + \dot{C}_{11} + (\dot{C}_{24} - \dot{C}_{25}) +$ $\dot{C}_{W8} + \dot{C}_5 + \dot{Z}_8 = \dot{C}_{14}$ $\frac{\dot{C}_{24}}{\dot{E}_{24}} = \frac{\dot{C}_{25}}{\dot{E}_{25}}$ (F Rule) $\dot{C}_{10}$=0 (Assumption)

Table 19 (Continued)

9	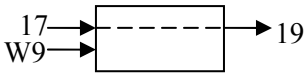	$\dot{C}_{17} + \dot{C}_{W9} + \dot{Z}_9 = \dot{C}_{19}$
10	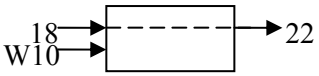	$\dot{C}_{18} + \dot{C}_{W10} + \dot{Z}_{10} = \dot{C}_{22}$

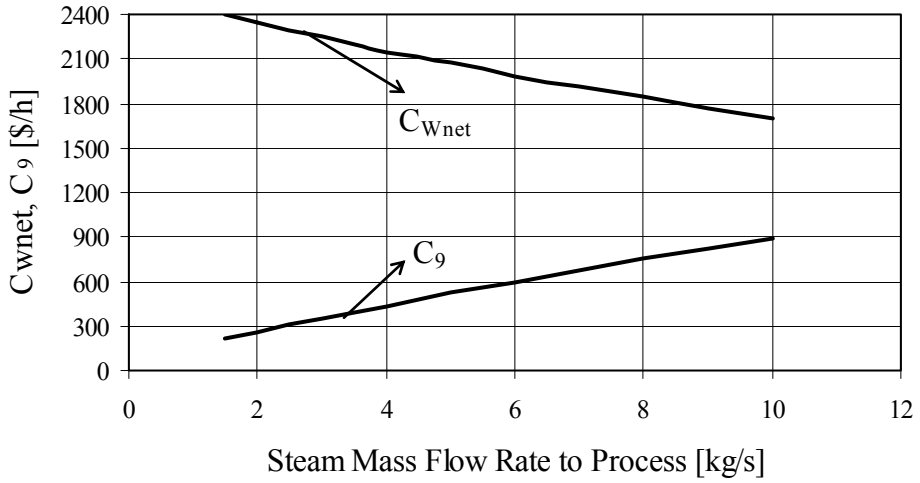

Figure 41: Change of Cost of Products of Bilkent Plant with Steam Mass Flow Rate to Process

Table 22: Cost Formation of Bilkent Plant for 15 t/h Steam to Process

State	Substance	$\dot{E}$ (kW)	$\dot{C}$ ($/h)	c ($/GJ)
A	Natural Gas	76050	1629	5.95
B	Air	0	0	0.00
C	Air	0	0	0.00
D	Natural Gas	76250	1702	6.20
E	Air	0	0	0.00
F	Exhaust Gas	45660	2023	12.30
G	Exhaust Gas	20547	910	12.31
H	Exhaust Gas	3054	135	12.31
I	Air	0	0	0.00
J	Air	0	0	0.00
1	Water	13474	1129	23.28
2	Water	2827	237	23.28
3	Water	1779	149	23.28
4	Water	510	-	-
5	Water	511	366	199.27
6	Water	1402	132	26.13
7	Water	4297	-	-
8	Water	4210	-	-
9	Water	4107	387	26.19
10	Water	237	0	0.00
11	Water	85	11	35.39
12	Water	291	-	-
13	Water	292	-	-
14	Water	802	401	139.11
15	Water	1172	-	-
16	Water	1439	440	84.99
17	Water	221	68	84.99
18	Water	1217	372	84.99
19	Water	222	72	89.96
20	Water	45	14	89.96
21	Water	177	57	89.96
22	Water	1232	385	86.89
23	Water	849	108	35.39
24	Water	409	0	0.00
25	Water	414	0	0.00

$\dot{C}_{W1}$	$32/h	$\dot{C}_{W6}$	$10/h	c_{W1}	$18.89/GJ	c_{W6}	$18.89/GJ
$\dot{C}_{W2}$	$3/h	$\dot{C}_{W7}$	$0/h	c_{W2}	$18.89/GJ	c_{W7}	$3.29/GJ
$\dot{C}_{W3}$	$1192/h	$\dot{C}_{W8}$	$0/h	c_{W3}	$13.96/GJ	c_{W8}	$18.89/GJ
$\dot{C}_{W4}$	$854/h	$\dot{C}_{W9}$	$0/h	c_{W4}	$37.69/GJ	c_{W9}	$5.77/GJ
$\dot{C}_{W5}$	$19/h	$\dot{C}_{W10}$	$4/h	c_{W5}	$18.89/GJ	c_{W10}	$18.89/GJ

CHAPTER 7

DISCUSSIONS

7.1 SELECTION OF THE GAS TURBINE SYSTEM FOR CASE STUDIES

In this thesis, case studies have the same gas turbine system which is the one that is used in CGAM problem. The reasons of this selection are discussed in this section.

Since the aim of case studies is to investigate the effect of different kinds of steam turbine and HRSG, all cases should have the same gas turbine system. Two different alternatives could be foreseen for this selection. The first one is selecting the latest industrial gas turbines. Assume that, MS5001, a model of General Electrics is chosen. From the available data, performance of MS5001, generator drive type, natural gas fueled gas turbine at ISO conditions (15°C, 101.325 kPa, 60% humidity, sea level) are as follows:

Table 23: Performance of MS5001, Generator Drive Type, Natural Gas Fueled Gas Turbine at ISO Conditions [42]

Output	26,830 kW
Heat Rate	12,687 kJ/kWh
Exhaust Flow	125.2 kg/sec
Exhaust Temperature	483 °C
Compressor Pressure Ratio	10.5

The available data are not sufficient to find the mass flow rates and thermodynamic properties of the states within the gas turbine system even if the isentropic efficiencies of compressor and gas turbine are assumed. Because there is no information about mass flow rate and positions of cooling flows. So, exhaust gas composition may not be calculated properly.

Even if the thermodynamic properties are clearly identified for an industrial gas turbine system, there are still problems. Unlike steam turbines, gas turbine systems are not custom designed and they are sold with certain properties and prices. The price of the components of the system are not given, only the price of whole system is given. If all the prices are assumed, the cost flow within the gas turbine system could be misleading. However, if the whole system is considered to be analyzed in thermoeconomic analysis, then the problem of assuming the price of each component disappears. At this time, the cost of electrical power output and the cost of combustion gases entering HRSG should be considered equal from product rule of SPECO method. From several studies in literature, it is seen that the cost of the streams mentioned could be very different with each other. So, this kind of an approach may be also misleading.

The second alternative for selection of the gas turbine system could be a proposed gas turbine system. Rather than designing a gas turbine system by the author, CGAM system is chosen because this system is very suitable for cogeneration applications. Since a gas turbine system with fixed properties is considered throughout the thesis, a similar analysis with that of the CGAM problem for different data set is thought to be unnecessary. It would be only repeating the calculations with different numbers.

Due to the reasons explained at above paragraphs, gas turbine system is chosen same as that of in the CGAM problem.

7.2 INFLUENCE OF AGGREGATION LEVEL IN THERMOECONOMIC ANALYSIS

If a system has more than one products, then aggregation level is of great importance in calculating the cost of the products. This level should be kept low enough. The most appropriate way is to analyze a system at component level. However, in some cases, two or more components can be considered together. The latter is applied, in general, if there is not enough information about some components in a system. Additionally, if a component serves another component, then these components might be considered together. For example, an expansion valve serves other components by reducing the pressure to the desired level of that component.

To illustrate, we can consider the bottoming cycle of case-3 as an aggregate system, which is shown in Figure 42.

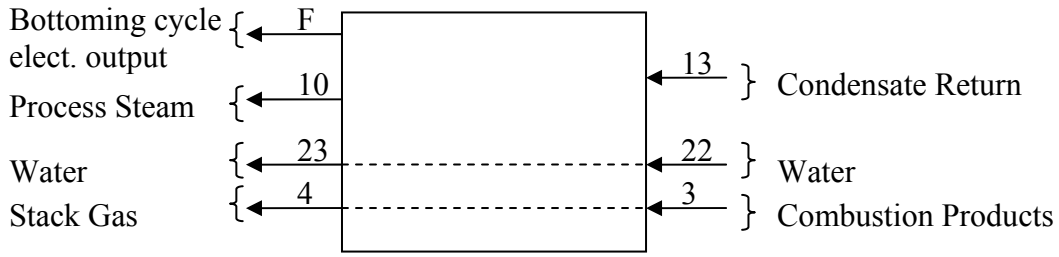

Figure 42: Control Volume of Bottoming Cycle of Case-3

From the cost balance of the control volume shown in Figure 42

$$\dot{C}_3 + \dot{C}_{22} + \dot{C}_{13} + \dot{Z}_{bottoming} = \dot{C}_4 + \dot{C}_{23} + \dot{C}_{10} + \dot{C}_F \qquad (117)$$

From fuel rule,

$$\frac{\dot{C}_3}{\dot{E}_3} = \frac{\dot{C}_4}{\dot{E}_4} \tag{118}$$

$$\frac{\dot{C}_{22}}{\dot{E}_{22}} = \frac{\dot{C}_{23}}{\dot{E}_{23}} \tag{119}$$

$\dot{C}_{22}$ is assumed to be zero, so from Equation (119) $\dot{C}_{23}$ is zero. Additionally, $\dot{C}_{13}$ should be assumed to be zero. The remaining auxiliary equation is due to product rule

$$\frac{\dot{C}_F}{\dot{E}_F} = \frac{\dot{C}_{10}}{\dot{E}_{10}} \tag{120}$$

After the cost balances and auxiliary equations are applied to the aggregate system, it is found that $\dot{C}_F$ =\$1444/h, $\dot{C}_{10}$ =\$882/h for 15 t/h steam to process.

When the aggregate level is chosen low enough as done in Section 5, it is found that $\dot{C}_F$ =\$1711/h, $\dot{C}_{10}$ =\$616/h.

In conclusion, it is clear that choosing the aggregate level influences the cost of the products for a system having more than one product significantly. Hence, it should be kept low enough.

CHAPTER 8

CONCLUSIONS

In this thesis, combined cycle cogeneration systems are investigated by energy, exergy and thermoeconomic analyses. General methodology of these methods are discussed and they are applied to case studies. First, three cases proposed by the author are discussed. Then, an existing plant, Bilkent combined cycle cogeneration plant is analyzed by the mentioned methods. Results of these analyses are given in related sections.

8.1 CONCLUSIONS OF CASE STUDIES

Three different configurations of combined cycle cogeneration systems are analyzed. In the first case, a back-pressure steam turbine and 2-pressure level HRSG; in the second case, a condensing steam turbine and 2-pressure level HRSG; and, in the third case, a condensing steam turbine and 3-pressure level HRSG is used. Effect of steam demand, HP steam drum pressure and pinch point on thermodynamic performance is discussed. Then, thermoeconomic analysis is carried out to calculate the cost of each product and see the cost formation for different steam demands.

When the effect of steam demand is investigated, it is seen that case-1 has the lowest FUE and PHR, which means this case is the most inefficient case in terms of energy concepts. The system in case-3 is slightly more efficient than the system in case-2 when FUE and PHR are taken into account. However, the best performance assessment parameter is exergetic efficiency since it takes into account the quality of energy. So, exergetic efficiencies of the cases are compared. It is seen that the order of efficiency of the cases do not change, however the values of the efficiencies decrease, i.e. exergetic efficiency of case 3 for a given steam demand is lower than FUE of that case for the same steam demand. Insights of this result are observed. It is

seen that high exergy loss in case-1 and high exergy destruction in dump condenser is the main reason of case-1 being inefficient. Additionally, the main difference of exergetic efficiencies between case-2 and case-3 arise from the higher exergy loss of case-2. Then, thermoeconomic analysis has been carried out to compare these cases. From results of this analysis, it is concluded that the cost of systems' products is the highest in case-1. Cost of process steam for case-2 is slightly lower than that for case-3, whereas cost of gas turbine electrical output and bottoming cycle electrical output for case-3 is slightly lower than case-2. So, a company owner may benefit from these results in arranging the company's economic policy. According to the selling prices, case-2 or case-3 might be more economic. For example, if selling price of process steam is higher, then case-2 may be more economic; if selling price of electrical power is higher, then case-3 may be more economic. If a more general conclusion is needed to be drawn, it can be said that combined cycle cogeneration systems with extraction-condensing steam turbine are thermodynamically and thermoeconomically more efficient. Increasing the pressure level of HRSG, increases slightly the cost of process steam and decreases slightly the cost of electrical output for the same steam demand.

Effect of HP steam drum pressure and pinch point is investigated in all cases. The results of this analysis may be helpful in thermodynamic and thermoeconomic optimization of combined cycle cogeneration systems. It is seen that, increasing the HP steam drum pressure has different effects on FUE for each case. For example, FUE increases in case-3; whereas FUE first decreases, then increases in case-1. However, exergetic efficiency of these cases increase as HP steam drum pressure increases. The reason of this increase is the decrease in exergy destruction of HRSG and dump condenser for case-1, slight decrease in total exergy loss and decrease in HRSG for case-3. Exergetic efficiency of case-2 is not very sensitive to HP steam drum pressure. When effect of pinch point is investigated, it may be observed that FUE and exergetic efficiency decreases as pinch point increases. However, it should be taken in mind that as pinch point decreases, cost of HRSG increases, which means an increase in cost of systems' products.

8.2 CONCLUSIONS OF BILKENT PLANT

An existing plant, Bilkent combined cycle cogeneration plant is analyzed with energy, exergy and thermoeconomic analyses. The aim of the study is investigating the current configuration of the plant, rather than optimizing for the site requirements.

From energy analysis, information about net electrical output, enthalpy difference of process, stack temperature, fuel utilization efficiency and power-to-heat ratio is obtained and the results are given in relevant sections. Exergy destructions are given for different steam demands. These results may be helpful for future improvements for the plant. Additionally, cost of products and cost formation is discussed. The plant owner may develop an opinion from these results and check the company's economic policy.

8.3 RECOMMENDATIONS FOR FUTURE WORKS

In this thesis, advanced thermodynamics techniques has been used to analyze systems. After accomplishing energy, exergy and thermoeconomic analyses, a basis for starting optimization is ready to use. A very clear schematic to indicate the steps that has been taken in this thesis and future works can be seen in Figure 43. As it can be seen from Figure 43, thermoeconomic optimization and multidisciplinary optimization could be carried out for future works.

Exergy and its links to environment is also an interesting topic. It is stated by the reseachers that environmental problems such as air pollution, solid waste disposal, etc. may be reduced by using exergy techniques. Some studies have been started at this topic. However, it should be stated that more work is needed for improving the topics of exergy and its links to economics, and exergy and its links to environment.

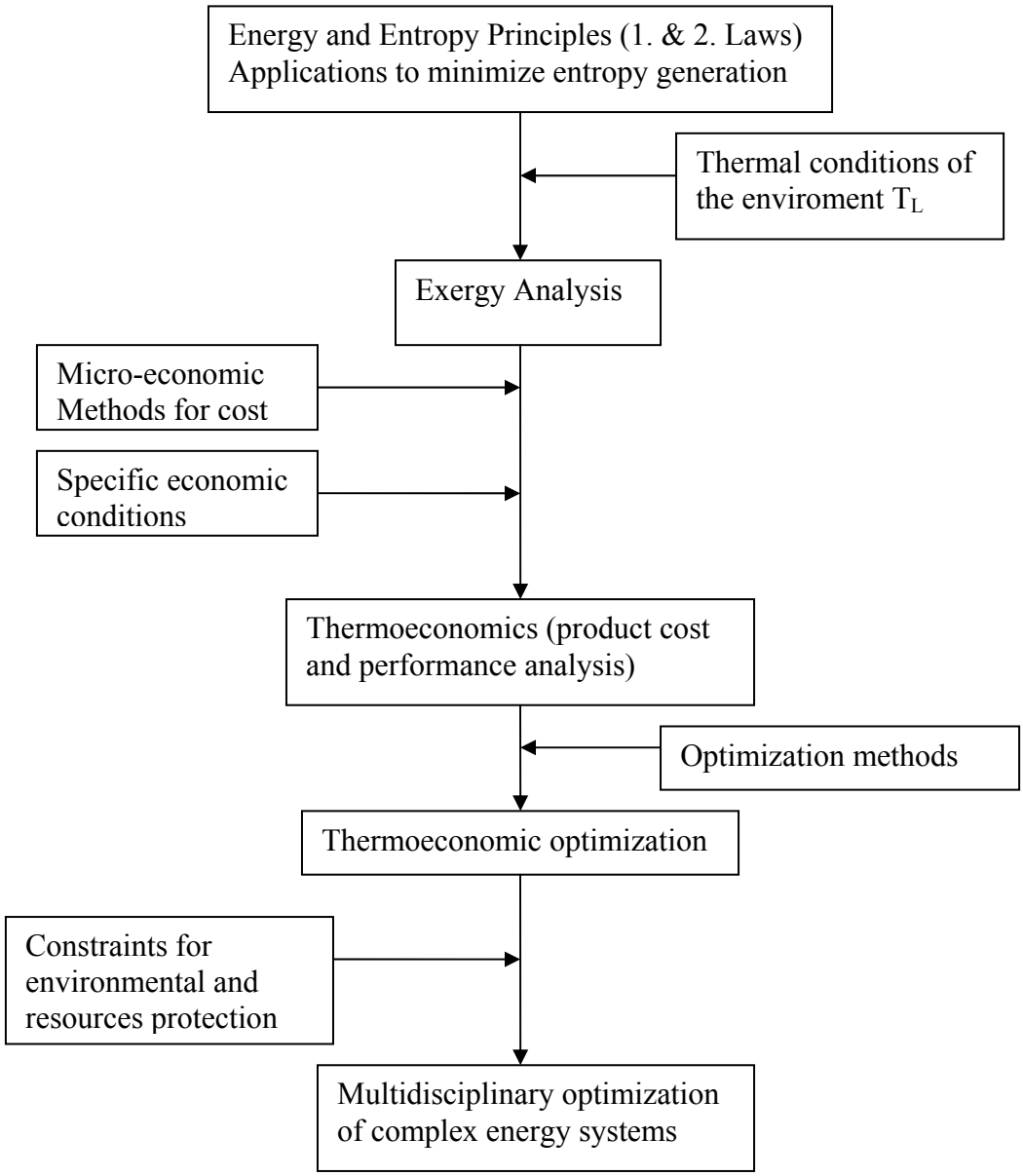

Figure 43: Initiation and the Role of Thermoeconomics within the Frame of Thermodynamic Optimization [15]

APPENDIX A

FORMULATION OF ENTHALPY AND ABSOLUTE ENTROPY OF IDEAL GASES

Table A.1 Variation of Enthalpy and Absolute Entropy with Temperature at 1 bar for Various Substances [1]

1. At T_{ref}=298.15 K (25°C), P_{ref}=1 bar

Substance	Formula	$\bar{h}°$ [kJ/kmol]	$\bar{s}°$ [kJ/kmol-K]
Nitrogen	$N_2(g)$	0	191.610
Oxygen	$O_2(g)$	0	205.146
Hydrogen	$H_2(g)$	0	130.679
Carbon dioxide	$CO_2(g)$	-393521	213.794
Water	$H_2O(g)$	-241856	188.824
Water	$H_2O(l)$	-285829	69.948
Methane	$CH_4(g)$	-74872	186.251

2. For $298.15 < T \le T_{max}$, P_{ref} =1 bar, with $y = 10^{-3}\,T$

$$\bar{h}° = 10^3 \cdot \left[H^+ + a \cdot y + \frac{b}{2} \cdot y^2 - c \cdot y^{-1} + \frac{d}{3} \cdot y^3 \right]$$

$$\bar{s}° = S^+ + a \cdot \ln T + b \cdot y - \frac{c}{2} \cdot y^{-2} + \frac{d}{2} \cdot y^2$$

The maximum temperature, T_{max}, is 500 K for $H_2O(l)$, 2000 K for $CH_4(g)$, and 3000 K for the remaining substances

Substance	Formula	H^+	S^+	a	b	c	d
Nitrogen[a]	$N_2(g)$	-9.982	16.203	30.418	2.544	-0.238	0
Oxygen	$O_2(g)$	-9.589	36.116	29.154	6.477	-0.184	-1.017
Hydrogen	$H_2(g)$	-7.823	-22.966	26.882	3.586	0.105	0
Carbon dioxide	$CO_2(g)$	-413.886	-87.078	51.128	4.368	-1.469	0
Water	$H_2O(g)$	-253.871	-11.750	34.376	7.841	-0.423	0
Water	$H_2O(l)$	-289.932	-67.147	20.355	109.198	2.033	0
Methane	$CH_4(g)$	-81.242	96.731	11.933	77.647	0.142	-18.414

[a]Table values for nitrogen are shown as reported in [34]. Corrected values for H^+, S^+, a, b, c, d are, respectively, -7.609, 51.539, 24.229, 10.521, 0.180, -2.315.

APPENDIX B

BASIC THERMODYNAMICS [1, 28, 29]

B.1 THE FIRST LAW OF THERMODYNAMICS

The first law of thermodynamics led to the concept of energy as a property by identifying two modes of its change for a closed system. The two modes are heat and work. This identification, in turn, leads to the law of the conservation of energy. The conservation of energy states that energy interaction at the system boundaries by matter flow, by heat and by work is equal to the change of the energy of the system.

For a steady state steady flow process, control volume energy rate balance may be written as

$$\dot{Q}_{C.V.} + \sum \dot{m}_i \left(h_i + \frac{V_i^2}{2} + g \cdot Z_i \right) = \sum \dot{m}_e \left(h_e + \frac{V_e^2}{2} + g \cdot Z_e \right) + \dot{W}_{C.V.} \qquad (1)$$

B.2 THE SECOND LAW OF THERMODYNAMICS

The second law of thermodynamics evolved around the fact that spontaneous processes can proceed only in a definite direction (towards equilibrium states). Heat by itself can only flow from a hot body to a cold body. Water by itself can only flow from higher to lower level. Combustion gases by themselves cannot go back to fuel and air. This led to the concept of entropy as a property that increases in irreversible interactions.

For a steady state steady flow process, control volume entropy rate balance may be written as

$$0 = \sum_j \frac{\dot{Q}_j}{T_j} + \sum_i \dot{m}_i \cdot s_i - \sum_e \dot{m}_e \cdot s_e + \dot{S}_{gen} \tag{2}$$

B.3. USEFUL CONCEPTS AND RELATIONS

B.3.1 Isentropic Efficiencies

The isentropic turbine efficiency η_{st} compares the actual turbine power $\dot{W}_{CV}$ to the power that would be developed in an isentropic expansion from the specified inlet state to the specified outlet pressure, $(\dot{W}_{CV})_s$

$$\eta_{st} = \frac{\dot{W}_{CV}}{(\dot{W}_{CV})_s} \tag{3}$$

The isentropic compressor efficiency η_{sc} compares the actual power input to the power that would be required in an isentropic compression from the specified inlet state to the specified outlet pressure.

$$\eta_{sc} = \frac{(\dot{W}_{CV})_s}{\dot{W}_{CV}} \tag{4}$$

An isentropic pump efficiency is defined similar to Equation (4)

B.3.2 Ideal-Gas Model

Entropy change between any two states of an ideal gas may be given as

$$\bar{s}(T_2, P_2) - \bar{s}(T_1, P_1) = \bar{s}°(T_2) - \bar{s}°(T_1) - \bar{R} \cdot \ln \frac{P_2}{P_1} \tag{5}$$

The enthalpy and entropy of the ideal gas mixtures can be determined as the sum of the respective properties of the component gases, provided that the contribution from each gas is evaluated at the condition at which the gas exits in the mixture. Thus

$$H = \sum_{k=1}^{N} n_k \cdot \bar{h}_k \quad \text{or} \quad \bar{h} = \sum_{k=1}^{N} x_k \cdot \bar{h}_k \tag{6}$$

$$S = \sum_{k=1}^{N} n_k \cdot \bar{s}_k \quad \text{or} \quad \bar{s} = \sum_{k=1}^{N} x_k \cdot \bar{s}_k \tag{7}$$

Enthalpy of an ideal gas depend only on temperature, $\bar{h}_k$ terms appearing in the equation above are evaluated at the temperature of the mixture. Entropy is a function of two independent properties. Accordingly, the $\bar{s}_k$ terms are evaluated either at the temperature and volume of the mixture or at the mixture temperature and the partial pressure P_k of the component. In the latter case

$$S = \sum_{k=1}^{N} n_k \cdot \bar{s}_k(T, x_k \cdot P) \tag{8}$$

The molecular weight M of the mixture is determined in terms of the molecular weights M_k of the components as

$$M = \sum_{k=1}^{N} x_k \cdot M_k \tag{9}$$

B.4 THE THIRD LAW OF THERMODYNAMICS AND ABSOLUTE ENTROPY

The third law deals with the entropy of substances at the absolute zero of temperature, and in essence states that the entropy of a perfect crystal is zero at absolute zero.

The particular relevance of the third law is that it provides an absolute base from which to measure the entropy of each substance. The entropy relative to this base is termed the absolute entropy.

When the absolute entropy is known at the standard state, the specific entropy at any other state can be found by adding the specific entropy change between the two states to the absolute entropy at the standard state. Similarly, when the absolute entropy is known at the pressure P_{ref} and temperature T, the absolute entropy at the same temperature and any pressure P can be found from

$$\bar{s}(T,P) = \bar{s}°(T) - \overline{R} \cdot \ln \frac{P}{P_{ref}} \quad \text{(ideal gas)} \tag{10}$$

The entropy of the kth component of an ideal-gas mixture is evaluated at the mixture temperature T and the partial pressure P_k. For the kth component of an ideal gas mixture Equation (10) takes the form

$$\bar{s}_k(T,P_k) = \bar{s}_k^o(T) - \overline{R} \cdot \ln \frac{x_k \cdot P}{P_{ref}} \tag{11}$$

APPENDIX C

CGAM PROBLEM [1, 25]

C.1 INTRODUCTION

A simple cogeneration system consisting of a regenerative gas-turbine system and a heat-recovery steam generator serves as an example to illustrate the application of thermoeconomic methods for evaluating and optimizing complex energy systems. The foremost professors and/or researchers of the thermoeconomic field discussed their approaches through this problem. The name CGAM stems from the initials of Christoph Frangapoulos, George Tsatsaronis, Antonio Valero and Michael Spakovsky.

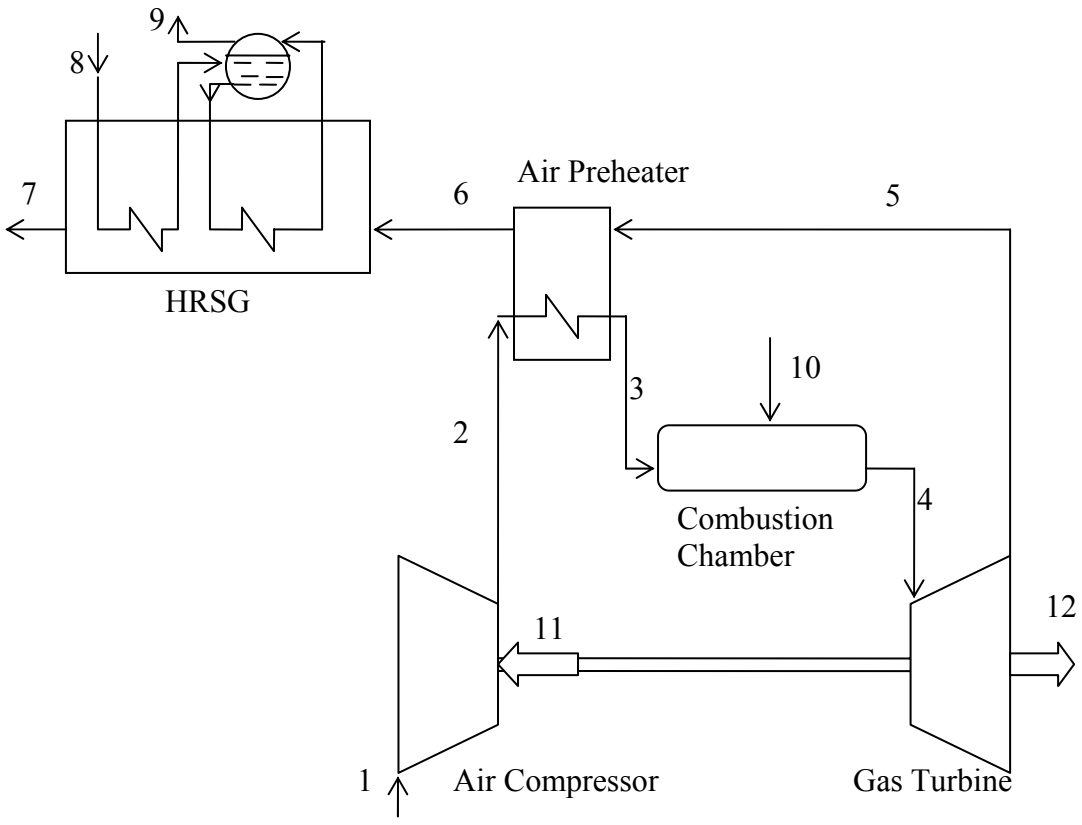

Figure C.1: Schematic of the Cogeneration System Discussed in CGAM Problem

Table C.1 Decision Variables and Parameters of CGAM Problem

Decision Variables	
Air Compressor Pressure Ratio	10
Combustion Chamber Inlet Temperature	850 K
Gas Turbine Inlet Temperature	1520 K
Isentropic Efficiency of Air Compressor	86%
Isentropic Efficiency of Gas Turbine	86%
Parameters	
Net Power Generated by the System	30 MW
Process Steam Conditions	20 bars, 14 kg/s
Air Compressor Inlet Conditions	25 °C, 1.013 bars
Air Preheater Pressure Drops	3% on the gas side 5% on the air side
Condensate Return Conditions	25 °C, 20 bars
Stack Pressure	1.013 bars
HRSG Pressure Drop	5% on the gas side
Fuel (Natural Gas) Conditions	25 °C, 12 bars
Combustion Chamber Pressure Drop	5%

In addition to the data tabulated in Table C.1, other considerations for the base-case design are as follows: Air molal analysis (%): 77.48 N_2, 20.59 O_2, 0.03 CO_2, 1.90 H_2O(g). Evaporator approach temperature is taken as 15 °C.

The assumptions underlying the cogeneration system model include the following:

- The cogeneration system operates at steady state
- Ideal-gas mixture principles apply for the air and the combustion products

- The fuel (natural gas) is taken as Methane modeled as an ideal gas. The fuel is provided to the combustion chamber at the required pressure by throttling from a high-pressure source.
- The combustion in the combustion chamber is complete. N_2 is inert.
- Heat transfer from the combustion chamber is 2% of the fuel lower heating value. All other components operate without heat loss.

C.2 ENERGY ANALYSIS

C.2.1 Governing Equations

Denoting the fuel-air ratio on a molar basis as $\bar{\lambda}$, the molar flow rates of the fuel, air, and combustion products are related by

$$\frac{\dot{n}_F}{\dot{n}_a} = \bar{\lambda}, \qquad \frac{\dot{n}_P}{\dot{n}_a} = 1 + \bar{\lambda} \tag{1}$$

Where the subscripts F, P, and a denote, respectively, fuel, combustion products, and air. For complete combustion of methane the chemical equation takes the form

$$\bar{\lambda}CH_4 + \left[0.7748N_2 + 0.2059O_2 + 0.0003CO_2 + 0.019H_2O\right] \rightarrow$$
$$\left[1 + \bar{\lambda}\right]\left[x_{N_2}N_2 + x_{O_2}O_2 + x_{CO_2}CO_2 + x_{H_2O}H_2O\right] \tag{2}$$

Balancing carbon, hydrogen, and nitrogen, the mole fractions of the components of the combustion products are

$$x_{N_2} = \frac{0.7748}{1 + \bar{\lambda}}, \qquad x_{O_2} = \frac{0.2059 - 2\bar{\lambda}}{1 + \bar{\lambda}}$$
$$x_{CO_2} = \frac{0.0003 + \bar{\lambda}}{1 + \bar{\lambda}}, \quad x_{H_2O} = \frac{0.019 + 2\bar{\lambda}}{1 + \bar{\lambda}} \tag{3}$$

The fuel-air ratio can be obtained from an energy rate balance as follows:

$$0 = \dot{Q}_{CV} + \dot{n}_F \overline{h}_F + \dot{n}_a \overline{h}_a - \dot{n}_p \overline{h}_p \tag{4}$$

As the heat loss is assumed to be 2% of the fuel lower heating value, we have

$$\dot{Q}_{CV} = -0.02 \dot{n}_F \overline{LHV} \tag{5}$$

From the results of Equations (1) to (5), and applying ideal gas mixture principles to determine the enthalpies of the air and combustion products, $\overline{\lambda}$ may be found.

From a control volume enclosing the compressor and turbine, energy rate balanced takes the form

$$0 = -\dot{W}_{CV} + \dot{n}_a \cdot (\overline{h}_1 - \overline{h}_2) + \dot{n}_p \cdot (\overline{h}_4 - \overline{h}_5) \tag{6}$$

The term $(\overline{h}_1 - \overline{h}_2)$ of Equation 6 is evaluated using the isentropic compressor efficiency

$$\eta_{sc} = \frac{\overline{h}_{2s} - \overline{h}_1}{\overline{h}_2 - \overline{h}_1} \tag{7}$$

The term $(\overline{h}_4 - \overline{h}_5)$ of Equation 6 is evaluated using the isentropic turbine efficiency

$$\eta_{st} = \frac{\overline{h}_4 - \overline{h}_5}{\overline{h}_4 - \overline{h}_{5s}} \tag{8}$$

Using Equations 1,6,7 and 8 $\dot{n}_a$ may be calculated. Then, $\dot{m}_a$ is found by using the molecular weight of air.

From a control volume enclosing the air preheater, energy rate balance takes the form

$$0 = \dot{n}_a(\bar{h}_2 - \bar{h}_3) + \dot{n}_p(\bar{h}_5 - \bar{h}_6) \quad (9)$$

After solving Equation (9) for $\bar{h}_6$, the temperature T_6 is obtained iteratively.

From a control volume enclosing the HRSG, energy rate balance takes the form

$$0 = \dot{n}_p(\bar{h}_6 - \bar{h}_7) + \dot{m}_8(h_8 - h_9) \quad (10)$$

After solving Equation 10 for $\bar{h}_7$, the temperature T_7 is obtained iteratively.

C.2.2 Results of Energy Analysis

Fuel-air ratio, $\bar{\lambda}$ is found to be equal to 0.0321. Molar analyis of the products is as follows: 75.07% N_2, 13.73% O_2, 3.14% CO_2, 8.06% H_2O. Power input to compressor is found to be 29.662 MW. Other results involving mass flow rate and thermodynamic properties of states are tabulated below.

C.3 EXERGY ANALYSIS

Exergy rates of states are calculated using the equations and considerations given in Section 4.2. For the chemical exergy of methane, liquid water and ideal gas mixtures, standard chemical exergies are used. Results are tabulated above.

Table C.2 Mass Flow Rate, Temperature, and Pressure Data for the Cogeneration System of Figure C.1

State	Substance	Mass Flow Rate (kg/s)	Temperature (K)	Pressure (bars)
1	Air	91.2757	298.150	1.013
2	Air	91.2757	603.738	10.130
3	Air	91.2757	850.000	9.623
4	Combustion Products	92.9176	1520.000	9.142
5	Combustion Products	92.9176	1006.162	1.099
6	Combustion Products	92.9176	779.784	1.066
7	Combustion Products	92.9176	426.897	1.013
8	Water	14.0000	298.150	20.000
9	Water	14.0000	485.570	20.000
10	Methane	1.6419	298.150	12.000

Table C.3 Exergy Data for the Cogeneration System of Figure C.1

State	Substance	$\dot{E}^{PH}$	$\dot{E}^{CH}$	$\dot{E}$
1	Air	0.0000	0.0000	0.0000
2	Air	27.5382	0.0000	27.5382
3	Air	41.9384	0.0000	41.9384
4	Combustion Products	101.0873	0.3665	101.4538
5	Combustion Products	38.4158	0.3665	38.7823
6	Combustion Products	21.3851	0.3665	21.7516
7	Combustion Products	2.4061	0.3665	2.7726
8	Water	0.0266	0.0350	0.0616
9	Water	12.7752	0.0350	12.8102
10	Methane	0.6271	84.3668	84.9939

Table C.4 Exergy Destruction Data for the Cogeneration System of Figure C.1

Component	Rate (MW)	y_D^* (percentage)	y_D (percentage)
Combustion Chamber	25.48	64.56	29.98
HRSG	6.23	15.78	7.33
Gas Turbine	3.01	7.63	3.54
Air Preheater	2.63	6.66	3.09
Air Compressor	2.12	5.37	2.49
Overall Plant	39.47	100.00	46.43

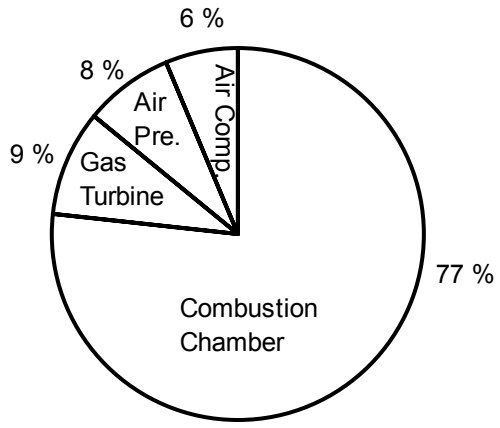

Figure C.2 Exergy Destruction Distribution of Gas Turbine System of the Cogeneration System of Figure C.1

C.4 ECONOMIC ANALYSIS

A detailed economic analysis was done for the cogeneration system of Figure C.1. Details of this analysis may be found in [1]. Results needed to be used in thermoeconomic analysis are given below.

Annual levelized carrying charges, operating and maintenance costs, fuel costs are found to be $\$10.527\times10^6, \$5.989\times10^6, \$10.411\times10^6,$ respectively. Total number of hours of system operation per year is taken as 7446. Other data and results are tabulated in Table C.5.

Table C.5 Economic Data for the Cogeneration System of Figure C.1

Component	PEC (10^3\$)	$\dot{Z}$ (\$/h)
Air Compressor	3735	753
Air Preheater	936	188
Combustion Chamber	338	68
Gas Turbine	3739	753
HRSG	1310	264
Other Plant Equipment	942	190

The levelized cost rate of fuel, which is supplied to the total system from outside, is found to be \$1398/h.

PEC values of Table C.4 are calculated from the following formulations:

$$\mathrm{PEC}_{ac} = \left(\frac{C_{11}\cdot \dot{m}_a}{C_{12}-\eta_{sc}}\right)\cdot\left(\frac{P_2}{P_1}\right)\cdot \ln\left(\frac{P_2}{P_1}\right) \tag{11}$$

$$PEC_{cc} = \left(\frac{C_{21} \cdot \dot{m}_a}{C_{22} - \frac{P_4}{P_3}} \right) \cdot \left[1 + \exp(C_{23} \cdot T_4 - C_{24}) \right] \tag{12}$$

$$PEC_{gt} = \left(\frac{C_{31} \cdot \dot{m}_g}{C_{32} - \eta_{st}} \right) \cdot \ln\left(\frac{P_4}{P_5} \right) \cdot \left[1 + \exp(C_{33} \cdot T_4 - C_{34}) \right] \tag{13}$$

$$PEC_{aph} = C_{41} \cdot \left(\frac{\dot{m}_g \cdot (h_5 - h_6)}{U \cdot \Delta T_{lm,aph}} \right)^{0.6} \tag{14}$$

$$PEC_{hrsg} = C_{51} \cdot \left[\left(\frac{\dot{Q}_{ec}}{\Delta T_{lm,ec}} \right)^{0.8} + \left(\frac{\dot{Q}_{ec}}{\Delta T_{lm,ev}} \right)^{0.8} \right] + C_{52} \cdot \dot{m}_{st} + C_{53} \cdot \dot{m}_g^{1.2} \tag{15}$$

Table C.6 Constants Used in the Equations (11)-(15)

Compressor	C_{11}=71.10 \$/(kg/s), C_{12}=0.9
Combustion Chamber	C_{21}=46.08 \$/(kg/s), C_{22}=0.995, C_{23}=0.018 (K^{-1}), C_{24}=26.4
Gas Turbine	C_{31}=479.34 \$/(kg/s), C_{32}=0.92, C_{33}=0.036 (K^{-1}), C_{34}=54.4
Air Preheater	C_{41}=4122 \$/($m^{1.2}$), U=18 W/(m^2K)
HRSG	C_{51}=6570 \$/(kW/K)$^{0.8}$, C_{52}=21276 \$/(kg/s), C_{53}=1184.4 \$/(kg/s)$^{1.2}$

C.5 THERMOECONOMIC ANALYSIS

Cost balances and auxiliary relations are formulated for each component of the cogeneration system. These formulations are as follows:

Air Compressor

$$\dot{C}_1 + \dot{C}_{11} + \dot{Z}_{ac} = \dot{C}_2 \quad (16)$$

$$\dot{C}_1 = 0 \text{ (assumption)} \quad (17)$$

Air Preheater

$$\dot{C}_2 + \dot{C}_5 + \dot{Z}_{ph} = \dot{C}_3 + \dot{C}_6 \quad (18)$$

$$\frac{\dot{C}_6}{\dot{E}_6} = \frac{\dot{C}_5}{\dot{E}_5} \text{ (F rule)} \quad (19)$$

Combustion Chamber

$$\dot{C}_3 + \dot{C}_{10} + \dot{Z}_{cc} = \dot{C}_4 \quad (20)$$

Gas Turbine

$$\dot{C}_4 + \dot{Z}_{gt} = \dot{C}_5 + \dot{C}_{11} + \dot{C}_{12} \quad (21)$$

$$\frac{\dot{C}_5}{\dot{E}_5} = \frac{\dot{C}_4}{\dot{E}_4} \text{ (F rule)} \quad (22)$$

$$\frac{\dot{C}_{11}}{\dot{W}_{11}} = \frac{\dot{C}_{12}}{\dot{W}_{12}} \text{ (P rule)} \quad (23)$$

HRSG

$$\dot{C}_6 + \dot{C}_8 + \dot{Z}_{hrsg} = \dot{C}_7 + \dot{C}_9 \quad (24)$$

$$\frac{\dot{C}_7}{\dot{E}_7} = \frac{\dot{C}_6}{\dot{E}_6} \text{ (F rule)} \quad (25)$$

$$\dot{C}_8 = 0 \text{ (Assumption)} \quad (26)$$

Solving linear Equations (16)-(26), cost formation within the system and cost of products may be calculated. Results are tabulated below.

The cost associated with other plant equipment must be apportioned to the two product streams on the basis of an estimate of the equipment contribution to the generation of each product stream. For simplicity, cost rate associated with other plant equipment is equally divided between steam and net power. Then, monetary loss associated with the exergy loss of stream 7is charged to steam and net power. In the absence of other criteria, the exergy values $\dot{E}_9 - \dot{E}_8$ and $\dot{W}_{12}$ may be used as weighting factors for apportioning the cost rate $\dot{C}_7$ between steam and electricity, respectively. The final adjusted cost rates of steam and net power is found to be \$1394/h and \$2223/h, respectively.

Table C.7 Cost Formation within the Cogeneration System of Figure C.1

State	$\dot{E}$ (MW)	$\dot{C}$ (\$/h)	c (\$/GJ)
1	0.000	0	0.00
2	27.538	2756	27.80
3	41.938	3835	25.40
4	101.454	5301	14.51
5	38.782	2026	14.51
6	21.752	1137	14.51
7	2.773	145	14.51
8	0.062	0	0.00
9	12.810	1256	27.23
10	84.994	1398	4.57
11	29.662	2003	18.76
12	30.000	2026	18.76

REFERENCES

[1] Bejan, A., Tsatsaronis G., Moran M., *Thermal design and optimization*, John Wiley and Sons Inc., U.S.A., 1996

.

[2] Bejan, A., *Advanced engineering thermodynamics*, 2nd ed. New York: Wiley, 1998

[3] Lazzaretto, A., Tsatsaronis, G., *On the calculation of efficiencies and costs in thermal systems*, In: Proceedings of the ASME Advanced Energy Systems Division, AES-Vol.39, 1999.

[4] Tsatsaronis, G., Cziesta, F., *Thermoeconomics*, In: Optimisation of Energy Systems and Processes Summer School, Gliwice, Poland, 2003.

[5] Karthikeyan, R., Hussain, M.A., Reddy, B.V., Nag, P.K., *Performance simulation of heat recovery steam generators in a cogeneration system*. International Journal of Energy Research 1998; 22:399-410

[6] Huang, F.F., *Performance assessment parameters of a cogeneration system*, In: Proceedings of ECOS'96, Stockholm

[7] Dincer, I., Rosen, M.A., *Exergy as a driver for achieving sustainability*. International Journal of Green Energy 2004; 1(1):1-19

[8] Narin, B., Göğüş, Y.A., *Application of the method of exergy splitting to cost evaluation of a retrofitted J-79 engine as cogeneration unit*, In: Proceedings of ECOS 2002, Berlin, Germany..

[9] Çengel, Y.A., Boles, M.A., *Thermodynamics: an engineering approach*, 4th ed., Dubuque, Iowa: McGraw-Hill, 2002

[10] Tawney R., Ehman J., Brown M., *Selection of cycle configurations for combined cycle cogeneration power plants*, In: ASME Turbo Expo 2000, Munich, Germany

[11] Boyce, M.P., *Handbook for cogeneration and combined cycle power plants*, ASME Press, New York, 2002.

[12] EDUCOGEN, *The European educational tool on cogeneration*, second edition, December 2001

[13] EDUCOGEN, *A guide to cogeneration*, March 2001

[14] Cownden, R., Nahon, M., Rosen, M., *Exergy analysis of a fuel cell power system for transportation applications*, Exergy Int. J. 1(2) (2001):112-121

[15] Göğüş, Yalçın A., *Thermoeconomic optimization*, International Journal of Energy Research, Vol.29, 559-580, 2005

[16] Foster Wheeler, *Bilkent combined cycle operating manual*, February 1999

[17] Dechamps, P. J., *Advanced combined cycle alternatives with the latest gas turbines*, Transactions of the ASME, Vol. 120, April 1998

[18] Pak, P.S., Suzuki, Y., *Exergetic evaluation of gas turbine cogeneration systems for district heating and cooling*, International Journal of Energy Research, Vol.21, 209-220, 1997

[19] Agazzani, A., Massardo, A. F., *A tool for thermoeconomic analysis and optimization of gas, steam, and combined plants*, Journal of Engineering for Gas Turbines and Power, Vol.119, 1997

[20] Scuibba, E., *Exergo-Economics: Thermodynamically sound system analysis as a step toward more rationl resource use*, International Summer School on Thermodynamic Optimization and Constructal Design, July 19-21, 2004, Istanbul

[21] Tsatsaronis, G., Moran, M. J., *Exergy-aided cost minimization*, Energy Conversion and Management, Vol.38, No. 15-17, pp.1535-1542, 1997

[22] Huang, F. F., *Performance evaluation of selected combustion gas turbine cogeneration systems based on first and second-law analysis*, Journal of Engineering for Gas Turbines and Power, Vol.112, 1990

[23] Bilgen, E., *Exergetic and engineering analyses of gas turbine based cogeneration systems*, Energy, Vol.25, pp.1215-1229, 2000

[24] Tsatsaronis, G., Lin, L., Tawfik, T., Gallaspy, D.T., *Exergoeconomic evaluation of a KRW-based IGCC power plant*, Transactions of the ASME, Vol. 116, April 1994

[25] Tsatsaronis, G., Pisa, J., *Exergoeconomic evaluation and optimization of energy systems-application to the CGAM problem*, Energy, Vol.19, No.3, pp.287-321, 1994

[26] Huang, F.F., Naumowicz, T., *Performance evaluation of a combined-cycle cogeneration system*,

[27] Erlach, B., Tsatsaronis, G., Cziesla, F., *A new approach for assigning costs and fuels to cogeneration products*, In: Proceedings of ECOS'01, pp. 759- 776, Istanbul

[28] Sonntag, R. E., Borgnakke, C., Van Wylen, G. J., *Fundamentals of thermodynamics*, Fifth Edition, John Wiley and Sons Inc., U.S.A., 1998

[29] El-Sayed, Y. M., *The thermoeconomics of energy conversions*, Elsevier, U.S.A., 2003

[30] Dincer, I., *The role of exergy in energy policy making*, Energy Policy, Vol.30, pp.137-149, 2002

[31] Fisk, R. W., VanHousen, R. L., *Cogeneration application considerations*, GE Power Generation

[32] Moran, M. J., Shapiro, H. N., Fundamentals of engineering thermodynamics, 4th ed., New York, Wiley, 2000

[33] Moran, M. J., *Availability analysis: A guide to efficient energy use*, ASME Press, New York, 1989

[34] Knacke, O., Kubaschewski, O., Hesselmann, K., T*hermochemical Properties of Inorganic Substances*, 2nd ed., Springer-Verlag, Berlin, 1991

[35] Habib, M. A.*, First and second law analysis of steam-turbine cogeneration systems*, Journal of Engineering for Gas Turbine and Power, Vol. 116, January 1994

[36] Tsatsaronis, G., Lin, L. *On exergy costing in exergoeconomics* , In: Computer-Aided Energy Systems Analysis, American Society of Mechanical Engineers, New York, AES-Vol.21, 1990.

[37] Ahrendts, J., *Die exergie chemisch reaktionsfahiger systeme*, VDI-Forschungsheft, 579, VDI-Verlag, Düsseldorf, 1977, pp.26-33

[38] Szargut, J., Morris, D.R., Steward, F.R., *Exergy analysis of thermal, chemical, and metallurgical processes*, Hemisphere, New York, 1988, pp.297-309

[39] Botaş Genel Müdürlüğü, *BOTAŞ*, http://www.botas.gov.tr/, Last update: 29.03.2005

[40] Aski Genel Müdürlüğü, *ASKİ*, http://www.aski.gov.tr/, Last update: 29.03.2005

[41] Turkiye Cumhuriyeti Merkez Bankası, *TCMB*, http://www.tcmb.gov.tr/, Last update: 29.03.2005

[42] GE Power, *Gas turbines technical comparisons*, http://www.gepower.com/prod_serv/products/gas_turbines_cc/en/downloads/gt_tech_sheet.pdf, Last update: 5.04.2005